FINAL THESIS SUBMISSION

Research into Adventitious Lung Sound Signals Originating From Pulmonary Tuberculosis Using Electronic Auscultation

Student: Mr. K.W Becker
Study Leader: Professor C. Scheffer
Co-supervisor: Dr. M. Blanckenberg

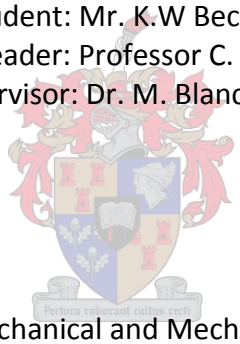

Department Of Mechanical and Mechatronic Engineering

Faculty of Engineering
Stellenbosch University

January 2009

Research into Adventitious Lung Sound Signals Originating From Pulmonary Tuberculosis Using Electronic Auscultation

By

Konrad Wilhelm Becker

Thesis Presented in partial fulfillment of the requirements for the degree of
Master of Science in Engineering
at Stellenbosch University

Department of Mechanical and Mechatronic Engineering
Stellenbosch University
Private Bag X1, 7602 Matieland, South Africa

Supervisor: Prof C. Scheffer
Co-supervisor: Dr. M. Blanckenberg

January 2009

Declaration

I, the undersigned, hereby declare that the work contained in this thesis is my own original work and that I have not previously in its entirety or in part submitted it at any university for a degree.

Signature: ……

K.W. Becker

Date: ……..

Abstract

Pulmonary tuberculosis is a common and potentially deadly infectious disease, commonly affecting the respiratory area. Over one-third of the world's population is infected with the tuberculosis bacterium. Since pulmonary tuberculosis damages the respiratory area, the sound properties of infected lungs differ from those of non-infected lungs. However, auscultation is often ruled out as a reliable diagnostic technique due to the random position and severity of damage to the lungs as well as requiring the personal and trained judgment of an experienced medical practitioner.

This project investigates a possible improvement in the pulmonary diagnostic and treatment field by applying electronic and computer-aided sound analysis techniques to analyze respiratory actions beyond human audible judgment.

Respiratory sounds of both healthy subjects and subjects who were infected with pulmonary tuberculosis were recorded from seven locations per lung on both the posterior and anterior chest walls, using self-designed hardware.

Adaptive filtering signal and analysis techniques yielded a wide range of signal features. This included analysis for time, frequency and both wheeze and crackle adventitious respiratory sounds.

Following the analysis, statistical methods identified the most attractive signal measurements capable of separating the recordings of healthy and unhealthy respiratory sounds. Selected signal features were used with neural network optimization to obtain a successful implementation for the semi-automated identification of healthy and unhealthy respiratory sounds originating from pulmonary tuberculosis, with a performance of over 80% for sensitivity, specificity and accuracy.

The success of categorizing the recordings justifies the capabilities of the digital analysis of respiratory sounds and supports an argument for further research and refinement into the assessment of pulmonary tuberculosis by electronic auscultation.

Further research is recommended, with improvements justified and highlighted in this report.

Opsomming

Tuberkulose is 'n algemene en aansteeklike siekte, potensieel dodelik, wat gewoonlik die asemhalingsarea aantas. Meer as 'n derde van die wêreldbevolking is met die tuberkulose-bakterie geïnfekteer. Aangesien tuberkulose van die longe die asemhalingsarea beskadig, verskil die klankeienskappe van geïnfekteerde longe van dié van ongeïnfekteerde longe. Beluistering is egter dikwels uitgesluit as 'n betroubare diagnostiese tegniek weens die lukrake ligging en erns van die skade aan die longe, en omdat die persoonlike en opgeleide oordeel van 'n ervare mediese praktisyn daarvoor vereis word.

Hierdie projek ondersoek 'n moontlike verbetering op die gebied van diagnose en behandeling van die longe deur elektroniese en rekenaargesteunde klankontledingstegnieke aan te wend om asemhalingswerking wat verder as die oordeel van die menslike gehoor strek, te ontleed.

Asemhalingsgeluide van gesonde subjekte sowel as subjekte wat met tuberkulose geïnfekteer is, is van sewe plekke per long op die agterste en voorste borswande opgeneem deur hardeware wat self ontwerp is, te gebruik.

Sein- en ontledingstegnieke met aanpasbare filtering het 'n wye reeks seinverskynsels gelewer. Dit het ontleding ten opsigte van tyd, frekwensie en toevallige fluit- en kraakgeluide tydens asemhaling, ingesluit.

Na afloop van die ontleding is die beste seinlesings wat die opnames van die gesonde en ongesonde lugweë kan skei deur statistiese metodes geïdentifiseer. Uitgesoekte seinverskynsels is met senuweenetwerkoptimering gebruik om die semi-geoutomatiseerde identifikasie van gesonde en ongesonde asemhalingsgeluide wat voortspruit uit tuberkulose, suksesvol in werking te stel, met 'n werkverrigting van 80% vir alle sensitiwiteit, spesifiekheid en akkuraatheid.

Die sukses met die kategorisering van die opnames regverdig die potensiaal om asemhalingsgeluide digitaal te ontleed en ondersteun 'n argument vir verderde navorsing en verfyning om te lei tot die evaluering van tuberkulose deur elektroniese beluistering.

Verdere navorsing word in die verslag aanbeveel, met verbeteringe wat geregverdig en uitgelig is.

Acknowledgements

I would like to express my sincere thanks to the following people for making my research possible:

- Professor Cornie Scheffer for the opportunity to study under your guidance with such flexibility and always maintaining a positive outlook on my progress.
- Dr. Mike Blanckenberg for the technical support and Dr. Andreas Diacon for the opportunity to complete my recordings while understanding more about rural healthcare.
- To all the nurses at the clinics for their patience and wonderful co-operation.
- Finally and most importantly to my parents who put me in the position to study in the first place.

Dedication

To my Granddad

Table of Contents

List of Figures

List of Tables

Nomenclature

Symbols

C	Capacitor
CO_2	Carbon Dioxide
dB	Decibels
Hz	Hertz
mm	Millimeter
ms	Milliseconds
O_2	Oxygen
pH	Logarithmic Hydrogen Concentration
R	Resistor
s	Second
V	Volt
λ	Forgetting Factor
μ	Micro (10^{-6})
σ^2	Input Variance

Abbreviations

A/D	Analogue-to-Digital
AIDS	Acquired Immune Deficiency Syndrome
ANN	Artificial Neural network
AR	Auto-Regressive
BERG	Biomedical Engineering Research Group
BP	Backprobagation
CAT scan	Computed Axial Tomography Scan
CC	Coarse Crackles
CF	Crest Factor
CHR	Committee for Human Research
CORSA	Computerized Respiratory Sound Analysis
CV	Cross Validation
DC	Direct Current
DNA	Deoxyribonucleic Acid
EC	European Community

ERS	**European Respiratory Society**
FC	**Fine Crackles**
FFT	**Fast Fourier Transform**
FIR	**Finite Impulse Response**
FN	**False Negative**
FP	**False Positive**
GUI	**Graphical User Interface**
HIV	**Human Immunodeficiency Virus**
HPF	**High Pass Filter**
IFN	**Interferon**
LPF	**Low Pass Filter**
MDR-TB	**Multiple Drug Resistant Tuberculosis**
MODS	**Microscopic Observation Drug Susceptibility**
MTB	**Mycobacterium Tuberculosis**
MTBV	**Mycobacterium Bovis**
NN	**Neural Network**
RLS	**Recursive Least Squares**
RMS	**Root Mean Square**
SOF	**Statistical Overlap Factor**
STFT	**Short Time Fourier Transform**
TB	**Tuberculosis**
TEWA	**Time Expanded Waveform Analysis**
TN	**True Negative**
TP	**True Positive**
WHO	**World Health Organization**
XDR-TB	**Extensively Drug-Resistant Tuberculosis**

Subscripts

Freq	**Frequency**
healthy	**Having no tuberculosis origin**
Mag.	**Magnitude**
peak	**Maximum value**
Resp.	**Respiratory**
rms	**Root Mean Square**
unhealthy	**Having tuberculosis origin**

1 Introduction

1.1 Background

Tuberculosis (TB) is a common and potentially deadly infectious disease, most commonly affecting the lungs[1]. Over one third of the world's population is infected with the Tuberculosis bacterium and new infections are occurring at a rate of one per second (National Institute of Allergy and Infectious Deseases, 1996). Latent Tuberculosis infections[2] are most common but one in ten infected will develop the active strain, which if left untreated has a 50% chance of death. In 2005, 1.6 million people globally died of active Tuberculosis (Fauci, 2007) with South Africa being identified as the country with the highest TB rate, with over 300 cases per 100 000 people in 2004 as cited in Figure 1 (World Health Organisation, 2006). The rising number cases in developing countries have been connected to the fact that immunosuppressive drugs and the human immunodeficiency virus (HIV) compromise many citizens' immune systems (National Institute of Allergy and Infectious Deseases, 1996).

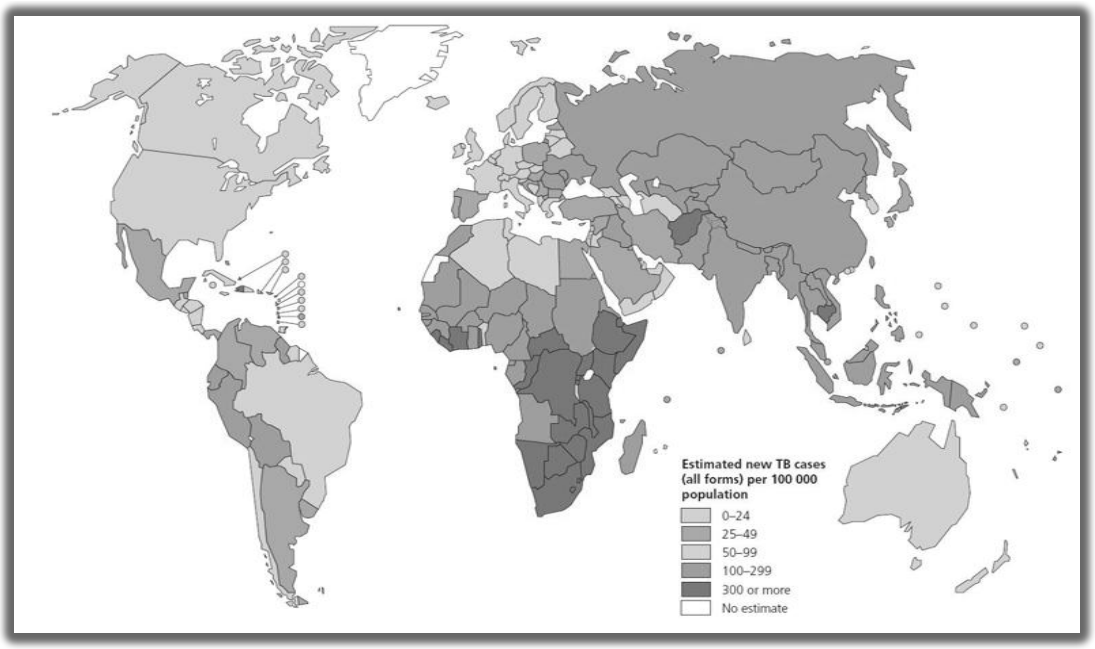

Figure 1: Estimated TB Incidences 2004 (World Health Oraganisation, 2006)

[1] Tuberculosis usually attaks the lungs (as pulomanry TB) but can also affect the central nervous system, circulatory system, genitourinary system, gastrointestinal system, bones joints and skin.
[2] The patient does not express any of the symptoms.

In 1993 the World Health Organization (WHO) declared TB a global emergency and launched a campaign called the "Stop TB strategy" (World Health Oraganisation, 2006). The strategy aims to halt and reverse the incidences of TB by 2015 and to have identified and treated 50 million people for TB. This includes an interest in the development of rapid and inexpensive diagnostic tests to assist diagnostics at the point of care. They also quote that "Rapid and cheap diagnosis will be particularly valuable in the developing world" (World Health Oraganisation, 2006).

Since pulmonary Tuberculosis damages the respiratory area, the sound properties of infected lungs differ to that of non-infected lungs. Therefore it would seem natural to assume that listening to the respiratory area (known as auscultation) is a viable and inexpensive diagnostic tool for pulmonary TB, but is often ruled out as a reliable technique due to the random position and severity of damage to the lungs. This is disappointing since auscultation remains one of the most common non-invasive diagnostic tools for assessing pulmonary health. Additionally, a common shortfall of the stethoscope is that it requires the personal and trained judgment of an experienced medical practitioner.

1.2 Motivation

Since the dawn of the computer era newly developed signal analysis techniques allow one to perform advanced signal analysis in the time, frequency and time-frequency domains. Such analysis techniques give more insight into the mechanical and mathematical components of sound signals resulting from respiration. With these new achievements in signal analysis a possibility to identify respiratory signal features that appear frequently in pulmonary tuberculosis patients exists. If such a characteristic property is found it may not only provide useful in the diagnostic field, but can also serve as a baseline for further research into whether the characteristic can serve as a surrogate marker[3]. This may prove valuable to medical practitioners when following the recovery of a patient undergoing treatment, since the current method of recovery tracking often involves repeated sputum testing, X-rays, blood testing and patient profiling (Blaivas, 2005).

Furthermore, the long-term establishment of a non-invasive and easily identifiable surrogate marker (or diagnostic tool) combined with modern internet communication, can pave the way for further capabilities. An advantage would be addressing a larger patient scope within rural areas through telemedicine (Earis and Cheetham, 2000).

[3] Any unique characteristic of a disease. This marker changes as the patient recovers and can be used to follow the recovery of the patient.

Current publications have indicated significant successes in using signal analysis, pattern recognition, mathematical modeling, neural networks and other methods to distinguish between adventitious and normal respiratory sounds. Resulting is an overwhelming volume of information motivating the application of electronic auscultation to identify adventitious sounds, or adventitious sounds common in respiratory diseases, and in turn diagnosis of the relevant diseases. However, to date no research in this field has focused on pulmonary TB, with no attempts since 1983 (Majumder and Chowdhury, 1981) were the basic observation of band pass filtered lung sound recordings on a storage oscilloscope indicated a distinct difference in wave shape between healthy and pulmonary TB infected lungs. This gap in the literature has left the question as to whether respiratory sounds originating from lungs infected with TB posses any unique features that are consistent for all cases of pulmonary TB.

With a call for new and cheap diagnostic techniques (World Health Organisation, 2006) it seems fair to encourage the investigation into adventitious lung sound properties as well as any other unique data than can be mathematically representative of the lung sound signals originating from pulmonary TB patients.

Consequently a hypothesis exists that the respiratory sounds associated with pulmonary tuberculosis front an opportunity to be fully investigated in fields beyond that of the mechanical stethoscope and human auditory judgment.

The origin of these respiratory sounds are thus set as originating from the lungs which include the specific organs of trachea, bronchi, bronchioles, and alveoli which make up part of the larger respiratory system[4].

1.3 Study Objectives

Therefore the aim of this project was to open a gateway towards the long term goal of improvement in the pulmonary TB diagnostic and treatment field by applying electronic and computer-aided sound analysis techniques to measure properties of lung sounds from pulmonary TB patients in an attempt to find any characteristic unique and consistent to respiratory sounds originating from TB infected lungs, and not present in healthy respiratory systems.

The research offered here is novel in three major categories:

- ❖ Evaluating the performance of an electronic respiratory recording device in third-world public clinics.

[4] The Anatomy of the respiratory system is discussed further in Section 2.1

- Analyzing recordings of respiratory sounds originating from a relatively difficult disease to diagnose.
- Investigate several the time domain, frequency domain, wheeze and crackle characteristics (instead of focusing on one characteristic) to identify which features correlate to TB with the highest degree.

1.4 Study Outline

To this point a discussion into the awareness of pulmonary tuberculosis, electronic auscultation research gaps and project objectives has been provided. In the chapters that follow, the necessary literature review and hypothesis execution is presented.

Chapter 2 contains a literature study into TB pathology and current methods of diagnosis and treatment. This is followed by detailed research into current methods of electronic lung sound analysis as well as electronic auscultation standards for both the medical and engineering industry, resulting in a study design that is presented in Chapter 3.

Chapter 4 proposes the hardware used to acquire the necessary data as well as the testing locations used for obtaining pulmonary tuberculosis participants, emphasizing certain aspects beneficial and harmful to the data acquisition stage of the project.

After the data acquisition phase, signal analysis techniques analyzed the data (Chapter 5) followed by data evaluation (Chapter 6) used to identify the most attractive signal features representing a difference between healthy and unhealthy data. Chapter 6 then also investigates the reliability of using the features in distinguishing between healthy and unhealthy data by measuring the accuracy of Neural Networks that use the signal features as inputs to categorize the data automatically into healthy and unhealthy groups.

Chapter 7 concludes the overall results of the project and suggests prospects towards potential future work.

2 Literature Review

2.1 Anatomy of Respiratory System and Origin of Lung Sounds

Since pulmonary tuberculosis affects the respiratory area, it is important to understand the basic physical environment of the common site of the disease, namely the respiratory system, as well as the origin of lung sounds as used by medical practitioners when conducting an auscultation procedure.

All the cells in the human body metabolically use oxygen (O_2) and discharge carbon dioxide (CO_2). The supply of this O_2 and removal of CO_2 is achieved by a mechanical process known as ventilation, which fills the respiratory organs with air (containing O_2) and expels CO_2. Additionally the respiratory system is also vital in maintaining body temperature and normal blood pH (A.D.A.M, 2008).

During the inhalation phase[5] of ventilation, air moves through the body by entering the nostrils, nasal cavity and the mouth. After moving through the trachea, the air moves into the left and right bronchi. These divide further into the bronchioles, which divide further into alveolar sacs, which contain alveoli (Figure 2 and Figure 3).

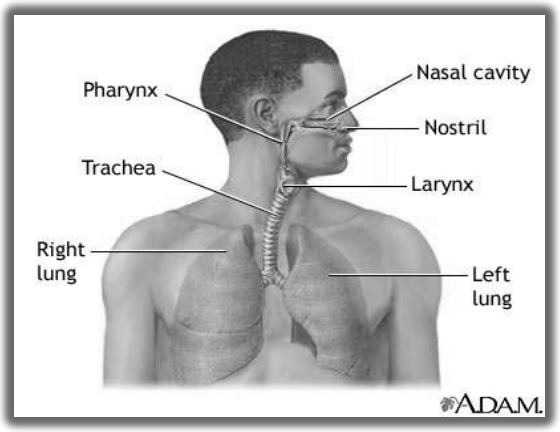

Figure 2: Organs of the Respiratory System (A.D.A.M, 2008)

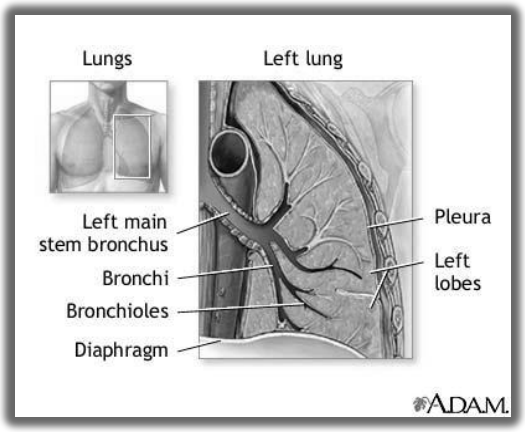

Figure 3: Detail of the Left Lung (A.D.A.M, 2008)

The bronchioles, alveolar sacs and alveoli make up the organ known as the lung and it is at the alveoli level where gaseous exchange takes place. This is also the unfortunate site of infection of pulmonary TB (A.D.A.M, 2008).

[5] Breathing into the lungs.

Gaseous exchange takes place as a result of maintaining homeostasis in the body. The alveolar walls are about 0.2 µm thick and permeable to gases. This allows O_2 to diffuse through the walls into the blood filled capillaries through the capillary wall (as shown in Figure 4 and Figure 5), as well as CO_2 to diffuse from the capillaries into the alveoli. This highlights the significant role the lungs play in gaseous exchange to the body (Farabee, 2001).

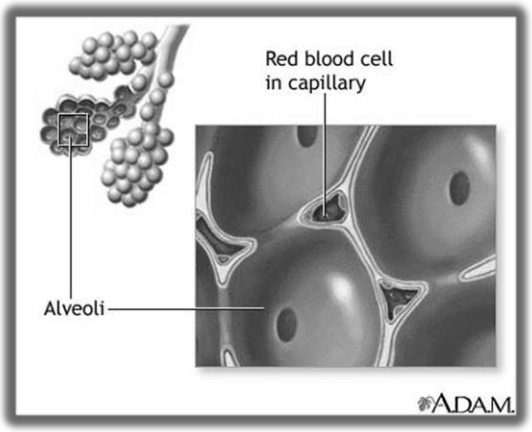

Figure 4: Alveoli and Capillaries

(A.D.A.M, 2008)

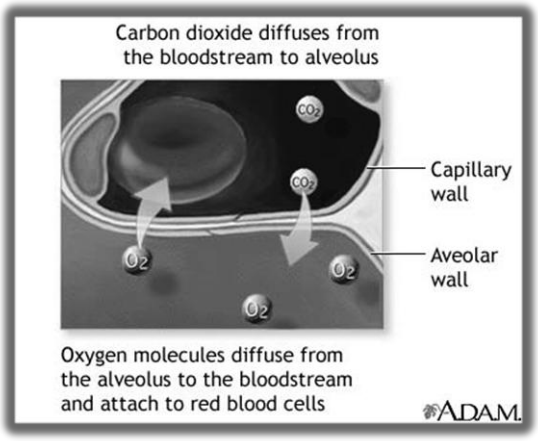

Figure 5: Gaseous Exchange

(A.D.A.M, 2008)

The lungs have a natural elasticity as they recoil from the expanded inhalation state. This causes air to flow out of the lungs until equilibrium is reached with respect to atmospheric pressure. This process of exhalation[6] is what removes CO_2 from the human body and completes the cycle for removing and supplying the relevant gases to the body (Farabee, 2001).

During inhalation and exhalation, certain lung sounds can be heard. Lung sounds are described as sounds that are generated by the movement of air as it travels through the bronchial tree. The fluctuations, vortexes shedding and oscillations of tissue are what allow one to hear the respiratory action, and is used by medical practitioners to assess respiratory health during auscultation. Thus, lung sounds can be classified in terms of sound measurements such as frequency and amplitude. When pulmonary diseases affect the shape and performance of lungs, differences in the respiratory sounds are often observed (Güler *et al.*, 2005).

[6] Expelling air out of the lungs.

2.2 Pathology of Pulmonary Tuberculosis

The following sections provide a closer look at pulmonary tuberculosis, including its pathology, symptoms, transmission and treatment.

2.2.1 Bacterial Species and Pathogenesis

The two primary mycobacteriums responsible for pulmonary TB[7] are *Mycobacterium tuberculosis* (MTB) and *Mycobacterium Bovis* (MTBV) and are slow growing aerobic bacteria that can withstand weak disinfectants and survive in an open air state for a few hours (Parish and Stoker, 1999).

Pulmonary TB infections begin when the micro bacteria reach the alveoli of the lungs and begin to replicate. Specialized white blood cells called Macrophages begin to surround the tuberculosis bacteria. If successful, the Macrophages ingest the bacteria or keep them sealed whereby a patient is said to have a latent form of pulmonary TB. However, the tuberculosis bacterium may use Macrophages to its advantage causing the white cells to clump together into a granuloma as shown in Figure 6 and Figure 7.

The bacteria multiply inside the granuloma, causing them to enlarge into noncancerous tumor-like nodules. The centers of these nodules often have a soft, crumbly, cheese-like consistency (MAYO Clinic Staff, 2006).

The destructed tissue and necrosis sites are replaced by tissue repair. Affected tissue is thus replaced by scarring, and open cavities fill with the white cheesy material which may also be coughed up causing further transmission (Grosset, 2003).

2.2.2 Symptoms

Symptoms of active pulmonary TB include the following (Blaivas, 2005):

- Minor cough.
- Fatigue.
- Unintentional weight loss.
- Coughing up blood.
- Phlegm producing cough.
- Fever and night sweats.
- Wheezing in breath sounds.[8]
- Chest pain.
- Breathing difficulty.

[7] Other microbacteriums include Mycrobacterium africanum, Mycrobacterium canetti and Microbacterium microti but these are less common.
[8] Wheezing is further discussed in Section 2.3.2.

- Crackles in breath after lung healing.[9]

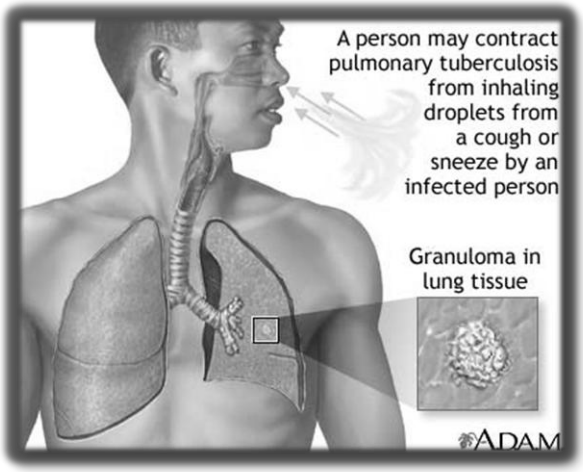

Figure 6: Granuloma in Lung Tissue (A.D.A.M, 2008)

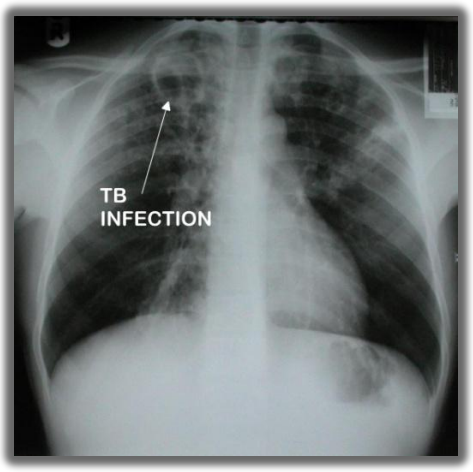

Figure 7: X-Ray Showing TB Infection

2.2.3 Transmission

The transmission of TB is advanced by the patient sneezing, coughing, speaking or spitting small aerosol sized droplets (Grosset, 2003). Many forms of TB are latent and transmission of the disease is only through the active strain of TB. However, an unaware and untreated person with active TB may infect between 10-15 people per year. This results in a high risk of new infections in third world areas where a high population density, limited isolation and weak immune systems (due to HIV) are prevalent (MAYO Clinic Staff, 2006).

2.2.4 Diagnosis

Diagnostic tests for pulmonary TB include (Blaivas, 2005):

- Chest X-ray. This is a medical image of the chest often observed for granuloma.
- Sputum cultures were samples of saliva are taken and analyzed for MTB.
- Tuberculin skin test. This is a test which yields a delayed hypersensitivity response to an injected purified protein derivative of the *M. tuberculosis* bacteria.

[9] Crackling as a symptom is further discussed in Section 2.3.2

- A medical procedure whereby a camera tube is inserted down the trachea in order to conduct a visual inspection of the trachea for granuloma known as bronchoscopy.
- Thoracentesis. A procedure removing of fluid from the pleura through a needle.
- Chest CAT scan (CT scan).
- Interferon (IFN) gamma blood test which searches for an immune response to proteins produced by M. tuberculosis.
- Microscopic-observation which is a new test used in developing countries which relies on sputum samples to detect the presence of TB bacteria.

All these procedures are combined in order to fully assess the presence of pulmonary TB. New diagnostic tools include the incorporation of deoxyribonucleic acid (DNA) diagnostics and Microscopic Observation Drug Susceptibility (MODS) (Moore *et al.*, 2006).

2.2.5 Treatment

Treatment includes the daily oral doses of anti-tubercular drugs for about six months. Many different forms of anti-tubercular drugs are available and a patient may have to try various types if their particular case is resistant to their current prescription (Fauci, 2007). Worse still, extended durations of treatment are often encountered when the patient has an Acquired Immune Deficiency Syndrome (AIDS) (Blaivas, 2005).

Treatment has to be completed, otherwise the TB bacteria may develop into a drug-resistant strain (Blaivas, 2005). Multidrug-resistant TB (MDR-TB) is any strain of TB that cannot be treated by isoniazid and rifampin (The British Society for Antimicrobial Chemotherapy, 2008). Extensive drug-resistant TB (XDR-TB) is the latest strain of TB at present and is resistant to the same treatments of MDR-TB (MAYO Clinic Staff, 2006).

Both MDR-TB and XDR-TB develop as a direct result of not completing the full treatment. This gives bacteria time to mutate to a level that can resist treatment with first-line TB drugs (The British Society for Antimicrobial Chemotherapy, 2008). MDR-TB can be treated but it requires at least 24 months of therapy with second-line medications (Ethnomed.org, 2005-2007) and even with treatment, many MDR-TB people may not survive (MAYO Clinic Staff, 2006).

2.3 Categories of Respiratory Sounds

So far the effects and seriousness of TB have been highlighted, along with the fact that pulmonary TB infects the respiratory area resulting in an altercation of respiratory sounds.

The following section provides a review of the terminology and an explanation of the physiological origin of respiratory sounds used by medical practitioners, also studied by many engineers in the electronic respiratory sound analysis field. These include the two main categories of *normal* and *adventitious* lung sounds.

2.3.1 Normal Lung Sounds

Breath sounds heard close to the chest can be described as "a distinct murmur corresponding to the flow of air into and out of air cells" (Sovijärvi *et al.*, 2000).

The lung itself cannot generate sound if pressure differences between the structures within the thorax or different lung volume levels do not exists. Breath sounds are probably generated by turbulence of the air at the level of lobar or segmental bronchi. In the smaller bronchi, the gas velocity decreases becoming less than the critical velocity to induce turbulence (and in turn sound). The airflow in smaller airways is therefore believed to be laminar and silent (Sovijärvi *et al.*, 2000).

Normal breath sounds generally have a soft acoustic character with the inspiratory phase being longer than the expiratory phase. This is in a ratio inspiration/expiration of about 2:1 during tidal breathing[10]. Expiration can be described as nearly silent. Breath sounds are also not uniform over the lung area and there are variations in sound intensity. At the base, the sound is less intense at the beginning of the inspiration and then gradually increases, and reaches it's maximum at about 50% of the vital capacity (Sovijärvi *et al.*, 2000).

2.3.2 Adventitious Lung Sounds

Adventitious lung sounds often indicate an abnormality in the lungs, such as an obstruction in the airway passages or a pulmonary disease. These adventitious lung sounds are classified into sub-categories in order to describe the nature of the adventitious sound. The two main groups of adventitious sounds are called *wheezes* and *crackles*. These are further divided into subsidiaries such as Coarse Crackles (CC), Fine Crackles (FC), stridors and rhonchus. Figure 8 illustrates where adventitious sounds, as well as their sub-categories, fall in the larger scope of lung and breath sounds, with the main adventitious sounds relevant to this project highlighted in grey.

[10] Normal breathing in and out.

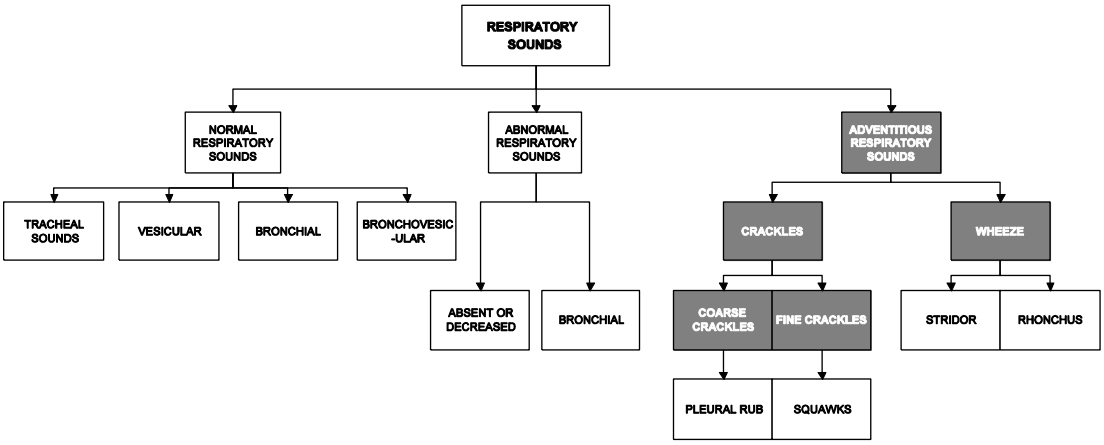

Figure 8: Structure of Respiratory Sounds

Origin of Crackles

Crackles are classified as discontinuous lung sounds. They are "explosive and transient in nature" (Sovijärvi *et al.*, 2000) and are frequent in respiratory diseases. Crackles seem to come from the acoustic energy released by pressure equalization or elastic stress due to the sudden opening of a restricted airway component (Sovijärvi *et al.*, 2000). This restriction may be due to increased elastic coil pressure around the alveoli (Sovijärvi *et al.*, 2000). They can therefore be identified as sudden peaks in acoustical energy, causing noticeable spikes of amplitude in the higher frequency bands. A further source of coarse crackles may be due to the air movement through sticky secretions in small airways (Hadjileontiadis, 2003) of which the acoustic nature can be temporary and lost when the patient coughs up phlegm.

Origin of Squawks

Squawks are classified as combination of musical, high-pitched wheezes and crackles. They appear in the latter half of inspiration, are mostly associated with FC (Hadjileontiadis, 2003), and known to originate from the oscillation of small airways after sudden opening (Sovijärvi *et al.*, 2000).

Origin of Pleural Rubs

Pleural rub is simply a brushing sound heard at a localized place on the chest wall. This pleural sound is most closely associated to CC as it is the effect of the thin membrane that wraps around the lung (visceral pleura) rubbing against each other.

The pleural rub can be heard simultaneous to the inhaling and exhaling of the patient (nursebob.com, 2007).

Origin of Wheezes

Wheezes are adventitious sinusoidal lung sounds that superimpose themselves onto the regular breathing sound waves. Wheeze sounds are audible over the mouth as well as the larynx and it should be noted that the measurement of wheezes across the chest wall is subject to damping, and hence the removal of sounds in specific frequency ranges is possible (Sovijärvi *et al.*, 2000).

Origin of Stridors

Stridors are believed to originate from a morphologic[11] or dynamic[12] obstruction of the larynx or trachea. This results in an exceptionally loud wheeze on inspiration (Sovijärvi *et al.*, 2000).

Origin of Rhonchus

Rhonchus has been defined as a low pitched wheeze which contains rapidly damping periodic waveforms and is shorter in duration compared to regular wheezes (Sovijärvi *et al.*, 2000).

2.4 Electronic Respiratory Analysis

An explanation of the origin of lung sounds was made apparent in Section 2.3. Section 2.4 deals with the mathematical measurements of respiratory sounds in the field of respiratory sound analysis.

2.4.1 Standardization of Electronic Respiratory Analysis

Since the field of respiratory lung sound analysis is still relatively new, there are no fixed guidelines and parameters for the acquisition, data storage and processing of lung sound recordings. A European Community (EC) project for Computerized Respiratory Sound Analysis (CORSA) was led by A.R.A. Sovijärvi, and focused seven European countries to develop guidelines for standardized recording and analysis of respiratory sounds (Piirilä and Sovijärvi, 1995).

The European respiratory review journal of 2000 presents the collaboration of Belgium, Britain, Finland, France, Germany, Italy and the Netherlands in order to

[11] Branch of biology dealing with the form and structure of organisms.
[12] The motion of respiration.

review over 1 672 research papers and set up guidelines aimed at curbing the variety of instruments, testing conditions and methods used by researchers around the world (Sovijärvi *et al.*, 2000). These standards are not compulsory but have been adapted and used extensively by researchers and engineers who conduct and publish research papers in the field of respiratory sound analysis.

Thus, this project also followed these guidelines as set in the ERS review of 2000. These guidelines offer a comprehensive outlook onto the different quantities for amplitude, pitch[13] and frequency of respiratory sound "waves" in order to classify them into their adventitious categories. (Sovijärvi *et al.*, 2000)

2.4.2 Acoustic Nature of Normal and Adventitious Respiratory Sounds

Signal analysis can occur across three main categories, namely the time domain, frequency domain and domains of mathematical and statistical modeling. Each of these categories is interchangeable and has further individual mathematical applications, as shown in Figure 9.

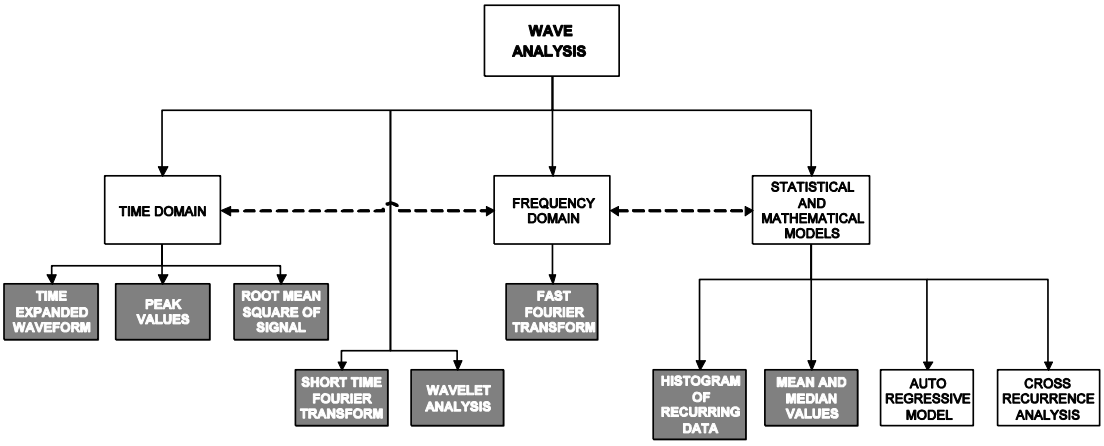

Figure 9: Domains of Signal Analysis

Some of the most common methods of displaying time domain data are using Time Expanded Wave Analysis (TEWA) and phonograms. Representations in the frequency domain include the Fast Fourier Transforms (FFT), showing the frequency content, as well as the Short Time Fourier Transforms (STFT) showing the FFT in small windows of time[14].

[13] The property of a sound or musical tone measured by its perceived frequency.
[14] A detailed explanation into each of these categories is provided in Chapter 5.

The following section highlights the uniqueness of displaying respiratory sounds in both the time and frequency domains[15].

Representation of Normal Respiratory Sounds

Figure 10 illustrates a normal respiratory sound and shows the signal amplitude varying with time. Respiratory sounds often do not show symmetry around any axis (irregular) and no symmetry at regular time intervals (non-stationary). Therefore, a normal breath sound can be modeled as Gaussian white noise (Sankur *et al.*, 1994). With the non-stationary characteristic, an argument can be made to use time windows small enough to assume a stationary wave (Charbonneau *et al.*, 2000) or the use of non-stationary chaotic wave analysis techniques (Conte *et al.*, 2004 and Reyes *et al.*, 2008).

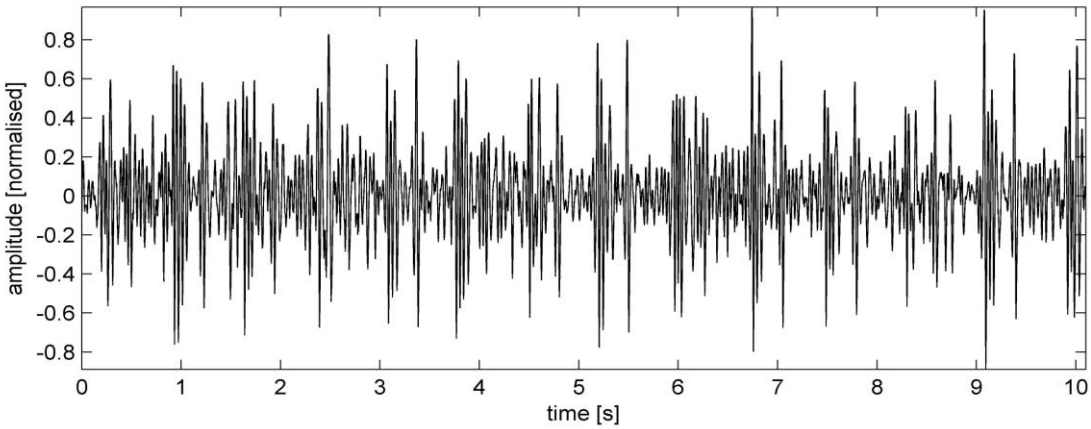

Figure 10: Wave Signal of Normal Respiration

The FFT in Figure 11 shows that the normal respiratory sound has most of its energy in the less than 50 Hz range. This is because most of the acoustical energy is coming from the heartbeat, muscle sounds and pleural rub that should also be filtered correctly prior to analyzing the respiratory sound (Yeginer and Kahya, 2007). It can be seen that relatively little acoustical energy exists beyond 250 Hz (Sovijärvi *et al.*, 2000), since less energy is contributed by each frequency band. If there were any adventitious sounds, there would appear a distinct alteration in the FFT spectrum since the adventitious sounds have higher amplitudes in one of the upper frequency bands. (Sovijärvi *et al.*, 2000)

[15] Detailed description of signal measurements is in Chapter 5.

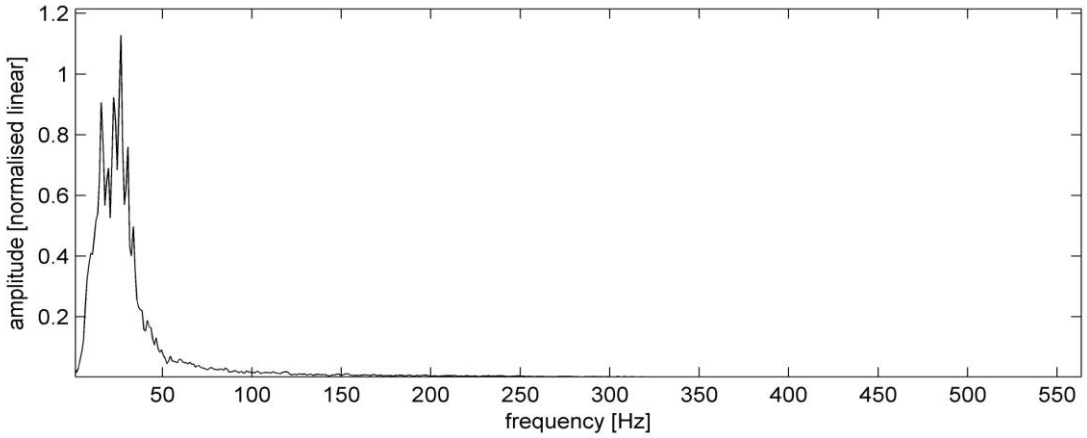

Figure 11: Fourier Transform of Normal Respiration

Figure 12 is a STFT (adapted FFT since frequency components change over time) that indicates that in the frequency spectrum there exists a few changes during the respiratory cycle with highest intensity (color) for a frequency maintained less than 100 Hz (unfiltered heart beat). There are a few indications of increased intensity in the spectrogram less than 200 Hz and therefore no indications of adventitious sounds (note that darker colors indicate higher intensity).

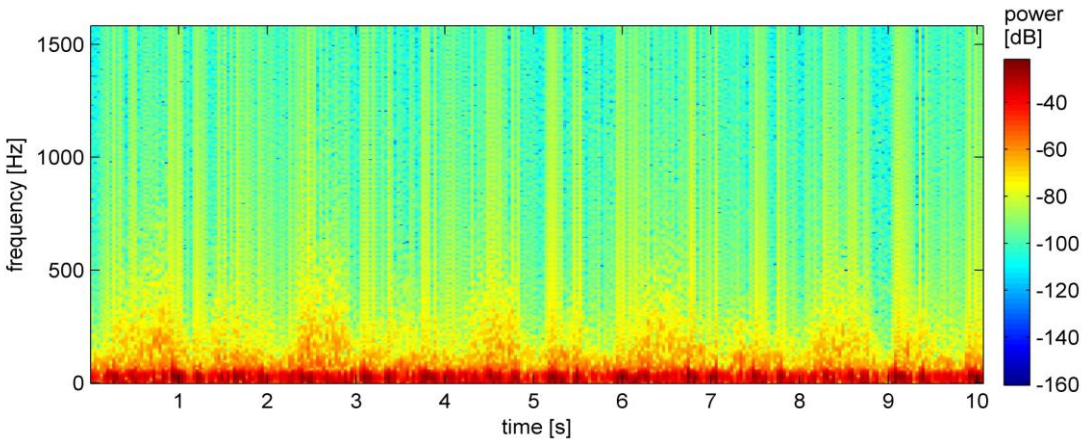

Figure 12: Short Time Fourier of Normal Respiration

Representation of Crackles

An example of a wave graph with identified crackle peaks is shown in Figure 13, as well as its FFT in Figure 14, showing a distinctive rise in sound intensity at higher frequency bands to that of the normal respiratory sounds.

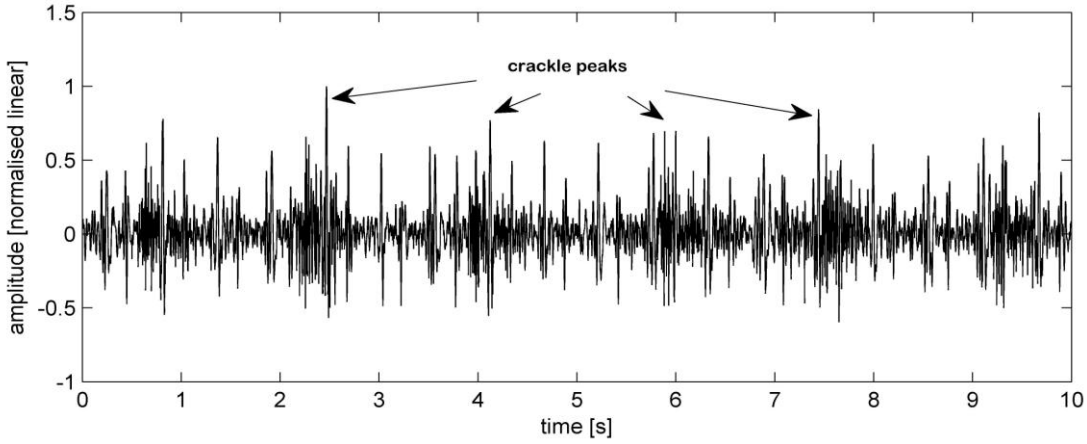

Figure 13: Wave Signal of Crackle Respiration

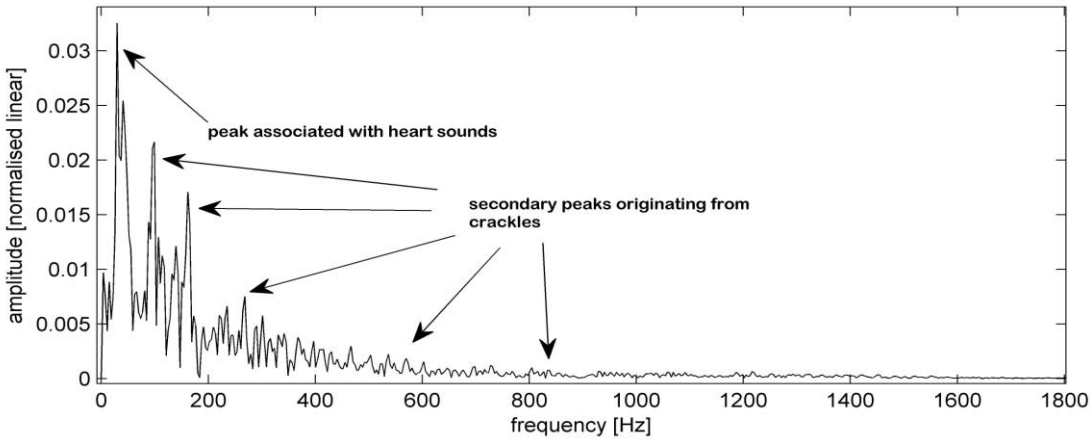

Figure 14: Fourier Transform of Crackle Respiration

In general, the analysis of crackles may be assigned to TEWA, spectral analysis and Auto-Regressive (AR) models. A crackle in TEWA has a very distinctive wave described by a sudden short deflection, followed by higher deflections. The quantative analysis of crackles is therefore achieved by calculating the start and end point of crackles as a percentage of the respiratory cycle from the start of inspiration to the end of expiration. Since recordings from a single patient will seldom be perfectly identical during a recording session, it is recommended that the mean values from three to five recordings be used (Charbonneau *et al.*, 2000).

To characterize the waveforms of crackles in TEWA the following measurements are recommended (Charbonneau *et al.*, 2000):

- Initial deflection width (IDW): the duration of the fist deflection of the crackle.
- Two-cycle duration (2CD): duration of the first two deflections of the crackle.
- Largest deflection width (LDW): width of the largest deflection of the crackle.

An example of these measurements is also illustrated in Figure 15 where a low value for each of these measurements is taken as FC and higher values are taken as CC, as listed in Table 1 (Charbonneau *et al.*, 2000).

Table 1: Measurements of Fine and Coarse Crackles

Crackle Sound	Measurement of 2CD
Fine Crackles	< 10 ms
Coarse Crackles	> 10 ms

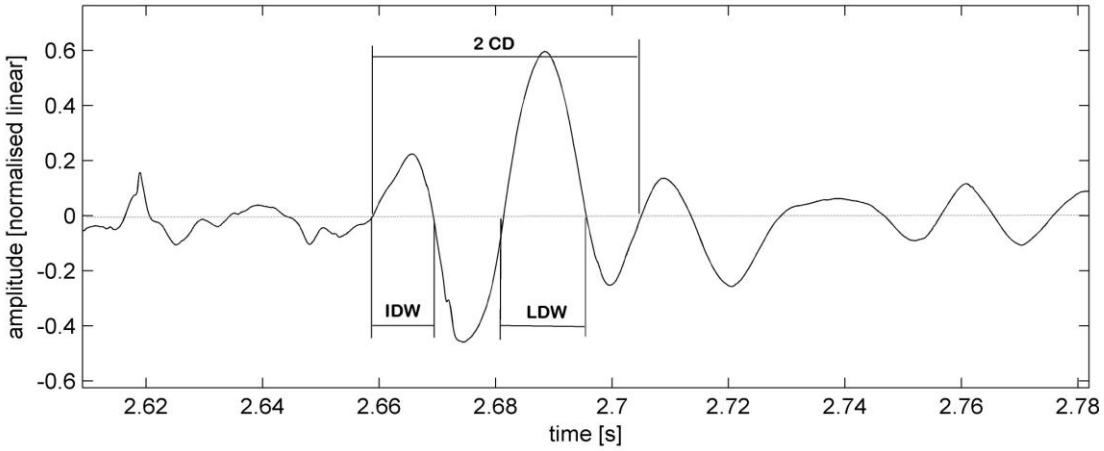

Figure 15: Time Expanded Waveform Measurements for Crackles

A STFT indicating higher sound intensity across higher frequency bands is a common indicator of crackles (Figure 16).

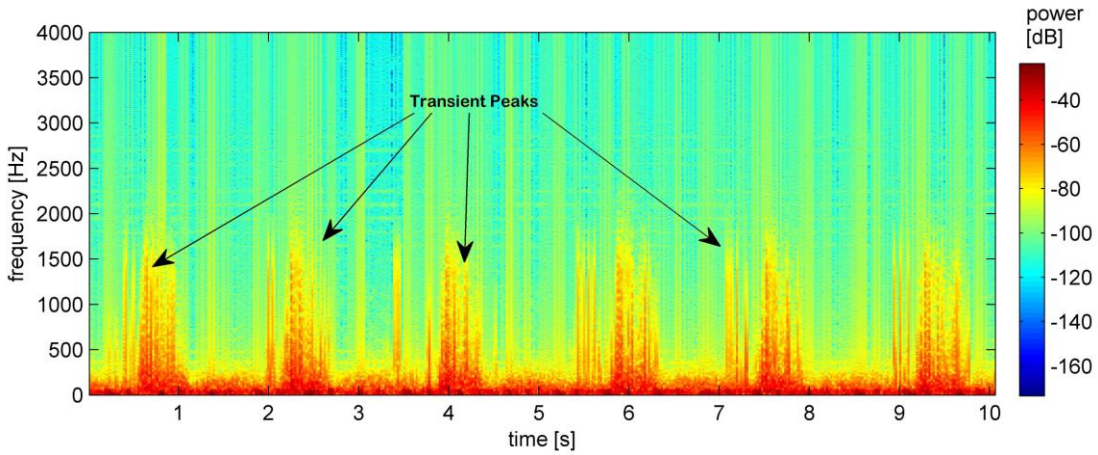

Figure 16: Short Time Fourier for Crackle Respiration

Motivations exist that since crackles occur across such a wide frequency range (100 – 2000 Hz) it is of less importance to conduct a FFT on the signal (Cheetham *et al.*, 2000). However if windowed samples are taken across various time steps in the signal, a window lying directly over a crackle waveform can yield a noticeable increase in amplitude for a given frequency band, as indicated in Figure 14.

Representation of Wheezes

Wheezes are pseudo-periodic signals and are characterized mainly by their duration and pitch. Literature reports a wide range of frequencies as summarized in a table of prior approaches by (Abhishek and Jithendra, 2008)Table 2. Table 2 illustrates a use of frequencies ranging from 150 Hz to as high as 1000 Hz. According Sovijärvi (2000), the American Thoracic society defines a wheeze to be continuous if the duration is longer than 250 ms however new CORSA guidelines define the duration to be longer than 100 ms and claim wheezes pushing higher frequencies (above 500 Hz) are only audible over the trachea. Generally the dominant frequency of a wheeze was thus fixed to 80 - 100 Hz and duration less than 80 – 100 ms duration (Sovijärvi *et al.*, 2000). As for the maximum duration of a wheeze, Taplidou (2007) claim duration to be less than 2 500 ms (Taplidou and Hadjileontiadis, 2007) reasoning this to be the maximum inspiratory or expiratory duration of a breath cycle at tidal breathing.

Table 2: Prior Approaches to Wheeze Analysis

Prior Approach	Frequency range	Wheeze Duration used
Time-Frequency Detection and Analysis of Wheezes. During Forced Exhalation	150 – 800 Hz	> 80 msec

Respiratory Health Screening using Pulmonary Function Tests and Lung Sound Analysis	200 & 500 Hz	-
When a "Wheeze" is not a Wheeze: Acoustic. Analysis of Breath Sounds in Infants	125 – 375 Hz	100 msec
WED: An Efficient Wheezing-Episode Detector. Based on Breath Sounds Spectrogram Analysis	100 – 800 Hz	>100 msec
Automated Breath Sound Analysis	100 – 1300 Hz	-
Lung Sound Analysis for Continuous Evaluation of Airflow Obstruction in Asthma	150 – 1000 Hz	250 msec
Lung Sound Recognition Using Model Theory Based. Feature Selection and Fusion	400 Hz	>250 msec

Figure 17, Figure 18 and Figure 19 illustrate a wheeze segment, its FFT (over small windows of time) and the STFT of the entire wheeze recording, respectively.

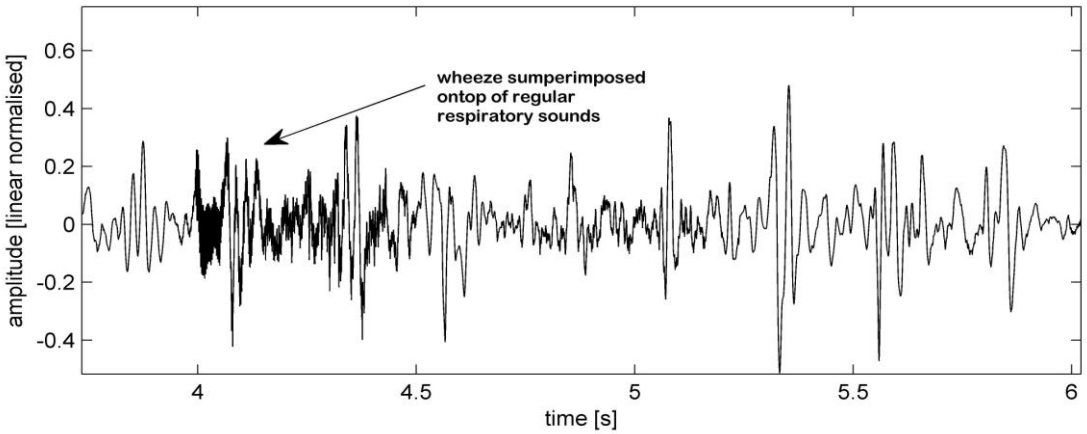

Figure 17: Wave Signal of Wheeze Respiration

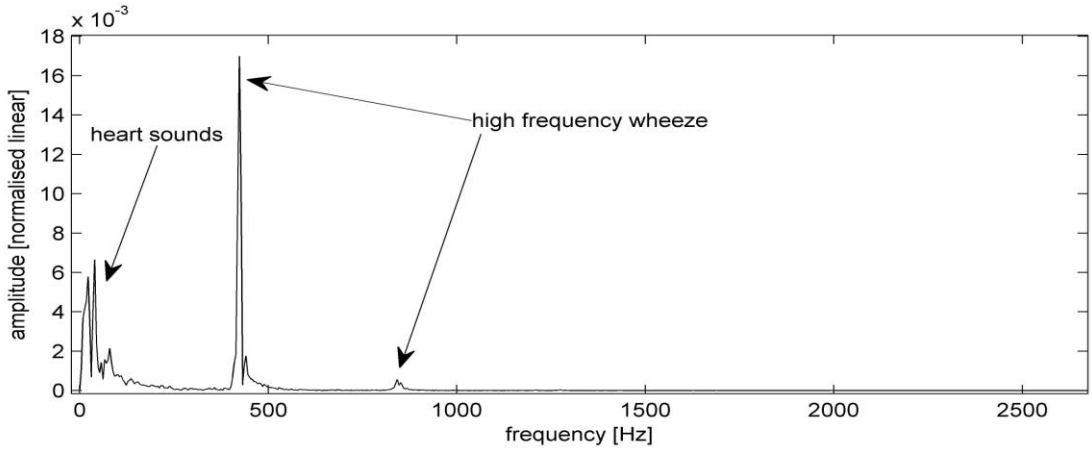

Figure 18: Fourier Plot of Wheeze Respiration

Figure 19 shows a clear rise in amplitude for a frequency range of 200 – 1000 Hz. These peaks are indicative of adventitious wheezing sounds when compared to the STFT of a normal respiratory sound. The arrows in Figure 19 indicate a fixed frequency range with fixed intensity over a period of time, which illustrates the periodic component of wheezes that superimpose on the respiratory sound as in Figure 17.

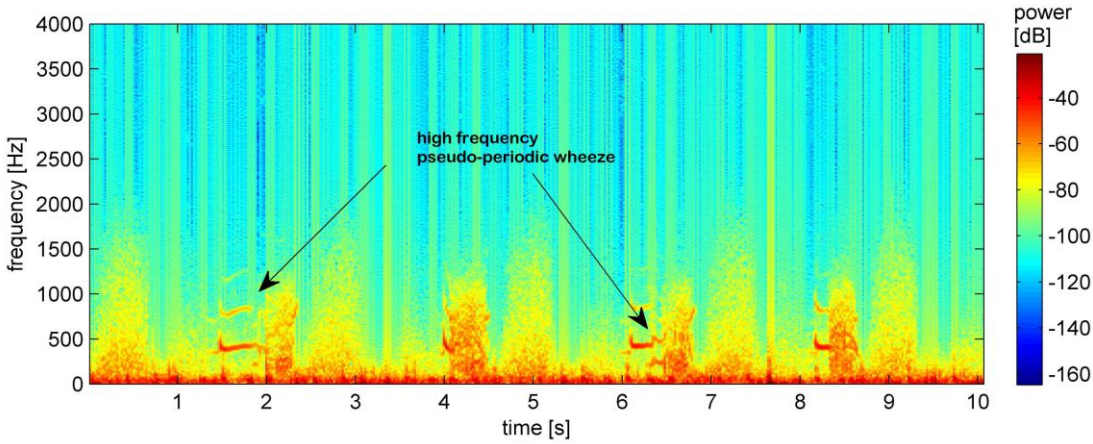

Figure 19: Short Time Fourier Plot of Wheeze Respiration

The methods applied to wheeze analysis are generally periodograms, FFTs and STFTs. Such methods allow for identification of the predominant frequency as well as the wheeze duration and timing. Importantly, the duration of a pseudo-periodic

sound superimposed on a breath sound should lie between 100 ms and 2.5 s (Sovijärvi *et al.*, 2000). A histogram of wheeze episodes (Jin *et al.*, 2008) and the mean frequency of multiple wheeze episodes are also relevant in the field of respiratory analysis (Sovijärvi *et al.*, 2000).

2.4.3 Relevance of Wave Analysis to Pulmonary Tuberculosis

Interestingly, it is already known that patients with lung fibrosis (also a result of lung healing found in pulmonary TB) show repeatable crackles in breathing cycles with waveforms similar to those indicated in Figure 13.

Figure 20 indicates the wave signal of an actual recording (PixSoft Inc, 2007) of a 16-year old patient diagnosed with TB over the left lung. The current auscultation syndrome is crackling and can be noted in both Figure 20 and the STFT spectrogram in Figure 21.

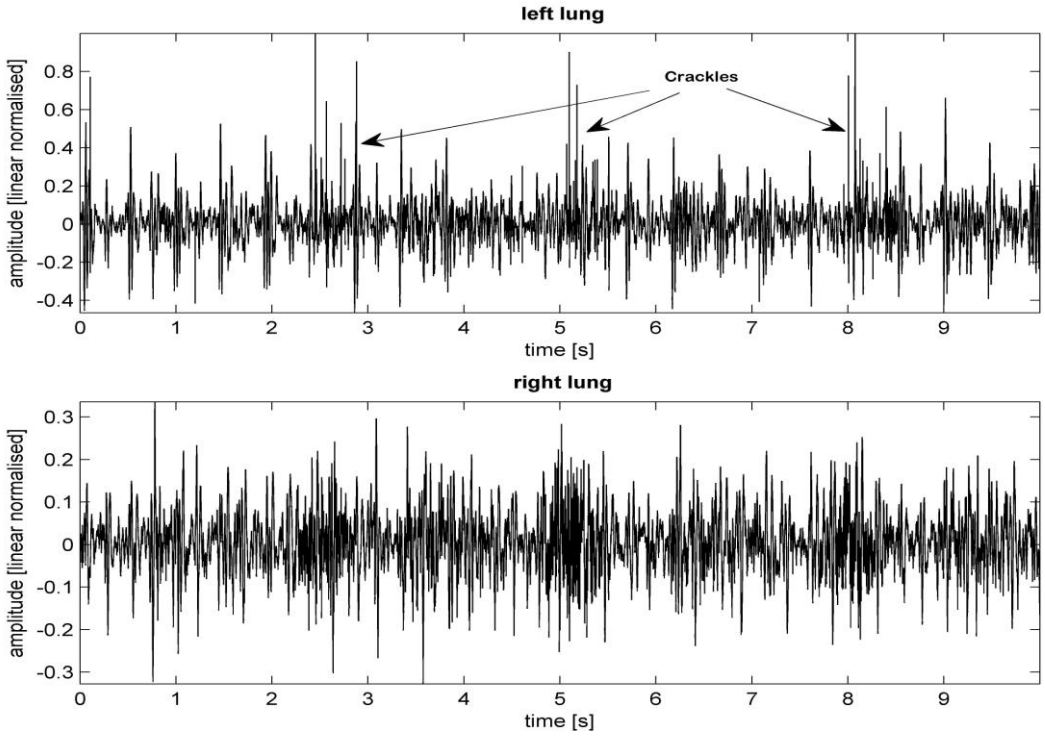

Figure 20: Wave Signal of Tuberculosis Patient

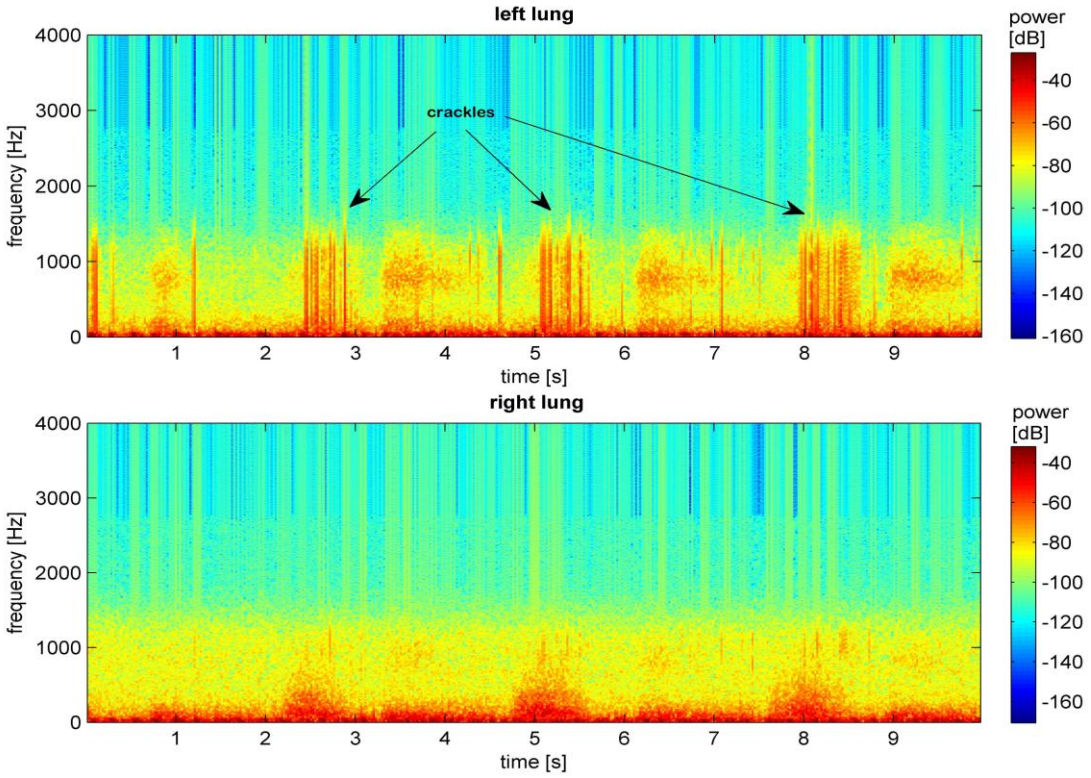

Figure 21: Short Time Plot of Tuberculosis Patient

From highlighting a possible connection between adventitious sounds and TB patients, the following chapters describe the planning, execution and outcomes of recording, extracting and investigating various signal measurements of unhealthy and healthy respiratory signals alike.

3 Study Design to meet Objectives

Given the introduction, objectives and literature review into the seriousness of pulmonary TB as well advances in electronic respiratory analysis, the following study design was drawn up to meet the objectives (as discussed in Chapter 1). These are divided into four main milestones namely:

- Acquisition of the data (Chapter 4): This included identifying various transducers capable of capturing and recording respiratory sounds. This was followed by an evaluation to determine the best device and equipment to offer reliable recordings while offering comfort for the participant being tested. There after the task to record at least 25 participants who have been diagnosed with pulmonary Tuberculosis and are currently undergoing treatment and 25 participants that have been examined and classified as healthy and having no respiratory disease.
- Analysis of the Data (Chapter 5): This required the analysis of the recorded respiratory sounds with respect to time, frequency and basic wheeze and crackles parameters and extracts predefined measurements describing these parameters or sub-parameters.
- Evaluation of the Data (Chapter 6): Group all the extracted measurements and calculate a Statistical Overlap Factor (SOF) to indicate the degree of separation of the means (and thus uniqueness) of the signal feature belonging to healthy or TB participants.
- Reliability of Data (Chapter 6): Train a Neural Network (NN) with the highest ranking extracted measurements, as determined by the SOF, in an attempt to achieve a semi-automated diagnosis of the recordings.

This study design in outlined in Figure 22.

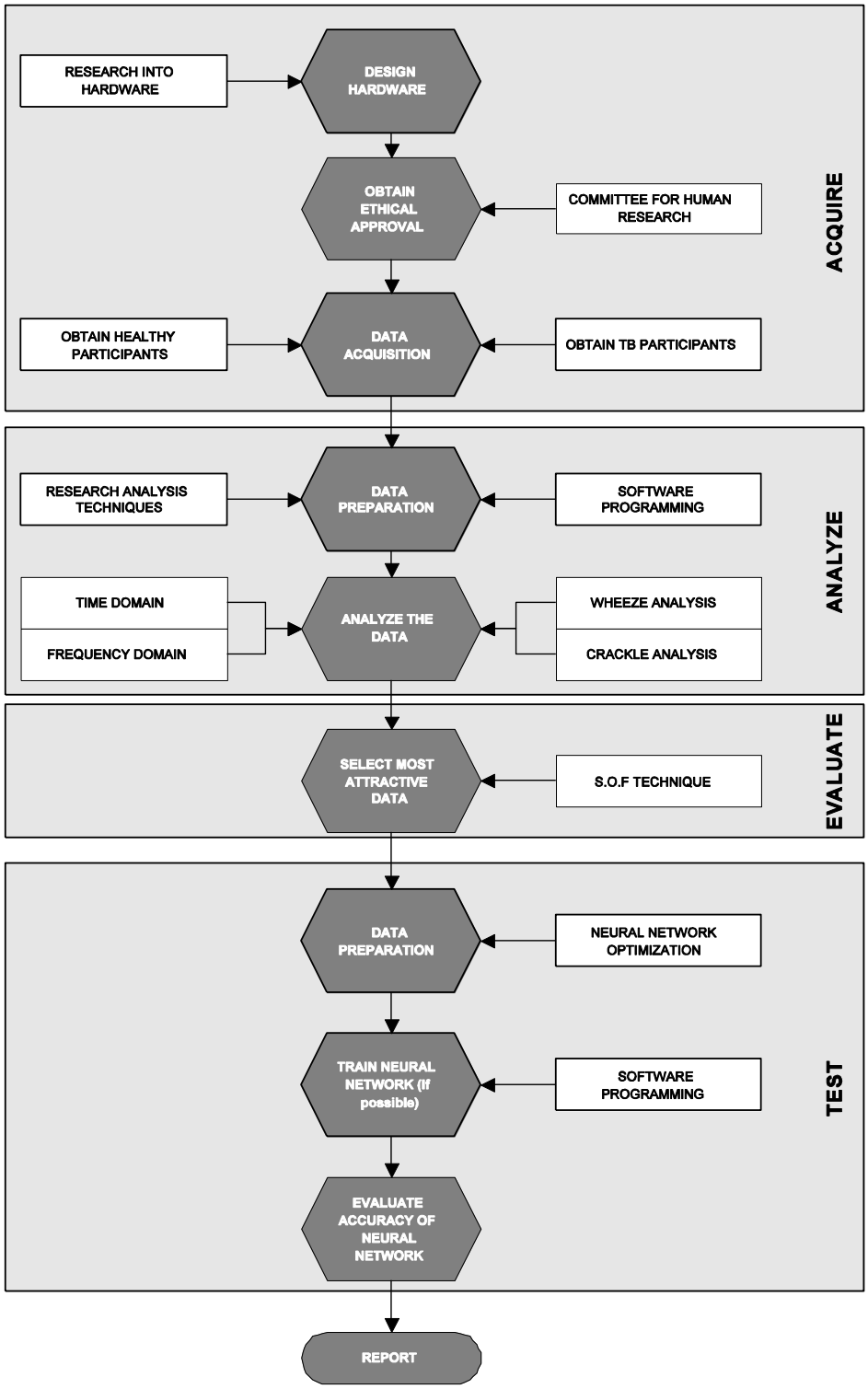

Figure 22: Study Design

4 Acquisition of Data

Data acquisition consisted of identifying the correct hardware and testing locations to obtain the recordings.

Commercial devices that exist for respiratory recordings include an auscultation "pad" supplied by © Stethographics, Inc. called the STG16 ™. The STG16 ™ in Figure 23 consists of multiple electronic stethoscopes from electret microphones embedded into a foam cushion that the participant lies on. The personal computer then uses software supplied by Stethographics and can display normal and adventitious lung sounds (Stethographics, Inc., 2007).

In competition to the STG16 is the Deep Breeze VRIxp System, depicted in Figure 24. The system uses forty active piezoelectric contact sensors and two inactive contact sensors, along with vacuum coupling to the patient's chest to record respiratory sounds (Deep Breeze Ltd., 2008).

Figure 23: Stethographics STG System (Stethographics, Inc., 2007)

Figure 24: Deep Breeze VRIxp System (Deep Breeze Ltd., 2008)

Using information on transducer performance and coupling recommendations (Kraman *et al.*, 2006), a personal recording device was designed and manufactured at the University of Stellenbosch (South Africa) specifically for the purpose of this project. This maintained testing the performance of a low-cost diagnostic device as well as to predetermine the viability of investing TB respiratory sounds before purchasing a commercial device.

4.1 Hardware Setup

The final hardware setup included an HP nx6110 Business notebook, an IOtech® ZonicBook Medallion series analog to digital (A/D) converter and the custom designed seven-channel electronic stethoscope system. The complete system is shown in Figure 25.

The seven-channel acquisition box consisted of seven Panasonic® Omni-directional Back Electret Condenser Microphone WM 61A Cartridges with a signal–to–noise Ratio of 62 dB and flat frequency response of 20 – 20 000 Hz as recommended by Vannuccini *et al.* (2006). The eighth channel of the ZonicBook acquired respiratory inhaling and exhaling movement using a Pneumotrace II piezo-electric belt (Figure 26).

Figure 25: Equipment Used for Data Acquisition

Figure 26: Pneumotrace II Respiratory Strap

The Microphones (Figure 27 and Figure 28) where housed in plastic conical shaped couplers, were un-vented (Vannuccini *et al.*, 2000), with capturing diameter of 30 mm and conical depth 5 mm as advised by Kraman *et al.* (2006). Development and machining was performed in-house at the University of Stellenbosch, South Africa.

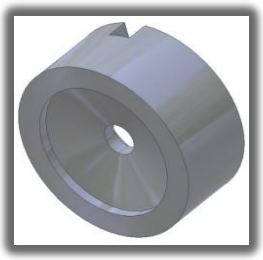

Figure 27: Stethoscope Housing Front View

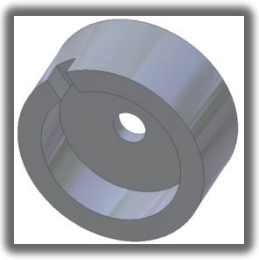

Figure 28: Stethoscope Housing Rear view

The signal for each WM 61A microphone was offset by 2.5 V with minimum and maximum voltage limits at 0 V and 5 V respectively (the supply voltage of the system). Additionally, the signal was amplified with gain of 30 by a Burr Brown OPA343 single-supply, rail-to-rail operational amplifier (Table 3). This is prior to transmission of the signal through a shielded cable to a second stage amplification by Burr Brown OPA4343 operational amplifiers. After the second stage amplifier the signal was sent through a shielded cable and a BNC plug connection to individual ports of the IOtech ZonicBook for digitization. This is illustrated in Figure 29.

Table 3: Stethoscope and Amplification per Microphone

Stethoscope Specifications	
Shape	Conical unvented
Diameter	30 mm
Depth	5 mm
Amplification Specifications	
Chip type	Burr-Brown OPA343
Offset	2.5 V
Max voltage	5 V
Total Gain	300 (30 and 10)

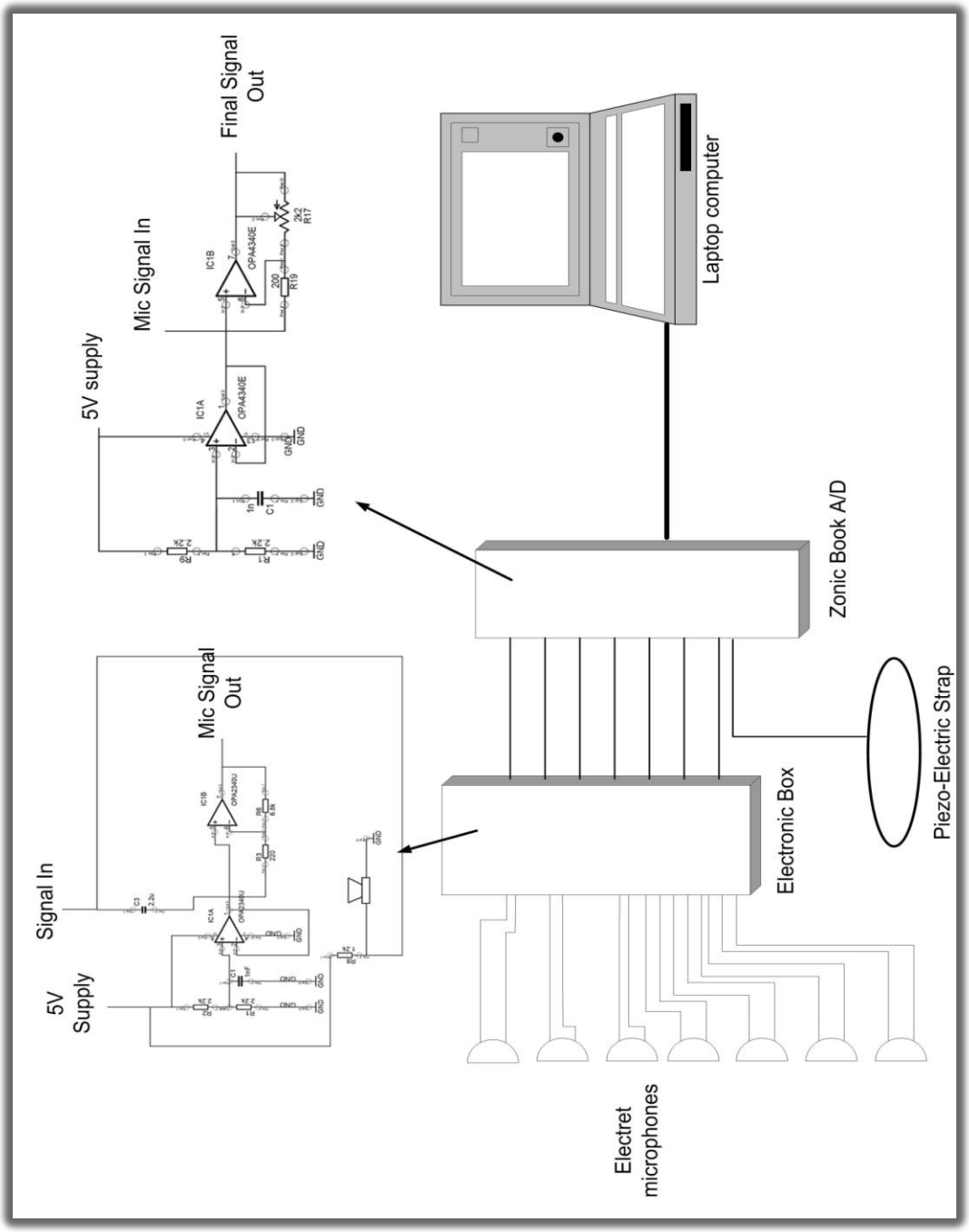

Figure 29: Hardware System

All electronics, printed circuit boards and electronic stethoscopes were designed and manufactured in-house at the University of Stellenbosch and are presented in more detail in Appendix B and Appendix C.

4.2 Testing Locations

Application for ethical approval, submitted to the Committee for Human Research (CHR) at the Faculty of health sciences of Stellenbosch University, included the necessary application forms, copies of patient informed consent forms, protocol reports and project proposals.

Meetings conducted with various medical practitioners from the faculty of health sciences respiratory research unit at Tygerberg Hospital (South Africa) recruited Dr. Andreas Diacon as a medical supervisor for the recording of pulmonary TB participants. A clinical drug trial taking place in Cape Town (South Africa) presented the necessary recording opportunities of TB participants.

The recording of patients on the trial incorporated the following advantages:

- Patients on the trial would have already met existing *inclusion* and *exclusion* criteria for the drug trial which guaranteed the patient of being infected with pulmonary TB and not other closely related pulmonary diseases[16].
- Patients had to return to their local clinics on a weekly basis which allowed for any re-recording of patients if the previous recording was not successful.
- Most of the patients would be starting treatment and therefore recordings would have the same infection status, namely that of untreated TB.

Recording commenced after the granting of ethical approval in February 2008 designated to three clinics around Cape Town. These clinics included:

- Mfuleni community clinic situated in the Mfuleni informal settlement outside Cape Town (Figure 30).
- Langa community clinic situated in Langa informal settlement in Cape Town (Figure 31).
- Chapel community clinic situated in the central area of Cape Town (Figure 32).

[16] Inclusion and Exclusion criteria for this trial are confidential

Figure 30: Mfuleni Community Clinic

Figure 31: Langa Community Clinic

Figure 32: Chapel Street Community Clinic

Figure 33: BERG Lab, Stellenbosch

The second floor laboratory of the Biomedical Engineering Research Group (BERG) at Stellenbosch University, South Africa (Figure 33) served as the location for testing healthy participants.

4.3 Signal Acquisition

The following section describes the attachment and recording procedure used to obtain the respiratory recordings of both the healthy and TB participants.

4.3.1 Stethoscope Placement

Signal acquisition included the fixture of the seven electronic stethoscopes and real time recording of the respiratory sounds from the healthy and TB participants' chest.

A meeting conducted in January 2008 with Dr. Diacon determined the seven microphones would cover the posterior and anterior chest in the most common locations of pulmonary TB infection. These are shown in Figure 34, illustrating microphones in the following locations:

- One electronic stethoscope over the trachea. (Figure 34 Position 1)
- One electronic stethoscope above the clavicle. (Figure 34 Position 2)
- One electronic stethoscope below the clavicle on the anterior chest. (Figure 34 Position 3)
- One electronic stethoscope on the lateral side between the 2nd and 4th intercostals space. (Figure 34 Position 4)
- Three electronic stethoscopes down the posterior chest along the Para-vertebral line. (Figure 34 Position 5,6 and7)

After being introduced to the nature of the project and a full explanation of the non-invasive recording procedure, persons interested were given the free choice of participation. This included all participants signing an informed consent form confirming the full understanding of the nature of the research and answering of any questions by the investigator. The informed consent form also indicated that the testing procedures were done according to international ethical testing standards as by the declaration of Helsinki compiled and reviewed by the World Medical Association (World Medical Association General Assembly, 2004).

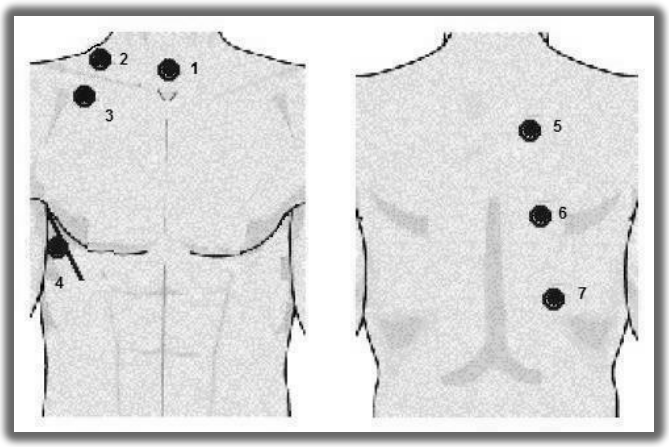

Figure 34: Microphone Placements for a Single Recording (Right Lung)

Being allowed to breathe with as little respiratory constriction as possible eliminated the use of tight or heavy jackets to house the microphones. Instead, thin double-sided adhesive tape (Earis and Cheetham, 2000) was used to attach the electronic stethoscopes to the skin as shown in Figure 35 and Figure 36.

Figure 35: Recording of Male TB Participant

Figure 36: Recording of Female TB Participant

4.3.2 Respiratory Recording Procedure

The recording procedure required participants to be seated in a chair in the upright position with all seven microphones and piezo-elastic strap attached.

The following respiratory maneuvers were then used during testing (Rossi *et al.*, 2000) :

- Five respiratory cycles recorded at tidal breathing.
- Three or four slow vital capacity maneuvers.

The procedure was repeated three times after which the stethoscopes were removed and placed over the adjacent lung.

TB recordings were subject to surgical masks and latex cloves being worn as well as all equipment being sterilized with appropriate antibacterial cleaners after completing recording sessions.

4.3.3 Environmental Conditions and Noise

Given the variability of geographical recording locations, environmental noise posed a constant risk to the quality of the recordings. Generally two types of noise exist as a threat to a respiratory recording. These were:

- Environmental noise: including traffic, people talking, doors slamming, nearby construction, radios playing and electronic disturbance in the form of tube lights, fans or cellular waves (Rossi *et al.*, 2000).
- Non respiratory and body sounds: This includes chest movement, heart beats, stomach and other organ noises, joint movement and pleural rubs (Rossi *et al.*, 2000).

Recording specifications of background noise below 45 dB (A) (Rossi *et al.*, 2000) were easier to maintain in the BERG lab during healthy recordings than that of TB recordings in public clinics. However, certain measures and arguments were adapted to minimize the background noise influence in the research. These included:

- If in future such a respiratory device is used as a viable diagnostic tool, its largest implementation would be out of noise-controlled environments since the largest patient scope with pulmonary TB exists in rural areas at community clinics.
- Originally the design of the hardware was for noise-controlled environments not realizing the possibility of uncontrolled noise recording environments. The device thus lacked the correct real-time noise cancellation.
- At all locations the investigator used a separate room reducing environmental noise to an extent.
- The use of three recordings per lung at four different geographical locations results in four different environmental noise profiles adding variability to the noise profile while maintaining any unique measurement to the respiratory sound.
- The electronic design contained appropriate ground connections and shielded cable, to minimize electronic interference.
- The electronic stethoscopes where padded with foam at the back to minimize the influence of environmental noise on the rear of the microphones.

In addition to the above-mentioned conditions adequate lighting, ventilation and temperature conditions provided comfort for the participant (Rossi *et al.*, 2000).

4.3.4 Digitization

Table 4 lists the common bandwidths used when investigating respiratory sounds (Vannuccini *et al.*, 2000).

Table 4: Common Bandwidths for Recording Respiratory Sounds

Respiratory Sound	Location: Trachea		Location: Chest	
	Lower Freq	*Upper Freq*	*Lower Freq*	*Upper Freq*
Normal Resp. Sounds	60-100 Hz	4000 Hz	60-100 Hz	2 000 Hz
Adventitious Sounds			60-100 Hz	6 000 Hz

Initially a sampling rate of 12 000 Hz was used for digitization as required by Table 4 to avoid aliasing frequencies[17]. However computer storage space became limited for such a high sampling rate over eight channels simultaneously. Table 6, showing the frequency bandwidths for adventitious sounds permitted the implementation of a lower sampling rate of 10 250 Hz. Subsequently re-sampling by software at 6 000 Hz maintained the nyquist frequency to a final analysis bandwidth of 60 – 3 000 Hz (Table 6) (Pasterkamp *et al.*, 1997).

Table 5: Common Bandwidths used in Respiratory Analysis

Respiratory Sound	Frequency Range	Acoustic Duration
Normal Sounds		
Over Lungs	100 – 1000 Hz	
Over Trachea	100 – 3000 Hz	
Adventitious Sounds		
Wheeze	100 – 1000 Hz	Typically 80 ms
Rhonchus	< 300 Hz	Typically 100 ms
Crackle		Typically < 20 ms

Table 6: Sampling Parameters Used

Bandwidth of Analysis	Analogue to Digital sampling	Digital to Digital re-sampling
60 – 3000 Hz	10 250 Hz	6000 Hz

[17] Refer to Appendix D for a definition of aliasing frequencies.

4.3.5 Filtering

High Pass and Low Pass Filtering

Two forms of filtering exist namely:

- Low-pass filtering (LPF): with a cutoff frequency in the upper frequency range to avoid aliasing.
- High-pass filtering (HPF): with a cutoff frequency in the lower frequency range in order to remove low level frequencies such as heart sounds and muscle sounds.

The result is a frequency band pass range in order to successfully study the respiratory sounds of which the parameters are illustrated in Table 7, with HPF stop band set at limits where heart, muscle and pleural sounds were deemed negligible yet still near to the frequency range for the start of adventitious sounds. Roll-off filter parameters were set according to literature research (Vannuccini *et al.*, 2000).

Table 7: Frequency Bandwidth Parameters

Filter Type	Stop Band	Roll Off
High Pass	150 – 200 Hz	18 dB Octave^{-1}
Low Pass	6000 Hz	24 dB Octave^{-1}

The LPF for the anti-aliasing of frequencies was covered for by the ZonicBook itself since the device already had anti-aliasing functionality designed into its hardware that can be set via its software.

Simple HPF of lung sound recordings to reduce heart sounds would remove significant components of lung sounds (Gnitecki and Moussavi, 2007) and there is a high degree of sensitivity of respiratory waveforms and phase shift to filter cut-off frequency parameters (Yeginer and Kahya, 2007). Therefore an adaptive filter algorithm removed low frequency heart sounds as well as (in severe cases) environmental noise from the recordings (Gnitecki *et al.*, 2003).

An adaptive noise cancellation scheme is illustrated in Figure 37 and consists of the following four components:

- The input or reference signal $r(n)$.
- The output of the adaptive filter $y(n)$.
- The desired filter response or primary signal $d(n)$.
- And the estimation error $e(n)$.

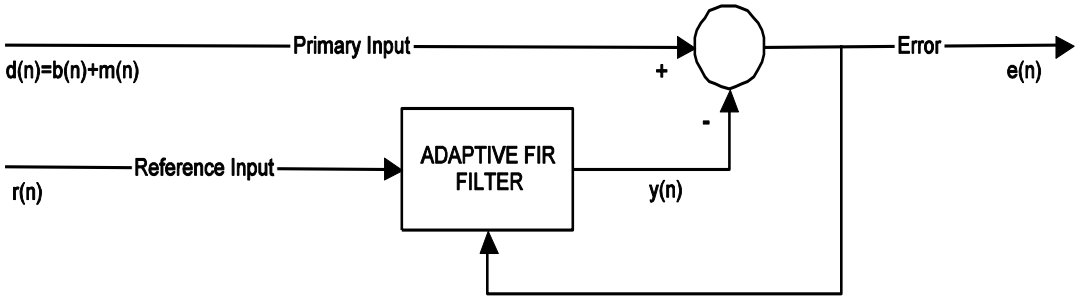

Figure 37: Adaptive Filter Algorithm

Figure 37 illustrates that a signal $d(n)$ consists of both a breath sound $b(n)$ and a heart sound $m(n)$. A reference input of pure heart sound $r(n)$ is provided into an adaptive Finite Impulse Response (FIR) filter which uses the minimization of error $e(n)$ between the primary and reference signal to update its filter weights to produce a new updated output $y(n)$.

In doing so the adaptive filter ensures that its parameters are set to filter the reference input $r(n)$ in such a manner that it matches the primary input. In the application illustrated in Figure 37 the filter adjusts itself to insure $y(n)$ represents $m(n)$ as closely as possible. The result is that the error $e(n)$ is the respiratory component $b(n)$ of the primary input $d(n)$.

The manner in which the input samples are arranged and the formula used to update the adaptive filter parameters depend on the specific type of filter scheme used. In this project the adaptive algorithm of Recursive Least Squares (RLS) was used and is given by the formulas:

$$\mathbf{k(n)} = \frac{\boldsymbol{\lambda}^{-1}\mathbf{P(n-1)u(n)}}{\mathbf{1} + \boldsymbol{\lambda}^{-1}\mathbf{u^H(n)P(n-1)u(n)}} \tag{4.1}$$

$$\mathbf{y(n)} = \hat{\mathbf{w}}^{\mathbf{H}}\mathbf{(n-1)u(n)} \tag{4.2}$$

$$\mathbf{e(n)} = \mathbf{d(n)} - \mathbf{y(n)} \tag{4.3}$$

$$\hat{\mathbf{w}}\mathbf{(n)} = \hat{\mathbf{w}}\mathbf{(n-1)} + \mathbf{k(n)e(n)} \tag{4.4}$$

$$\mathbf{P(n)} = \boldsymbol{\lambda}^{-1}\mathbf{P(n-1)} - \boldsymbol{\lambda}^{-1}\mathbf{k(n)u^H(n)P(n-1)} \tag{4.5}$$

The variables for these equations are listed in Table 8 with initial memory weighting factor, filter length and initial input variance set according to the literature (Gnitecki *et al.*, 2003) and provided in Table 9.

From Table 9 the filter length specifies the length of the filter weights vector and the forgetting factor (0 to 1) corresponds to λ in the equations. It specifies how quickly the filter "forgets" past sample information. The initial filter weights are specified by $\hat{w}(0)$ and the initial input variance σ^2 sets the initial value of P(n) given by:

$$P(n) = \frac{1}{\sigma^2} I \qquad n=0 \qquad (4.1)$$

Table 8: Table of Recursive Least Squares Variables

Variable	Description
n	The current algorithm iteration
u(n)	The buffered input samples at step n
P(n)	The inverse correlation matrix at step n
k(n)	The gain vector at step n
$\hat{w}(n)$	The vector of filter step estimates at step n
y(n)	The filtered output at step n
e(n)	The estimation error at step n
d(n)	The desired response at step n
λ	The exponential memory weighting factor

The RLS adaptive algorithm was used to successfully remove heart sounds from the recordings using the original recording as the primary input and an equi-ripple LPF version of the same signal as the desired input. The parameters and model for the system are illustrated in Table 9 and Figure 38 respectively.

As illustrated in Figure 38, the original signal has two phases associated to it. Firstly, the signal undergoes an equi-ripple LPF to obtain the low frequency component of the signal. Due to the destructive nature of simply subtracting this component of the signal it is sent through an RLS adaptive filter to identify the exact low frequency component of the primary signal and then adapt the filter weights to successfully remove the low frequency components from the primary input signal.

Table 9: Model Parameters for Environmental and High Pass Filtering

	High pass filtering	Environmental noise filtering
Equi-Ripple LP Filter		
Structure	Direct form FIR	
Order	76	
Stable	Yes	
Freq Pass	0.1 Hz	
Freq Stop	150 Hz	
Amplitude Pass	0	
Amplitude Stop	-80 dB	
RLS Filter		
Filter length	2	32
Forgetting factor	1	1
Initial input variance	0.1	0.1
Initial Value of Filter weights	0	0

Environmental Noise Filtering

Severe cases of environmental noise at rural clinics, resulted in the electronic stethoscope normally placed over the trachea, being used to record the environmental noise, which later then served as a noise reference input into the second phase of the RLS filter configuration (Figure 38). This reference signal could then identify the true environmental noise component of the primary input which was then removed from the original recording.

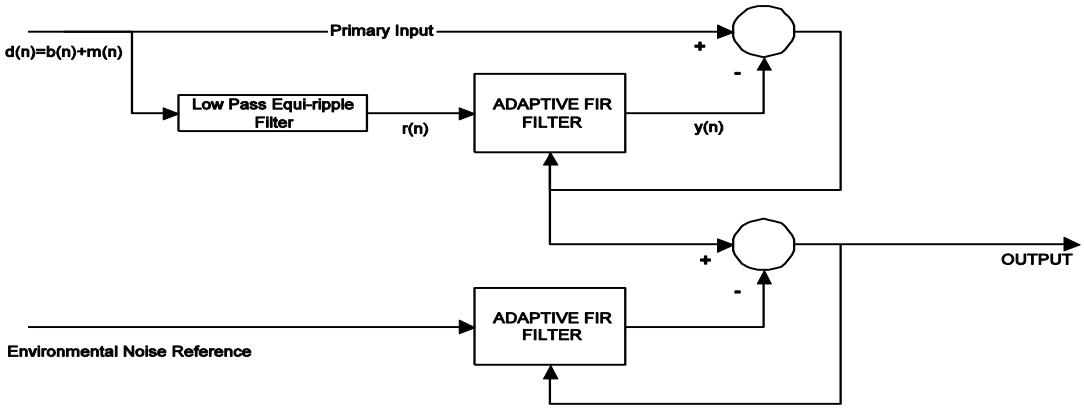

Figure 38: Filtering Structure for Removal of Heart Sounds & Environmental Noise

The spectrogram in Figure 39 shows how the maximum amplitude (dark red) shifts from the low level less than 50 Hz range into the respiratory range above 100 Hz after undergoing the adaptive filtering in Figure 38.

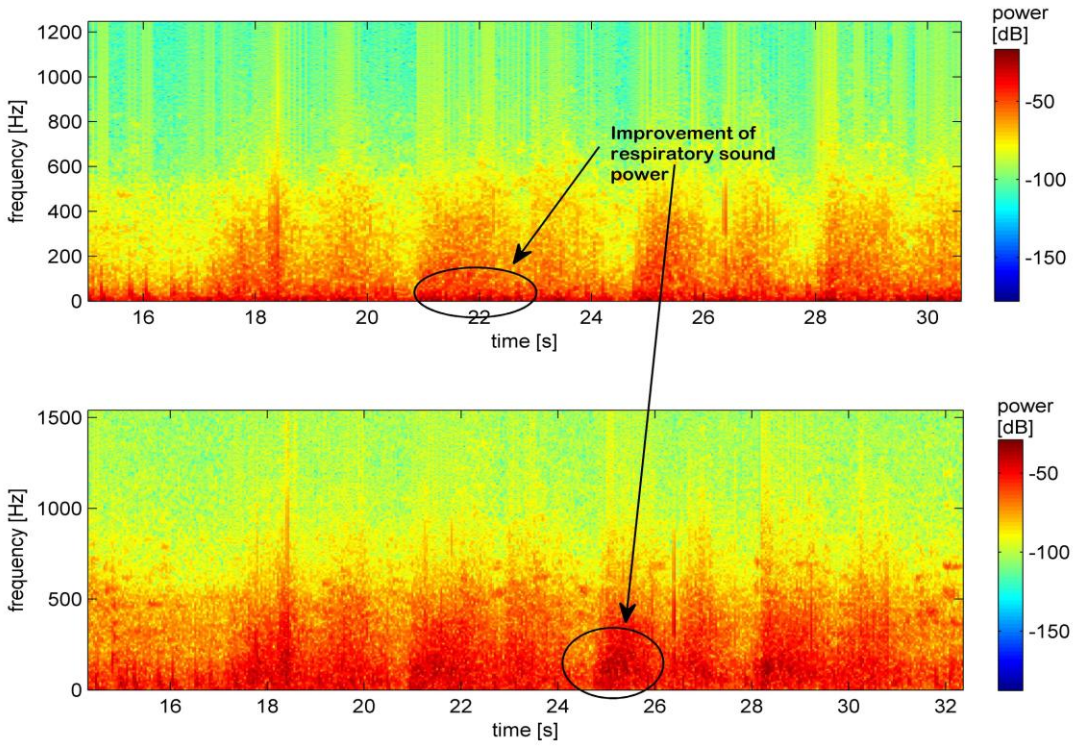

Figure 39: Spectrogram of Respiratory Recording before & After Filtering

5 Analysis of Data

Normalization between minimum and maximum values of 0 and 1 respectively set each recording to have the same possible maximum output amplitude of 1 so as to zero the effect of different ambient conditions prevailing during recording at different locations, and also the subject to subject variability (Jain and Vepa, 2008).

This was achieved using two functions set in Matlab's "Signal processing toolbox". The first function scans the entire vector of values that represent the time / amplitude data of the wave signal and identifies the maximum and minimum values in that vector. The maximum numerical value is set to a limit of one and the smallest value set to a numerical limit of zero. All other values between those two limits are then scaled respectively. Given that all values are scaled, an offset of the entire signal occurs. Therefore a second function was used to detrend the scaled signal. The detrend function removed the mean from the set of data thus eliminating the influence of any constant offsets in the signal.

Therefore the signal analysis techniques that were applied investigated signals with the same limits of normalization. The structure of the employed analysis techniques are shown in Figure 40.

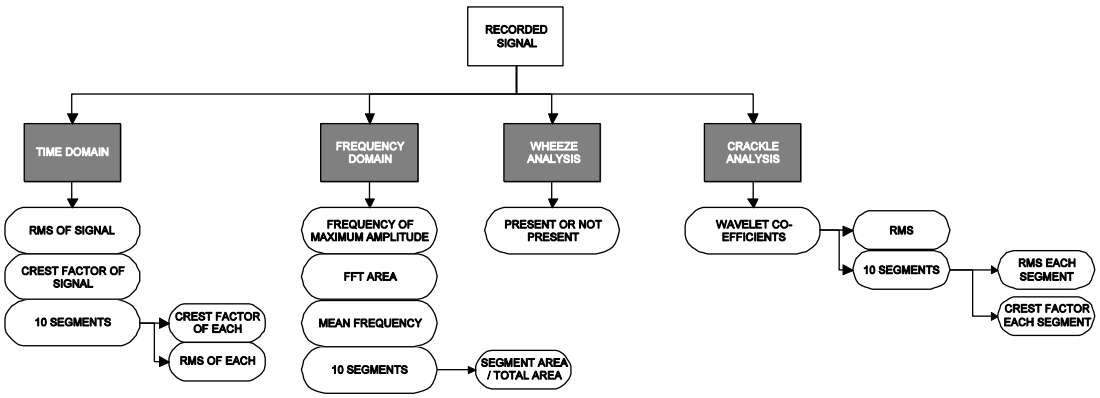

Figure 40: Overview of Signal Measurements

The structure indicates analyses completed in four distinct groups namely:

- Time analysis.
- Frequency analysis.
- Wheeze parameter analysis.
- Crackle parameter analysis.

These four sections were sub-divided into further measurement domains to provide additional data with all analysis technique being completed in Matlab® R2007b.

5.1 Overview

Time domain features included investigation into the RMS of the signal as well as dividing the signal into ten segments and a calculation of the RMS of each segment. Since analysis was done over a single breath cycle, the first five segments would roughly cover inspiration and the following five breaths expiration. Participants where asked to inhale and exhale to indications by the author thus maintaining an average time window of 2.5 s. A crest factor, discussed in Section 5.2.5, was calculated for each of the ten segments as well as saving the maximum crest factor of the ten and the average of all ten crest factors. The measurements are illustrated in Figure 41.

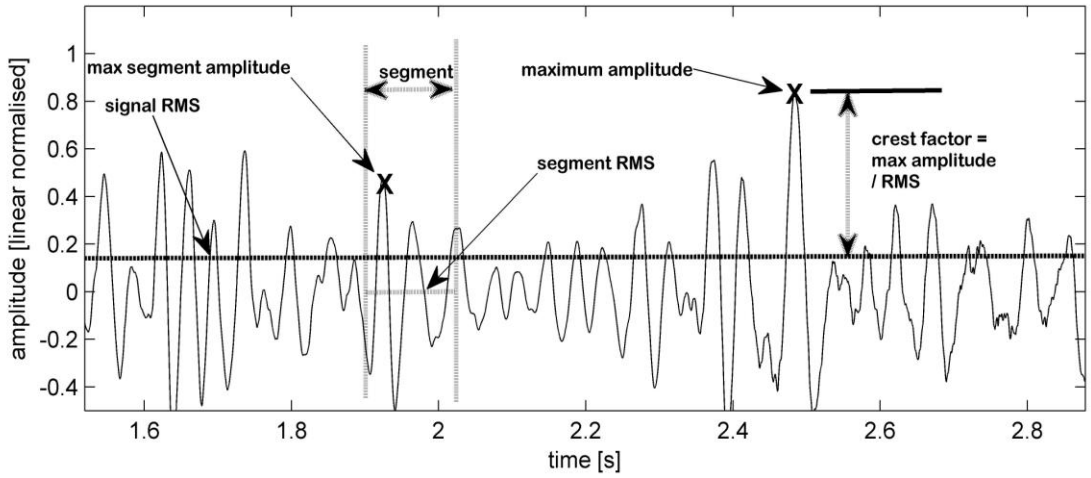

Figure 41: Measurements Done on Time Signal

The FFT of each recording was used to obtain the frequency with the maximum amplitude. Further frequency domain features included the maximum frequency divided by the area (energy) under the FFT as well as dividing the FFT into frequency octave bands. The area of each frequency octave band divided by the total area of the entire FFT supplied necessary quantative “band energy over total energy” ratio, as illustrated in Figure 42. Octave bands set up were 0-17 Hz, 18-45 Hz, 46-90 Hz, 91-180 Hz, 181-360 Hz, 361-720 Hz, 721-1440 Hz and 1440-3000 Hz respectively.

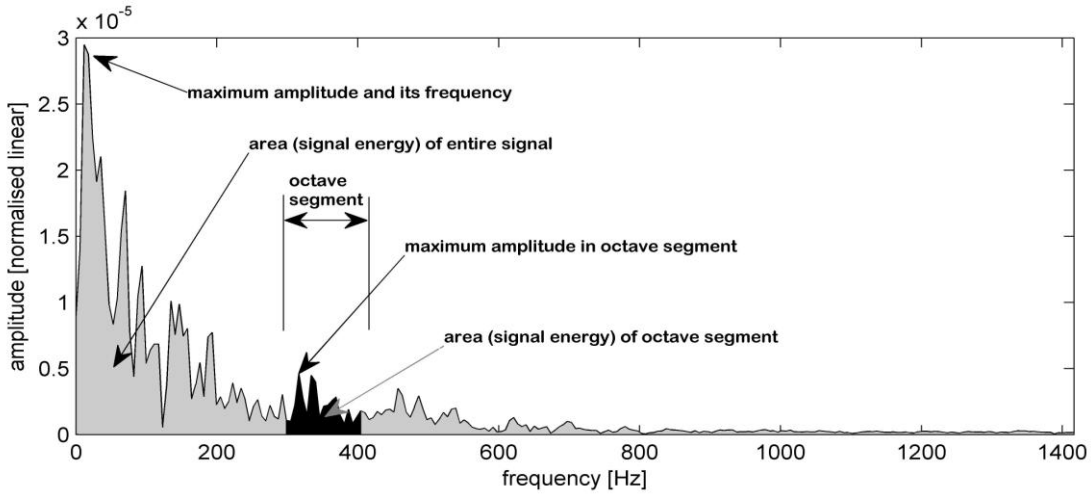

Figure 42: Measurements Done in Frequency Domain

Analysis of wheeze characteristics was performed in a manner of only identifying whether signal characteristics exist, that match those that define a wheeze, in order to establish whether wheeze analysis is relevant in future research. These definitions include the pitch and duration that a pseudo-sinusoidal signal should be present in the respiratory recording in order to classify it as a wheeze. Therefore, wheeze analysis was merely in the form of an answer for the presence or absence of wheeze characteristics. This answer is conclusive from an algorithm responsible for identifying wheeze characteristics within a respiratory recording according to the pitch and duration specifications. This method is illustrated in Figure 43, which in this case would yield an answer of 1 indicating wheeze characteristic presence.

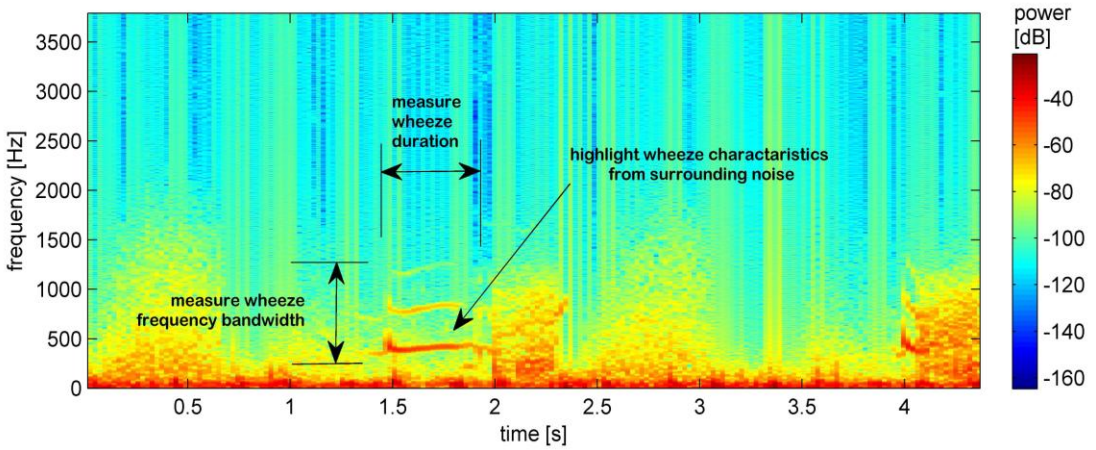

Figure 43: Measurements to Determine Wheeze Presence

Crackle analysis involved choosing a mother wavelet (of particular shape)[18] and measuring the degree of similarity of scaled and shifted versions of the mother wavelet to that of the respiratory signal. The outcome, in the form of wavelet coefficients, was used to obtain statistical data such as the mode, mean, median and range of wavelet coefficients. Figure 44 shows the plot of wavelet coefficients (Daubechies 5 level 5 in this example)[19] where peaks indicate a high degree of similarity between the mother wavelet and the respiratory signal. The plot of wavelet co-efficients was also broken into ten segments of which the maximum and RMS of each segment was also taken into account. In the digital domain, the coefficients are expressed as a vector of numbers that can be represented in a histogram (Figure 45) illustrating the mean, range, minimum and maximum values. This was completed for four specific wavelet nodes discussed in detail in Section 5.2.4.

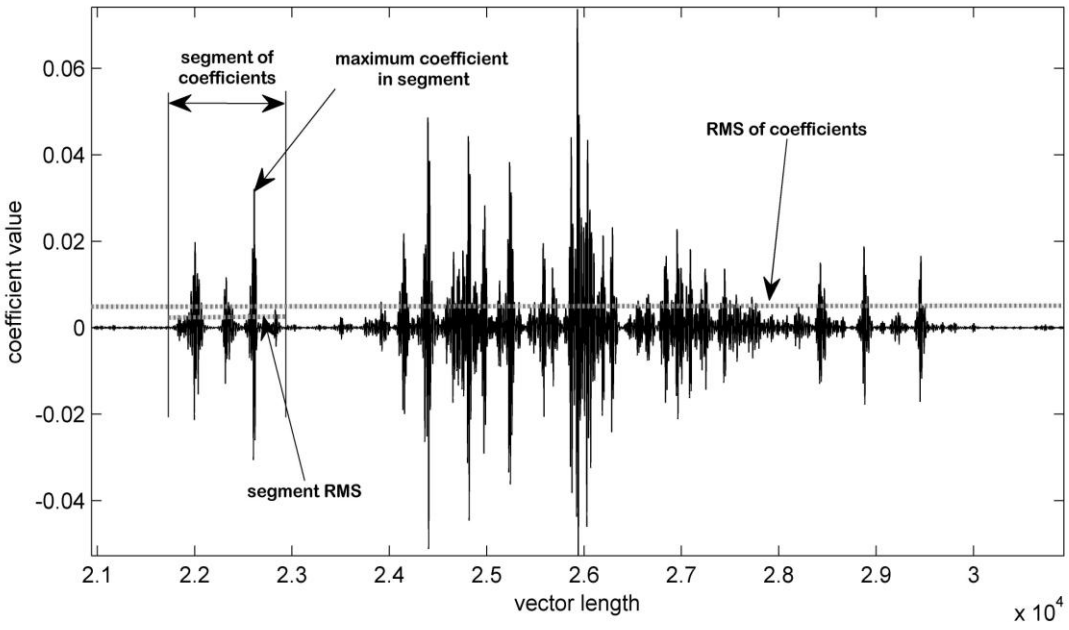

Figure 44: Measurements Done on Wavelet Coefficients

[18] Discussed in detail in Section 5.2.4 and Appendix G
[19] Consult Figure 50.

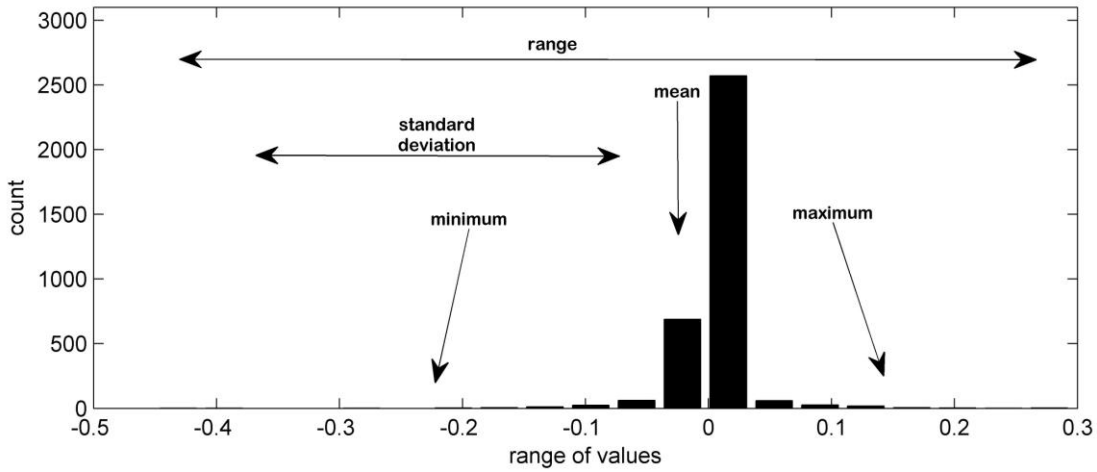

Figure 45: Histogram of Wavelet Data (example data)

5.2 Equations and Methods Used

5.2.1 Time Domain Analysis

Analysis in the time domain consisted of conventional plotting of wave data in the time / amplitude format. Further data extracted was the Root Mean Square (RMS) of the signal represented by Equation 5.1 for any continuous analogue variable (Figola and Beasley, 2000):

$$y_{rms} = \sqrt{\frac{1}{t2 - t1}\int_{t1}^{t2} y^2\, dt} \tag{5.1}$$

Where y_{rms} is the square root of the mean of a signal $y(t)$ over time $t_2 - t_1$. A time dependent analog signal $y(t)$ can be expressed by a discrete set of N numbers over time t_1 to t_2 through the conversion (Figola and Beasley, 2000):

$$y(t) \rightarrow \langle y(r\ \sigma t)\rangle \qquad r = 1, \ldots, N \tag{5.2}$$

Where r is the numerical sampling number and σt is the sampling interval if the analog signal. When in the from of digitized numerical data, the vectors RMS can be calculated given (Figola and Beasley, 2000):

$$Y_{rms} = \sqrt{\frac{1}{N}\sum_{i=1}^{N} y_i^2} \tag{5.3}$$

where y_i is the numerical data of length N.

5.2.2 Frequency Domain Analysis

Frequency domain analysis entailed calculating the FFT of the time series data representing a signal's contributing sine and cosine functions in complex exponential form:

$$X(f) = \int_{-\infty}^{\infty} x(t)\, e^{-j2\pi ft} dt \tag{5.4}$$

This means a signal $x(t)$ can be expressed in the frequency $x(f)$ domain as its coefficient $x(t)$ times a complex exponential $e^{-j2\pi ft}$, where f is the frequency.

Subsequently the continuous transformation of an analogue signal, once digitized, cannot be calculated so Equation 5.4 takes on a discrete form (Enderle *et al.*, 2005):

$$X(m) = \sum_{k=0}^{N-1} x(k) e^{-j\frac{2\pi mk}{N}} \tag{5.5}$$

The index m represents the digital frequency index, $x(k)$ is the sampled approximation of $x(t)$, k is the discrete time variable, N is an even number that represents the number of samples for $x(k)$ and $X(m)$ is the Discrete Fourier transform of $x(k)$ (Enderle *et al.*, 2005).

An interesting variation to the FFT is the STFT which is an adaptation to spectrally analyze time waveform data for frequency content within small units of time, since the frequency content of a non-stationary biomedical signal is changing constantly

over time. Thus a standard FFT only represents the average frequency content for the entire signal but not the frequency content at specific time instants.

Thus the STFT, given by the formula:

$$X(t,f) = \int_{-\infty}^{\infty} x(t) \cdot h*(t-\tau) e^{-j2\pi ft} dt \tag{5.6}$$

utilizes a windowing function $h*(t-\tau)$. Rippling effects of the sharp window border were avoided using a regular Hamming window with 50% overlap.

In the digital domain the time/amplitude signal is represented with a vector of amplitude quantities. Thus for both the FFT and STFT certain parameters were set to control spectral resolution as well as time windows limits. The parameters used are listed in Table 10.

Table 10: Parameters for Frequency Analysis

	Windowing			Frequency Length
	Type	Size	Overlap	
Fourier Transform	Hanning	1024 points		
Short Time Fourier	Hamming	512 points	50 %	0 – 3000 Hz

The equation:

$$Window\ Size = Sampling\ Frequency \times Time \tag{5.7}$$

yields the following frequency and time windows for the FFT and STFT (Earis and Cheetham, 2000):

Table 11: Window Sizes used for Frequency Analysis

	Window Size	Sampling Frequency	Time Frame	Minimum Frequency
FFT	1024	6000 Hz	170 ms	5.85 Hz
STFT	256	6000 Hz	42.7 ms	23.43 Hz

These limits, governed by computer processing limitations, were still in accordance with the literature (Charbonneau *et al.*, 2000) and accounted for smaller time frames to be analyzed which can in turn assume better stationary limits of the signal.

5.2.3 Wheeze Parameters: Spectral Analysis

The importance of extracting wheeze parameters was discussed in Section 2.3.2. A process of evaluation on a spectrogram of a signal to single out and highlight wheeze features was implemented based on a successful routine proposed by Taplidou (2007), and used the following steps of evaluation:

- "*Subtraction of the underlying basic breath sounds from the total breath sound*" (Taplidou and Hadjileontiadis, 2007). This involves a smoothing technique that estimates the trend of the frequency content of the windowed signal at each time instance. The estimation of this trend is based on a filtering method known as the cosine taper method[20] removing large amplitude variations (and thus high frequency noise) between samples, producing a smoother signal.
- "*Peak detection in the TF plane*" (Taplidou and Hadjileontiadis, 2007). Every frequency at every time window had to be greater than the mean of all the frequency amplitudes in the spectrogram plus twice the standard deviation of the frequency amplitudes in the spectrogram. Any signal amplitudes in the spectrogram below these values were removed.
- Group the remaining peaks in the spectrogram and measure the length of the peak duration in the time domain whereby durations in the range 250 ms – 2.5 s were considered wheezes (Sovijärvi *et al.*, 2000).

Figure 46 and Figure 47 show the spectrogram of a recorded signal from a healthy participant possessing wheeze characteristics. The results of the above evaluation technique on the recording are visible in the two illustrations[21].

[20] Variation to the box filtering method performed by Taplidou (2007).
[21] It should be noted that the algorithm highlights the wheeze *characteristics* following a routine proposed by Taplidou (2007) and the performance of the algorithm designed by the author may not perform in exactly the same manner as proposed by Taplidou.

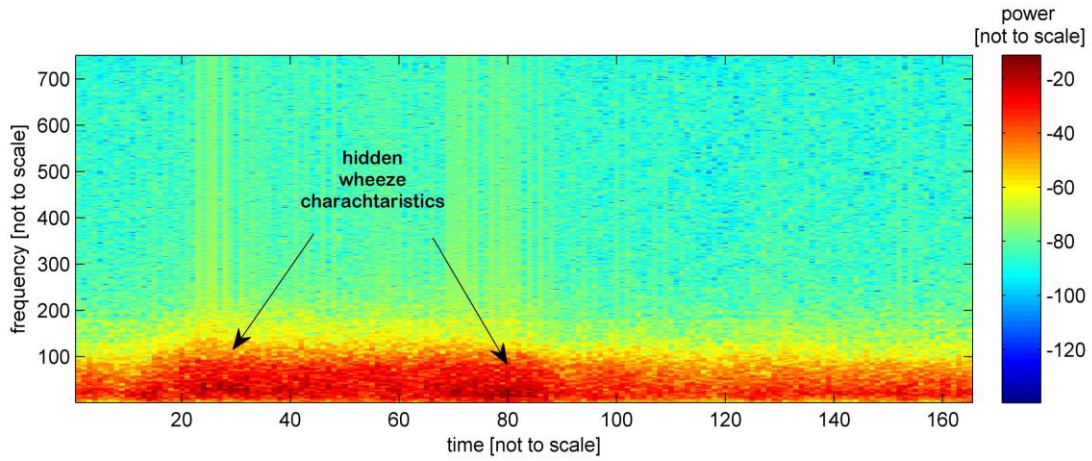

Figure 46: Spectrogram with Hidden Wheeze Characteristics

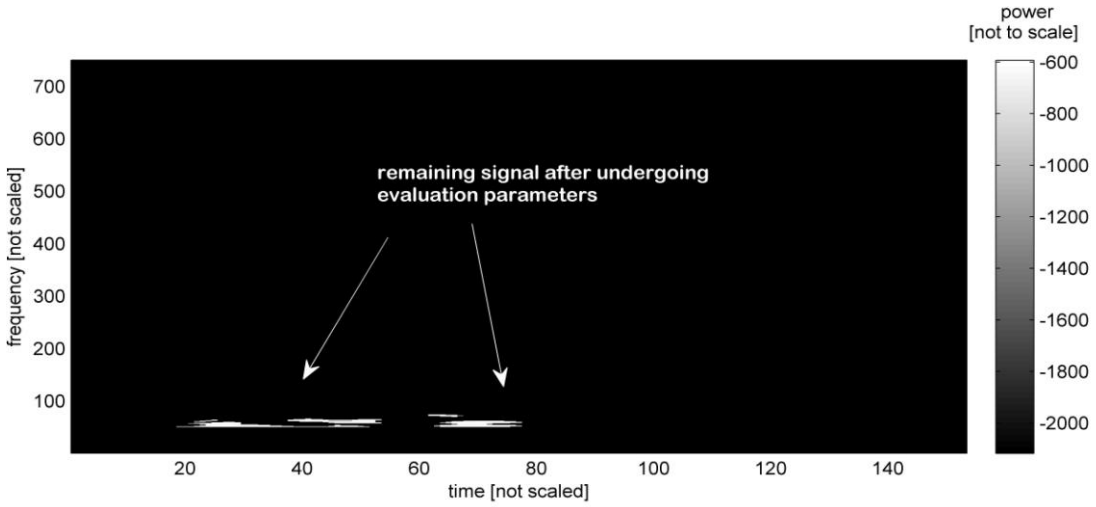

Figure 47: Spectrogram of Wheeze Characteristics after Evaluation

5.2.4 Crackle Parameters: Wavelet Analysis

Crackle parameters were obtained using an analytical method known as wavelet analysis (Kandaswamy *et al.*, 2004).

The successful execution of decomposing a signal into its wavelet coefficients required the correct selection of a *mother wavelet*. Many forms and variations exist and are often selected on a visual inspection basis. Visual inspection of the wavelets showed the *Daubechies* 5 wavelet to be the closest match to a typical crackle

waveform as defined in Figure 15 (Figure 48 and Figure 49 below further clarifies the decision).

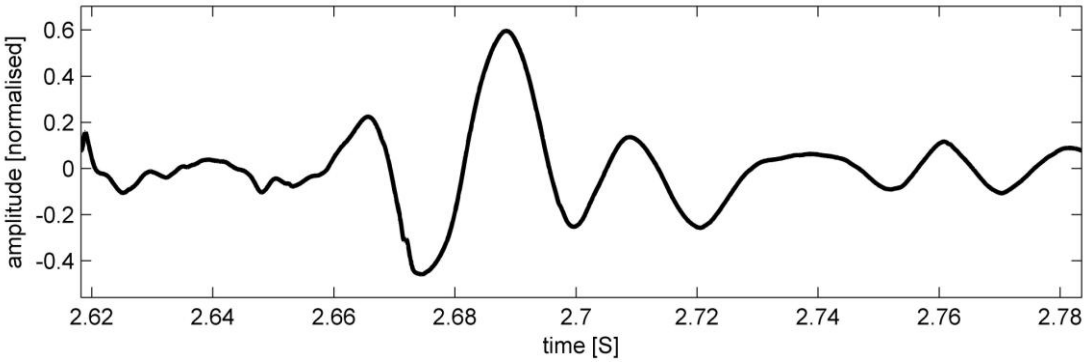

Figure 48: Crackle Wave (Example)

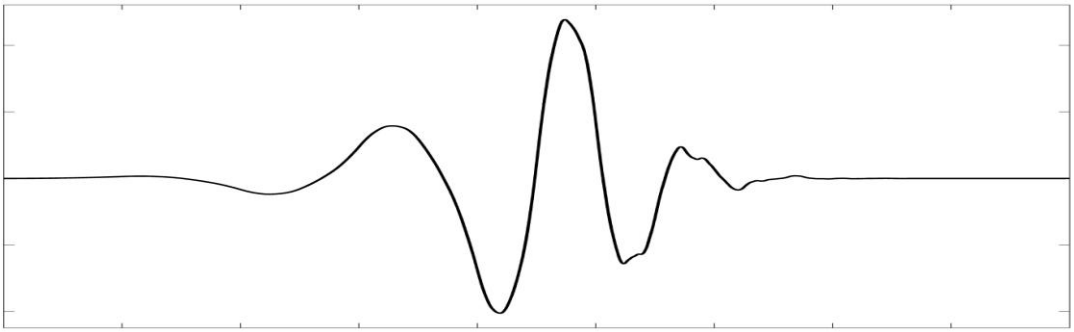

Figure 49: Daubechies Wavelet (Level W0)

Wavelet decomposition consists of decomposing a signal into its LP *approximations* and HP *details* using shifted and scaled versions of the mother wavelet. In a second round the detail from the previous level is again broken into further approximations and details. This process is repeated to a desired level (Figure 50).

Comparison of the approximations and details between ten healthy and ten crackle recordings downloaded from the internet (PixSoft Inc, 2007 and The Institute of Fundamental Electronics, 2006) showed that a decomposition up to level 5 using nodes (5, 2), (5, 3), (5, 6) and (5, 7) had the highest degree of similarity between individual recordings but difference between healthy and unhealthy TB pathological recordings. The decision shown in Figure 50 illustrates the wavelet decomposition tree for a healthy recording (on top) and pulmonary TB recordings (below) for nodes (5, 2), (5, 3), (5, 6) and (5, 7).

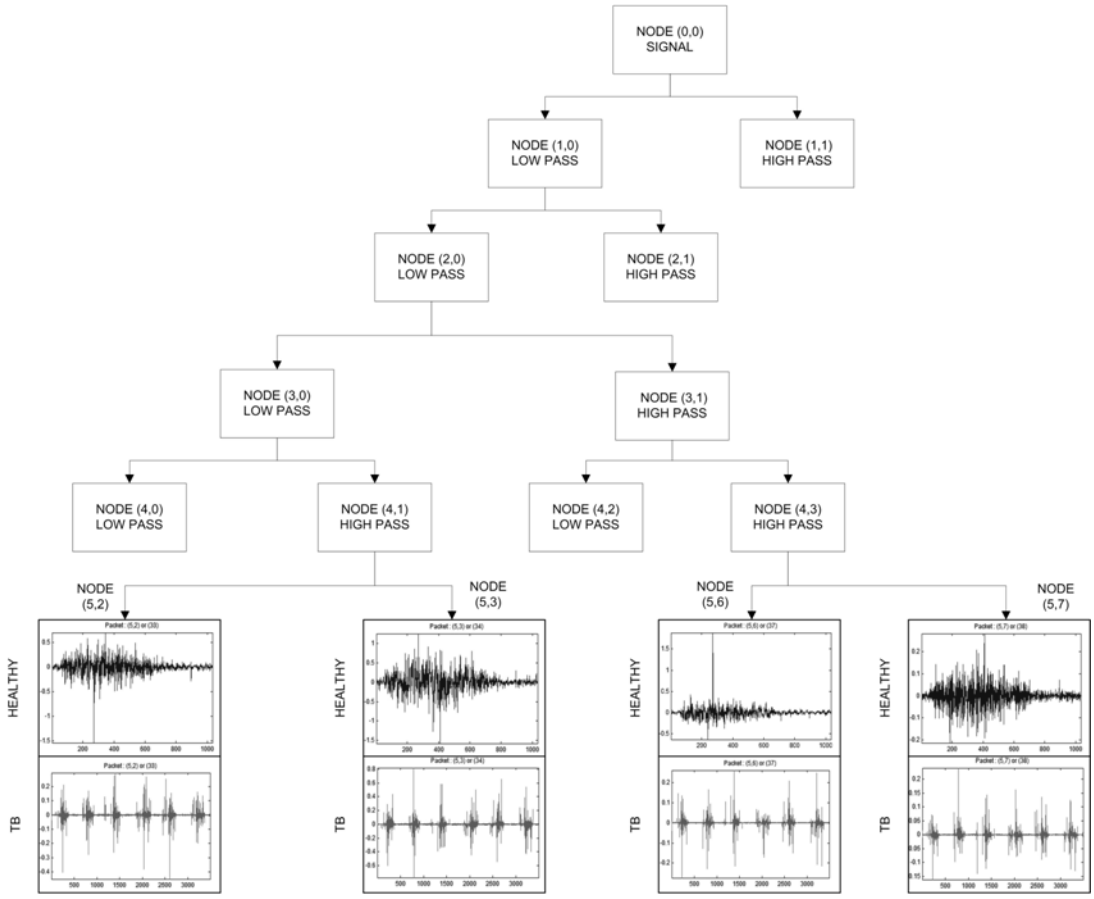

Figure 50: Nodes Chosen for Wavelet Decomposition

Thus the application of Daubechies 5 level 5 to the recordings provided data as part of the crackle measurement investigation. Figure 51 illustrates a healthy recording (four breaths prior to splitting into single breath cycles) along with its respective wavelet decomposition at level 5 of a Daubechies wavelet. Decomposition at level 5 was indicative of a low degree of Daubechies matching since the signal maintains a high level of respiratory noise throughout its sampling length.

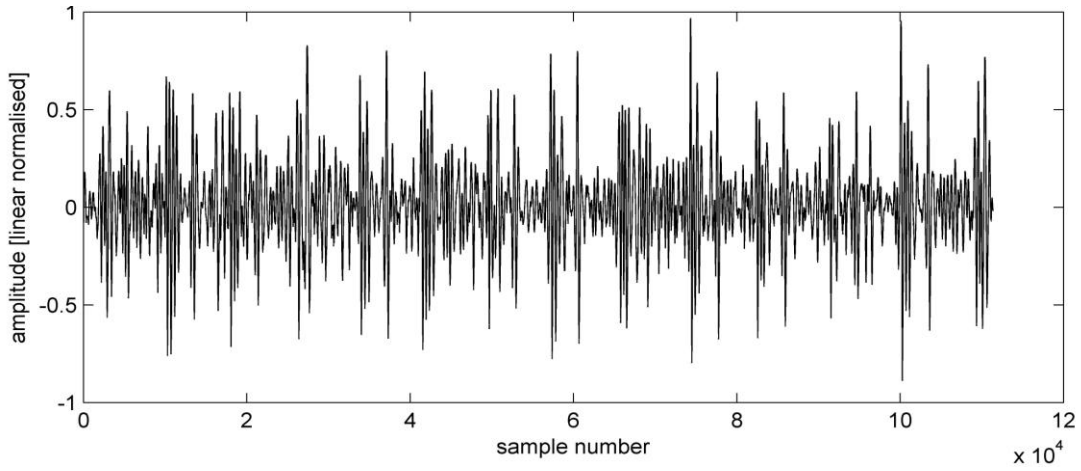

Figure 51: Original Signal of Healthy Participant (Four Breaths)

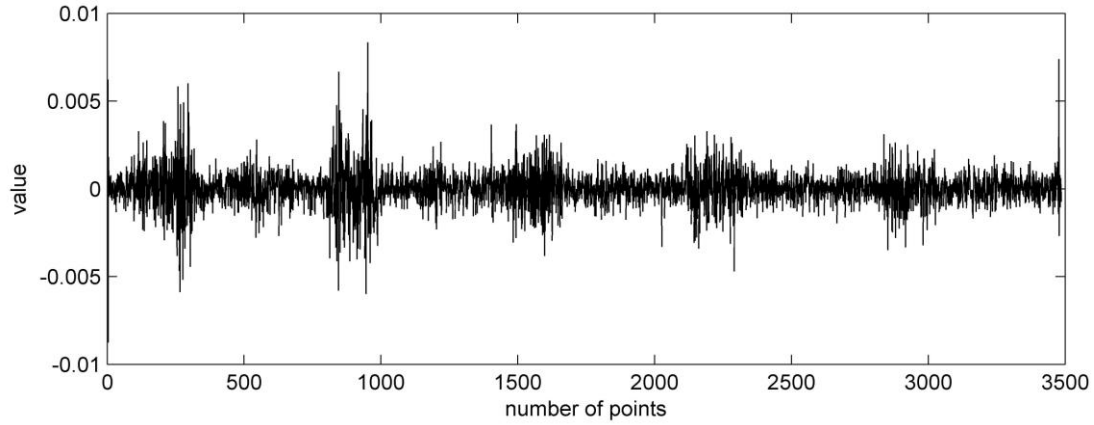

Figure 52: Decomposition (node 5,7) of Healthy Recording (Four Breaths)

This differs when compared to recordings done to pulmonary TB participants as illustrated in an original recoding done on the lower clavicle shown in Figure 53. Clues in the figure are already indicative of crackle waves prior to the wavelet analysis.

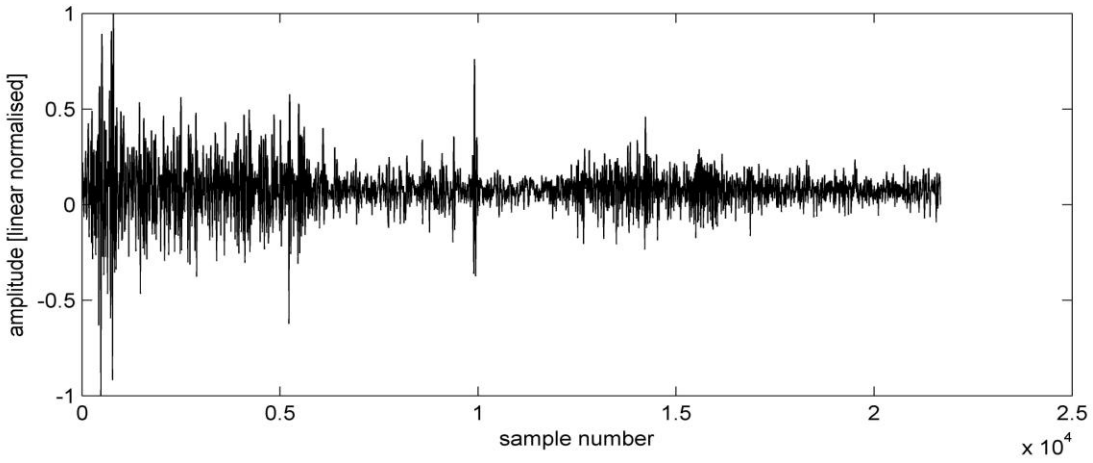

Figure 53: Original Recording TB Participant (Single Breath)

Decomposition at level 5 of a Daubechies 5 wavelet analysis showed a significant increase in Daubechies relationship (comparing Figure 52 and Figure 54, y-axis) for the recording done in Figure 53. Such analysis was repeated across all microphone positions and all participants as the final method chosen for crackle analysis.

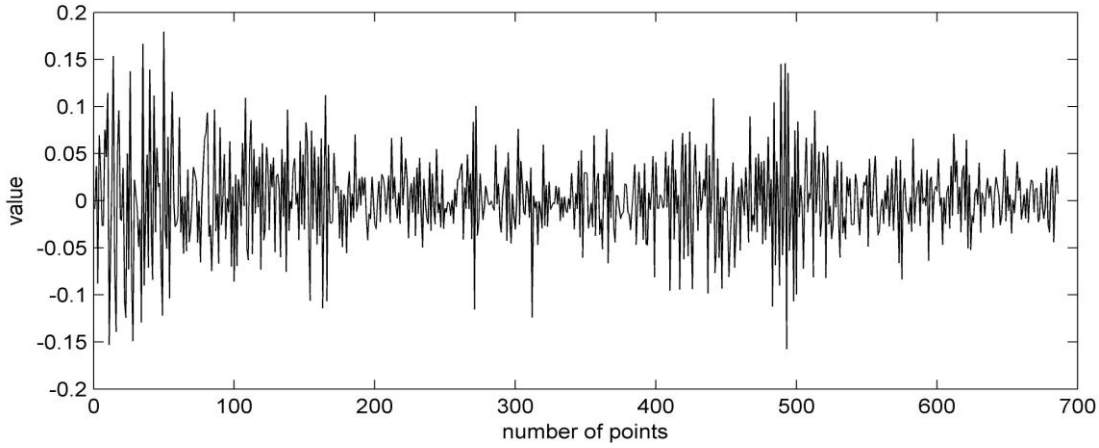

Figure 54: Decomposition (node 5,7) of TB Recording (Single Breath)

5.2.5 Further Useful Parameters

Further useful parameters included were:

- The mean of various FFTs and crackle parameters.
- The median of crackle wavelets

- The crest factor of various TEWA data, FFTs and crackles.

The mean of a set of data can be described as the average as represented by the following equation:

$$\bar{y} = \frac{1}{N}\sum_{i=1}^{N} y_i \tag{5.6}$$

Where the sum of all y_i values divided by the number of values in the sequence, N, gives the average value $\bar{y}$.

The median $\check{y}$ differs slightly from the mean by which the median is the centre-most value in an ordered set of data $\vec{y}_1\{ordered\}$ from smallest to largest. In the case of an even number of data points the median is the mean of the two most central points in the data set. This can be summarized as:

$$\check{y} = \frac{\vec{y}_1\{ordered\} + \vec{y}_2\{ordered\}}{2} \quad N = even \tag{5.7}$$

$$\check{y} = \vec{y}_1\{ordered\} \;\; N = odd \tag{5.8}$$

A final parameter calculated called the crest factor (CF) is given by:

$$Crest = \left|\frac{x_{peak}}{x_{rms}}\right| \tag{5.7}$$

and is a measurement of a waveform (x), calculated from the peak amplitude ($|x|peak$) of the waveform divided by the RMS (time-averaged) value of the waveform. Therefore crest factors for TEWA analysis was calculated, often over windowed segments of the signal to give a *running crest factor.*

5.3 Graphical user Interfaces (GUI)

The preparation of the time, frequency, wheeze and crackle data used computer programming divided into three distinct stages with each stage masked into a

Graphical User Interface (GUI). Storing of data in Matlab (*.mat) file format allowed for reloading into the Matlab workspace for further evaluation and/or processing.

The three GUI's designed were:

- A "Preview" GUI responsible for previewing the exact data recorded by the ZonicBook to make sure all microphones and respiratory straps were in working order and to evaluate the quality of the recording. If the recording was unsuccessful the participant was politely asked if that particular trial could be repeated (refer to Appendix E).
- A "Filter and Split" GUI for re-sampling the digital data from 10 250 Hz to 6 000 Hz as well as executing the RLS filter, as mentioned in Section 4.3.5, removing any heart, muscle and extreme environmental noise from the signal. After filtering the three deep breaths for each test, they were manually split into individual sets of data (single complete breaths). Tidal breathing was discarded after various attempts proved the acoustic power to be too low.
- An "Auscultation" GUI for analyzing the three breath cycles for all the time, frequency, wheezes and crackle parameters discussed in Section 5.1.

The auscultation GUI served as the key program in analyzing the data into those mentioned in Section 5.1 of which the techniques were discussed in detail in Section 5.2.

6 Evaluation and Reliability of Data

The following section discusses the assembly and evaluation of the characteristics calculated from Chapter 5. These signal measurements where by the characteristics with the greatest degree of separation between healthy and pulmonary TB participants (separation of the averages of the data) but smallest variance within their own cluster are used as training inputs into a neural network. The effectiveness of the neural network is then discussed.

6.1 Selection of Top Parameters

Gathering of all the respective RMS, CF values, frequency and amplitude values, wheeze answers, crackle coefficient and histogram statistical data produced a total of 202 signal features for a single breath. The distribution of these 202 measurements across the four analysis groups is explained in Table 12.

Table 12: Range of Analysis Values to Analysis Group

Analysis Group	Value Number
Time Domain	1 - 33
Frequency Domain	34 - 45
Wheeze Parameters	46
Crackle Parameters	47 - 202

Being repeated for a total of 27 healthy and 33 pulmonary TB participants and given that each participant contributed three breath sounds for mostly left and right lungs, a total of 156 healthy participant breath sounds and 189 TB participant breath sounds were obtained (Table 13).

Sequential alignment of the three breaths from each participant as well as successive participants led to the creation of a stacked data block of 156 healthy breaths and a separate stack of 189 TB breaths.

Table 13: Total Recordings Obtained and Used

	Healthy	TB

Number of Participants	27	33
Number of Lungs	2	2
Number of Breaths	3	3
Total Breaths	162	198
Discarded Recordings	2 (6 Breaths)	3 (9 Breaths)
Total Used	**156**	**189**

Figure 55 shows the 202 wave measurements were arranged in rows along the x-axis, the seven microphones in columns along the y-axis and stacked breaths and participants in the z-axis. The result is two such stacks, one for healthy and one for unhealthy data.

The addition of similar characteristic measurements for similar microphone positions was achieved by maintaining a single row and column position and adding values in the z-axis respectively. This allowed for calculating the average value for any signal characteristic measurement.

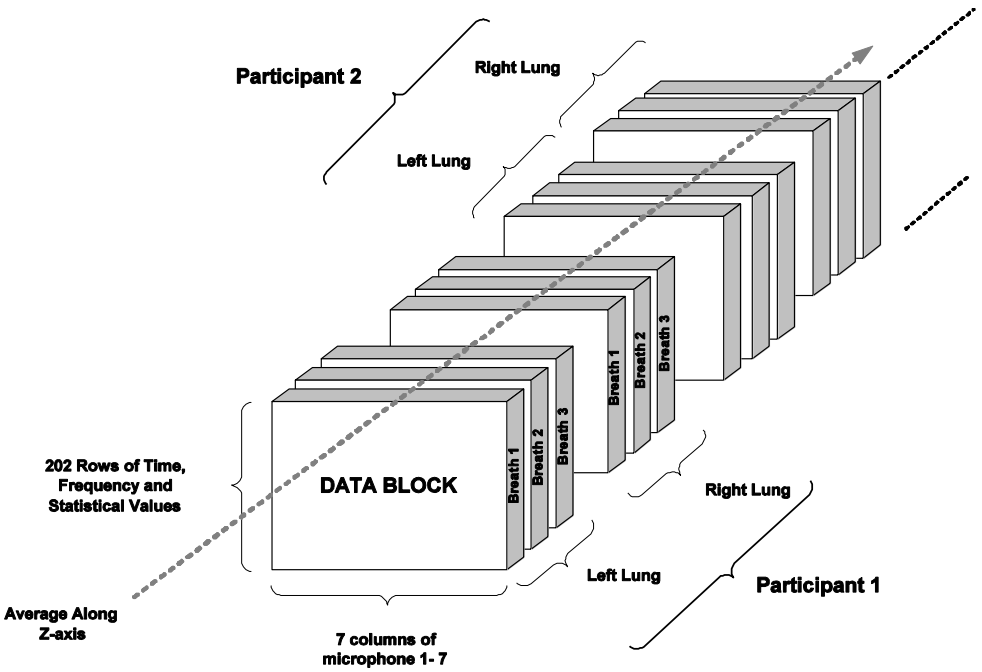

Figure 55: Arrangement of Data Blocks

As a result the SOF for each of the 202 characteristics at each microphone was calculated. The SOF is given by:

$$SOF = \left| \frac{\bar{x}_{Healthy} - \bar{x}_{Unhealthy}}{(\sigma_{Healthy} + \sigma_{Unhealthy})/2} \right| \quad (6.1)$$

where $\bar{x}_{Healthy}$ is the average of the particular characteristic for healthy participants, $\bar{x}_{Unhealthy}$ is the average of pulmonary TB participants, $\sigma_{Healthy}$ the standard deviation of the characteristic data for healthy participants and $\sigma_{Unhealthy}$ the standard deviation of pulmonary TB participants.

In essence the SOF indicated the degree of separation of means of the data between healthy and pulmonary TB participants but also considers the variance as a degree or overlap between the data.

Figure 56 clarifies that microphones 3 (lower clavicle), 5 (upper posterior chest) and 6 (middle posterior chest) provided the widest range of data with SOF values greater than 0.4 and continuity of a signal characteristic across more than one microphone. (Already noted is the fact that the locations of microphones 3, 5 and 6 are paired to the most common sites of pulmonary TB infection seen from the corresponding radiographs, as judged by the medical practitioner for this research.)

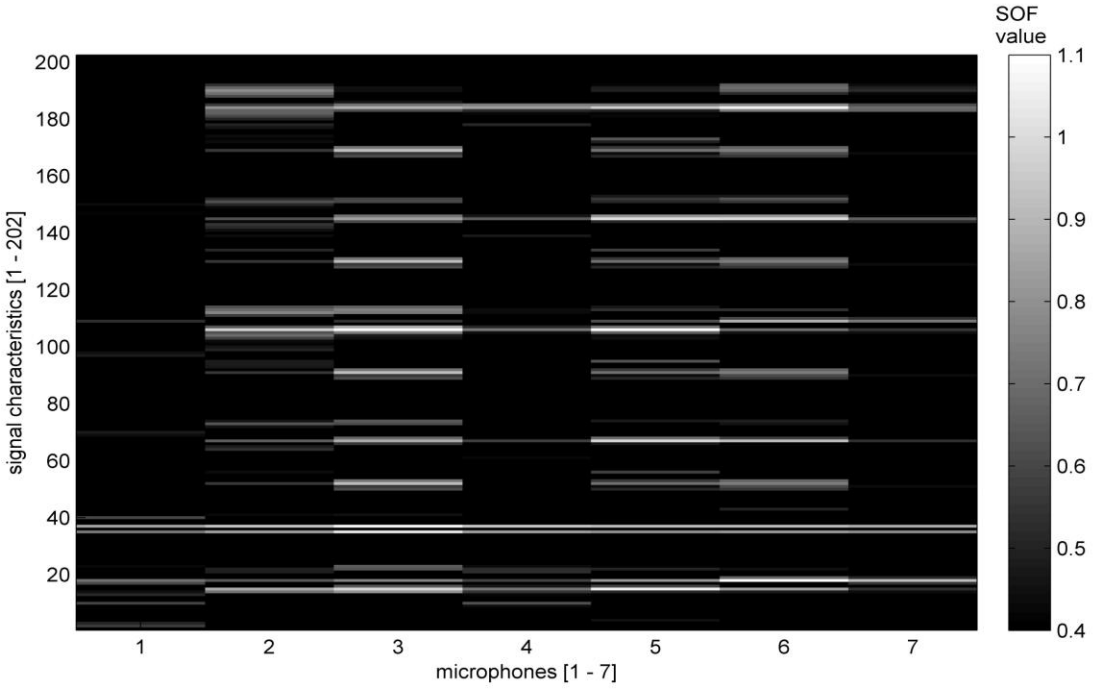

Figure 56: Evaluation of Statistical Overlap Factors

In order to understand which of the four categories from Table 12 contributed the most to the SOF values, a histogram of SOF values above 0.4 was drawn and indicated in Figure 56. A histogram divided into 202 categories was considered too fine for overview purposes and thus set to display histogram data in 15 groups. The limits of the 15 groups where then assigned back to their corresponding categories as defined in Table 12. Therefore it needs to be emphasized that Figure 57 indicates only the major contributing measurements towards SOF factors above 0.4

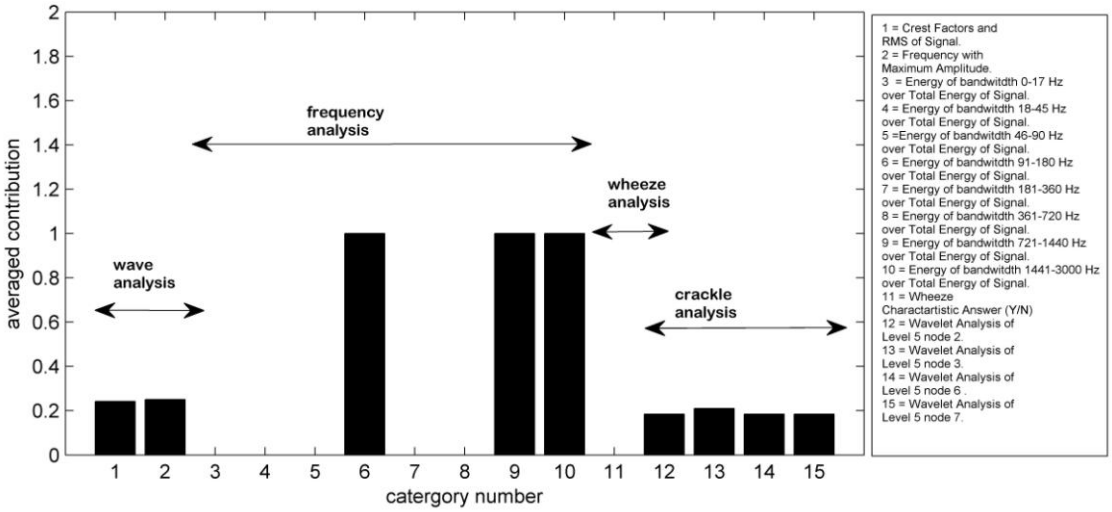

Figure 57: Overview of SOF Values above 0.4

From Figure 57 it is clear that major SOF contributions came from the following factors:

- The energy (area under FFT) ratio of octave bands to total energy for octave bands in frequency range 91-180 Hz and 721 – 3000 Hz respectively.
- The frequency with the maximum amplitude.
- Crest Factors and RMS on wave signal.
- Crackle parameters of participants.

Table 14 lists the 14 highest SOF values[22] as well as their corresponding SOF magnitudes, microphone locations and type of signal measurement. Although varying in microphone location and type of signal measurement, a proposition exists that the types of signal measurements (as overviewed in Figure 57) can be grouped into a theory stating that:

[22] The top 14 are chosen since thiis the number of inputs required by the Neural Network and referred to again in Section 6.2

"A difference exists between healthy and TB participants in the sense that TB participants show a higher degree of crackle parameters and this in turn contributes to the higher amplitude in higher frequencies as shown in the FFT octave bands of Figure 57."

Table 14: Fourteen Highest SOF Factors

SOF Mag.	Measurement Num.	Microphone Position	Signal Measurement
1.126	18	6: Middle Posterior Chest	RMS of 5th of 10 Segments on the Respiratory Signal.
1.109	106	5: Upper Posterior Chest	RMS of 2nd of 10 Segments on the Wavelet Co-efficients Level 5 Node 2.
1.097	37	3: Lower Clavicle	Mean of the FFT of Entire Respiratory Signal.
1.086	106	3: Lower Clavicle	RMS of 2nd of 10 Segments on the Wavelet Co-efficients Level 5 Node 2.
1.059	184	6: Middle Posterior Chest	RMS of 2nd of 10 Segments on the Wavelet Co-efficients Level 5 Node 7.
1.052	35	3: Lower Clavicle	Frequency at Which Maximum Amplitude occurs.
1.045	15	5: Upper Posterior Chest	RMS of 2nd of 10 Segments on the Respiratory Signal.
1.002	145	5: Upper Posterior Chest	RMS of 2nd of 10 Segments on the Wavelet Co-efficients Level 5 Node 6.
0.998	145	6: Middle Posterior Chest	RMS of 2nd of 10 Segments on the Wavelet Co-efficients Level 5 Node 6.
0.991	67	5: Upper Posterior Chest	RMS of 2nd of 10 Segments on the Respiratory Signal.
0.980	15	3: Lower Clavicle	RMS of 2nd of 10 Segments on the Respiratory Signal.
0.979	106	2: Upper Clavicle	RMS of 2nd of 10 Segments on the Wavelet Co-efficients Level 5 Node 2.
0.961	184	5: Upper Posterior Chest	RMS of 2nd of 10 Segments on the Respiratory Signal.
0.959	37	4: 2nd Intercostals space	Mean of the FFT of Entire Respiratory Signal.

Preceding any conclusions to the validity of such findings was the design and optimization of a neural network to categorize the data automatically into its respective healthy or TB participant groups using the above data as inputs.

6.2 Configuration of Neural Network

Artificial Neural Networks (ANNs) are widely used in the biomedical field for modeling, data analysis, and diagnostic classification procedures. The effectiveness of an ANN to correctly classify recordings into its respective healthy and unhealthy categories was investigated using the highest scoring SOF parameters as inputs to the NN.

Finding the optimal NN training algorithm was achieved using cross-correlation validation (CV) approach across four different training algorithms (Kandaswamy *et al.*, 2004). These algorithms were:

- Adaptive learning rate back propagation (BP).
- Resilient BP.
- Scaled conjugate gradient.
- Levenberg-Marquardt algorithm.

Execution of the CV approach partitioned the available healthy and TB data into six sections whereby the learning model was trained on five of the six partitions and tested on the sixth partition. A system evaluation parameter in Matlab provided a mean absolute error for that particular training and testing round after which one of the five partitions was rotated with the sixth partition to yield a second round of training and testing data sets. This procedure was repeated six times of which the average mean absolute error was obtained over the six rotations.

Subsequently, the number of input parameters was varied between five and 15 input parameters using the top five to top 15 parameters belonging to the highest SOFs as listed in Table 14. Additionally the tolerance on the NN was varied between 0.1 and 1 with the CV technique being used to evaluate each.

Pre-analysis of the training performance across different input parameter numbers and tolerance levels indicated the optimal number of input parameters to be 14 and tolerance level 0.4, respectively. These results are justified with Figure 58 and Figure 59 showing the *resilient BP* training algorithm to have the lowest error[23] for a tolerance of 0.4 and number of input parameters at 14.

[23] Correlates to findings by (Kandaswamy *et al.*, 2004)

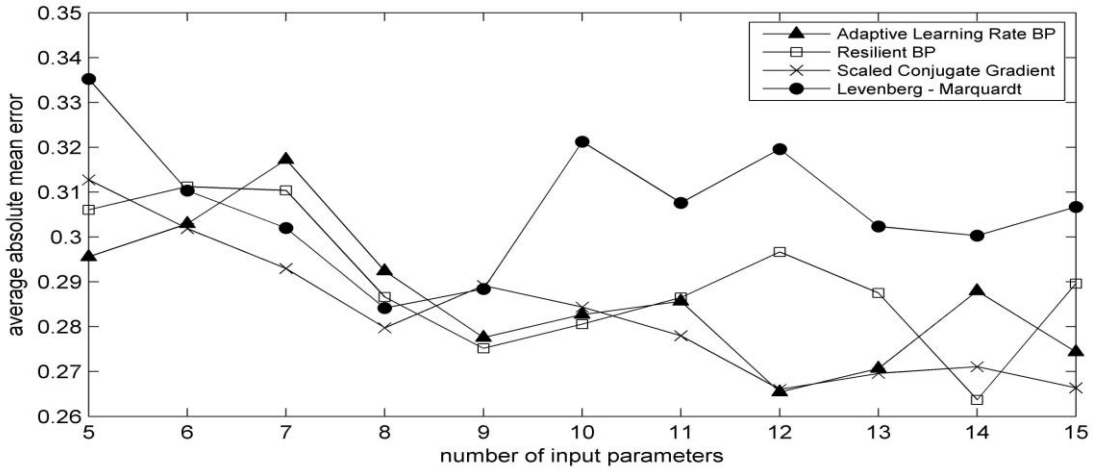

Figure 58: NN Training Evaluation for varying input parameters

For Figure 58 the tolerance was fixed at 0.4 illustrating the resilient backpropagation to have the lowest error of 0.63 which is the same performance for resilient backpropagation at a tolerance of 0.4 in Figure 59.

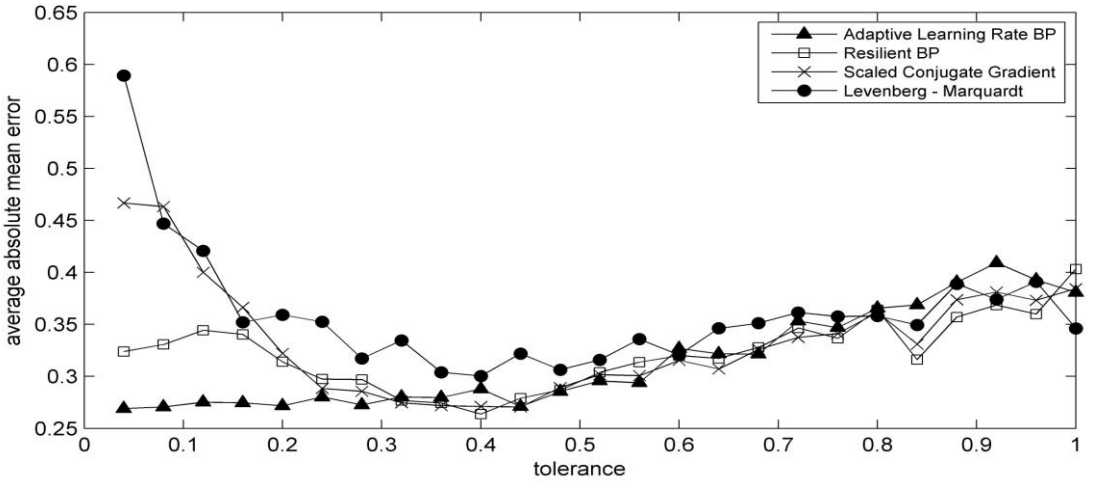

Figure 59: NN Training Evaluation for varying input parameters

Therefore it was decided to use the backpropagation algorithm along with a tolerance of 0.4 and using the top 14 input parameters from Table 14.

6.3 Evaluation of Network Configuration

The detection performance of the algorithm is depicted in terms of the ability of the NN to categorize the data successfully into its respective healthy and unhealthy categories. This means a network can one of four possible outcomes:

- A True Positive outcome where the NN correctly identifies the breath as having pulmonary TB.
- A False Positive outcome where the NN identifies a breath as having pulmonary TB when in fact it does not.
- A true Negative where the NN correctly identifies the recording as having no pulmonary TB.
- A False Negative where the NN identifies the breath as not having pulmonary TB when in fact it does.

The measures defined below indicate the performance of the NN in quantative terms being the sensitivity (SE), likely hood of the NN to maintain its decision, the specivity (SP), indicates confidence, and the accuracy (AC), the overall correctness of the NN. The formulas for the SE, SP, AC are listed below where TP, TN, FP, and FN are the number of true positive, true negative, false positive, and false negative pulmonary Tuberculosis detections, respectively:

$$SE = \frac{TP}{TP + FN} \tag{6.2}$$

$$SP = \frac{TN}{TN + FP} \tag{6.3}$$

$$AC = \frac{TN + TP}{TN + TP + FN + FP} \tag{6.4}$$

The performance of the NN parameters was evaluated by fixing the training data and testing data. Therefore the NN was trained on a data set and tested on a smaller data set that comprised of data taken from the training set. Therefore the NN was in essence tested on data it had already seen in the training phase. The CV approach performed still maintained a system of rotating and testing the data six times but ensuring that the testing set was always comprised of the training set. The CV approach was repeated 10 times, taking the average of the six CV TP, TN, FP, FN and then averaging the ten average TP, TN, FP, FN performances. These averaged TP, TN,

FP, FN values yielded an average and repeatability study of SE, SP and AC. The results are summarized in Table 15[24]

Table 15: Testing of Configuration Settings

Initial Setup	
Num Input parameters	14
Hidden layers	1
Num neurons	28
Epochs	500
Training method	Resilient Back Propagation
Network Training	
Training data size	5/6th of data
Healthy Participant	5/6 * 156 = 130 breaths
TB Participant	5/6 * 186 = 155 breaths
Testing data size	Taken from training data
Healthy Participant	26
TB Participant	31
Performance	
Evaluation Method	Cross Validation
Measures	TP=Correct Evaluation that Participant has TB
True Positives (TP)	
Overall Average	27.83
False Positives (FP)	
Overall Average	3.17
True Negatives (TN)	
Overall Average	21.17
False Negatives (FN)	
Overall Average	4.83
NN Configuration Sensitivity	**85.21 %**
NN Configuration Specificity	**86.98 %**
NN Configuration Accuracy	**85.96 %**

The results above indicate favorable testing conditions but do forewarn that the NN can lack confidence in its decisions when presented on making a choice on data it has already been trained on.

[24] Data Provided in Appendix J

The following section provides an evaluation of the same NN setup by testing the NN on data that had not been used in the training set. In turn this evaluates the overall diagnostic capabilities of the NN to foreign patient data.

6.4 Reliability of Chosen Signal Measurements

Final NN system conditions and performance are shown in Table 16 with specificity, sensitivity and accuracy calculated as an average of six trial runs swapping the data used for training and testing as with the CV approach.

The evaluation made use of the full data set, dividing it into five sixths of the data for training and the last sixth for testing. The last sixth was then rotated to the front of the data set and training and testing repeated again. This was repeated six times fulfilling the CV method.

In turn this CV method was also repeated ten times to justify the repeatability of the CV approach to the network. The results are presented in Table 16[25].

Table 16: reliability and Performance of NN

Initial Setup	
Num Input parameters	14
Hidden layers	1
Num neurons	28
Epochs	500
Training method	Resilient Back Propagation
Network Training	
Training data size	5/6th of data
Healthy Participant	5/6 * 156 = 130 breaths
TB Participant	5/6 * 186 = 155 breaths
Testing data size	1/6th of data
Healthy Participant	1/6 * 156 = 26 breaths
TB Participant	1/6 * 186 = 31 breaths
Performance	
Evaluation Method	Cross Validation
Measures	TP=Correct Evaluation that Participant has TB
True Positives (TP)	
Overall Average	25.57
False Positives (FP)	
Overall Average	5.43

[25] Data Provided in Appendix J

True Negatives (TN)	
Overall Average	20.73
False Negatives (FN)	
Overall Average	5.27
NN Sensitivity	**82.91 %**
NN Specificity	**79.24 %**
NN Accuracy	**81.23 %**

When considering that the NN used crackle and frequency parameters, the above results compare favorably when compared to previous papers that investigated crackle classification. Such papers include accuracy results of 80-100 % to distinguish between FC, CC and Squawks in research by Hadjileontaidis (2003) and multiple researches on the significance of crackle parameters in diseases such as fibrosis, asbestosis, bronchiectasis, COPD, heart failure, pneumonia and sarcoidosis, summarized in a paper by Piirila and Sovijärvi (1995). With this project's result, it seems plausible to add crackle parameters in pulmonary TB to the above-mentioned list of diseases. This would, however, include a significant in-depth analysis into what type and degree of crackles are specifically unique to pulmonary TB that may differentiate it from other respiratory diseases as well as a larger patient scope being tested. Nevertheless, this project has highlighted a key component to an often ignored respiratory disease and deserves consideration in the development of emerging real-time classification techniques such as k-NN classifiers yielding accuracy between 92-100 % (Alsmadi and Kahya, 1996) in clinical environments as discussed by Alsmadi (2006).

7 Conclusions and Recommendations

7.1 Conclusions

With advances beyond the traditional stethoscope, opportunities exist to study respiratory sounds beyond conventional auditory judgment. Capabilities to record and store respiratory action will aid medical practitioners to compile and archive larger and more effective patient portfolios when combined with consultation reports and medical images. This fronts an opportunity to compile patient profiles including medical images, sounds and inspection alike.

With the application of computer technology comes a better understanding and measurement of pulmonary acoustics and a new relevance to clinical significance. Computer analysis is developing beyond that of the human ear and clearly exhibits a much wider range of data when analyzed digitally. Such factors become a powerful tool when combined with the digital information exchange capabilities of the internet as well as portable computer devices allowing ambulant and bedside diagnosis and monitoring of patients.

Electronic auscultation remains fairly new and unexplored, with standardization occurring as late as 2000. Thus, one should not expect computer-based auscultation to replace the stethoscope-bearing clinician anytime soon, but a call for new, innovative, portable and cheap diagnostic techniques towards pulmonary health should justify the need to further develop and evaluate the importance of computer aided sound analysis in medical applications.

One such diagnostic application relevant to this thesis was pulmonary tuberculosis. Statistics and WHO reports have indicated the disease worthy of attention and is particularly prevalent in South Africa and other developing countries.

In an attempt to justify and defend accusations that diagnosis of the disease cannot be achieved through auscultation, a project was set to fully investigate a wide range of signal analysis techniques in a search for any measurement unique to pulmonary Tuberculosis and different to that of a healthy respiratory system.

Project planning included designing a hardware device capable of recording and digitizing respiratory sound action from various locations across the anterior and posterior chest and compiling a data set of healthy and unhealthy (TB infected) respiratory breaths. Digital editing and adaptive filtering executed successful removal of environmental noise and low frequency heart and muscle disturbances before being analyzed. Analysis of the signal yielded 202 unique signal features per microphone across seven microphones, per lung. Such values covered a wide range

of data including insight into the time, frequency and adventitious natures of wheezes and crackles.

Of the 202 values, a statistical overlap factor indicated the values with the highest degree of separation between healthy and unhealthy recordings which were successively selected as possible inputs in a neural network for automated categorizing of the data into its healthy and unhealthy groups. Network optimization included a cross-validation approach across four different training algorithms of which final network error evaluation proved the top 14 input measurements needed to be used.

A final neural network system comprising of 14 input parameters, one hidden layer and cross validation training using resilient backpropagation, yielded an overall accuracy of 81.23 %.

When observing the fact that 4 out of the 14 input parameters belonged to the mean of the FFT of the time signal, and three of the 14 input parameters belong to the RMS of Daubechies wavelets, a presumption exists that TB patients may well exhibit more frequent crackle parameters. Such parameters are exposed with TB wave characteristics that match better to scaled and shifted versions of the Daubechies wavelet (as compared to healthy participants) which in turn adds energy contributed by high frequency components in the FFT, thus altering the mean value. Confirmation of such ideologies are further confirmed with the remaining input parameters and highest scoring statistical overlap factors also belong to Daubechies wavelet packets.

As a side note, wheeze detection did not yield worthy results for differentiation of pulmonary TB and healthy respiratory recordings. Although it should be noted that the method used was of a very personal and specific nature. Furthermore, statistical data such as averages, ranges and minimum and maximum values performed on wavelet co-efficients did not contribute to the list of input parameters for the NN.

Given the wide arrangement of analysis completed using basic tools within a limited time frame, these findings are in no means fit to revolutionize the auscultation industry, especially with reference to pulmonary Tuberculosis diagnosis. The success of categorizing the recordings mentioned above merely justifies the capabilities and opportunities that exist with the combined effort of medical practitioners and engineers. An extension of the sample population for future work is imperative to be able to justify these promising results as clinically publishable.

Future work would include system hardware and software performance improvement along with repeatability studies and are highlighted in the section that follows.

7.2 Recommendations

The largest threat to any sound analysis is analyzing sound that should not be there. The comprehensive and successful execution of signal analysis for the project was vulnerable to environmental testing conditions in the clinics as well as difficulty in maintaining constant deep inspiratory and expiratory breath maneuvers with TB participants suffering severe damage to the respiratory area. In turn healthy participants often exhibited what is known as “white coat syndrome” where by the physiological realization by the participant that they are being recorded prohibits them from truly breathing at regular tidal or deep breaths.

In addition, artifacts such as the participants coughing, adhesive tape coming loose, high degree of electrical disturbance and environmental noise all contributed to certain recordings being labeled unusable and resulted in frequent re-recordings.

As a recommendation to improve the above problems the following applications and improvements to hardware were noted:

- Even though application of a portable diagnostic device is favored to be available in most commonly rural clinics the validation of this trial needs to be confirmed with recordings possessing noise <45 dB as recommended by CORSA (Rossi *et al.*, 2000). Such recordings are then achievable by relocating participants to a testing room guaranteed to be shielded against such noise conditions.
- Moreover the addition of one extra microphone should be available solely to record environmental noise which should be subtracted from the respiratory signal at hardware level before digitization from analogue to digital.
- Even though short-term recordings are recommended to be taken in the supine position, the adhesion of microphones to the skin can be improved through embedment of the microphone housing in foam-like mattresses. Such a design permits the use of the patient’s weight to apply contact to the microphone housings other than relying on the adhesion performance of the double-sided tape.
- The true potential of the ZonicBook can be optimized with the correct application to high performance laptops thus allowing for increased sampling rates and higher resolution recordings. Optional software should also be incorporated to allow real-time viewing of the entire recording so as to evaluate data quality on site. This would inhibit the difficulty of only evaluating a recording once it had been plotted after participants had left.

Given the broad spectrum of analysis completed in this project the conclusion can motivate further research to focus more intensely on the aspects of crackle analysis and frequency domains. This would be achieved through:

- Increasing the window size performed on the Fourier transform and short time Fourier analysis. By increasing the window size the resolution of frequency steps that are analyzed become finer. For this project a window size of 1024 points on the Fourier transform on 6000 Hz digital sampling meant that a resolution of 5.8 Hz was maintained which could be refined for a more detailed analysis.
- With the infectious nature of tuberculosis, mouth pieces or air flow meters could not be implemented. Inhaling and exhaling positions could only be measured through the piezo-electric chest strap used in the project. A further point for debate is the fact that all recordings where calibrated between maximum amplitude of one and minimum of zero. With all recordings having these ranges of normalization a large adjustment is made to the data in the sense that all participants have the same maximum breathing respiratory loudness. This in turn altered the entire analysis to studying the maximum frequency and shifts in frequency components but in no way supplies quantative data on amplitudes. This fact needs urgent addressing with further research done on supplied disposable flow meters and recordings done at fixed and varied flow rates. Such data would research the nature of sound and frequency amplitude at different flow rates which influence the amplitude of respiratory sounds (Rossi *et al.*, 2000).
- The application of wavelets to signals is a successful and widely used application that can be approved with confidence in this project. Wheeze detection using spectral analysis requires the resolution of the spectrogram to be fairly high as well as high level of knowledge in programming to extract the trends. The routine developed in this project was tested against three samples downloaded from the internet specified as characteristic wheeze recordings. Further testing on three healthy participant recordings also tested the wheeze algorithm designed for this project to be 100 % successful, however having only used three healthy and three unhealthy trial runs to evaluate the performance, the true effectiveness of analyzing the wheeze characteristics over the entire participant data set remains questionable and subject to improvement. Most modern algorithms developed in 2008 include making use of histograms of sample entropy for wheeze detections (Jin *et al.*, 2008) and are less computationally intensive than having to compute high time and frequency resolution spectrograms.

Literature warns of crackle characteristics being lost temporarily when a participant clears his/her throat or coughs (Gnitecki and Moussavi, 2007) and this was noted with many recordings in this project showing a high variability in wavelet crackle analysis between the breaths of a single participant. Therefore three or preferably more than three breaths need to be maintained per patient in order to maintain an

average over the three breath cycles. Furthermore, a larger patient scope needs to be addresses with specific focus on what areas of the lungs are infected with TB and aligned with the position of microphone.

Spectral analysis using STFT poses a resolution tradeoff since good time localizations requires a small time window whereas a good frequency location requires a small window in the frequency domain, which is the inverse to time domain and thus actually a larger window than the time domain. Thus alternative techniques should be investigated to improve time and frequency localizations that could also assist the analysis on the specific crackle shape, as neglected in this project. The empirical mode decomposition (EMD) is a technique for processing non-linear and non-stationary signals. Emerging techniques in 2008 indicate the successful use of EMD's to identify intrinsic modes (IMF's) and represent those modes as a Hilbert-Huang spectrum. Such spectrums relate better to the emerging crackle wave shape in relation to TEWA and could thus be used as a means to analyze the type and time localization of crackles (Reyes *et al.*, 2008).

As a final long-term goal, after the justification of such findings mentioned above, a further scope for research would be the monitoring of the consistency of relevant characteristics found during the recovery period of a pulmonary TB patient. If these characteristics are consistent throughout a patient's recovery from TB it can be concluded that although lungs heal from TB the physical and acoustic damage is permanent. If the characteristics return to those of healthy people it can be concluded that after healing the respiratory system returns to normal acoustically and this in turn justifies the recording during recovery to serve as a surrogate marker.

7.3 Final Thoughts

Although there has been a drastic advancement and improvement in electronic respiratory sound analysis it has yet to find its place in the clinical field. From this project it is evident that even with basic hardware and relatively unstable recording environments, it is possible to filter and analyze respiratory recordings whereby useful parameters can be extracted.

Among the common applications of electronic respiratory analysis are the recording and exchange of respiratory action, presentation of important wave parameters and the creation of records of these presentations for better patient profiling, patient monitoring and recovery (Earis and Cheetham, 2000).

Disadvantages such as increased cost and physical size are decreasing with the further developments, portable technology and brand competitive pricing. Such

factors allow for portability to remote locations, often the case with doctors visiting clinics, or the opportunity for most medical staff to have a personal computer and recording device in their practice.

References

A.D.A.M. (2008). *Respiratory System Information*. [online]. [Accessed 11 Sept 2008]. Available form World Wide Web: <http://pennhealth.com/health_info/body_guide/reftext/html/resp_sys_fin.html#intro>

Abhishek, J. and Jithendra, V. (2008). Lung Sound Analysis for Wheeze Episode Detection. *In*: *30th Annual International IEEE EMBS Conference, 2008*. Vancouver,:, pp.2582 - 2585.

Alsmadi, S. and Kahya, Y. P. (1996). Design of a DSP-based Instrument for Real-time Classification of Pulmonary Sounds. *Comp. Biol. Med.*,Vol. **38**, pp.53-61.

Blaivas, A. J. (2005). *Pulmonary Tuberculosis Health Article*. [online]. [Accessed Mar 2007]. Available form World Wide Web: <http://www.healthline.com/adamcontent/pulmonary-tuberculosis>

Charbonneau, G., Ademovic, E., Cheetham, B., Malmberg, L., Vanderschoot, J., and Sovijärvi, A. (2000). Basic Techniques for Respiratory Sound Analysis. *Eur. Respir. Rev*,Vol. **10**(77), pp.625-635.

Cheetham, B., Charbonneau, G., Giordano, A., Helistö, P., and Vanderschoot, J. (2000). Digitization of Data for Respiratory Sound Recordings. *Eur. Resp. Rev.*,Vol. **10**(77), p.621–624.

Conte, E., Vena, A., Federici, A., Giuliani, R., and Zbilut, J. (2004). A Brief Note on Possible Detection of Physiological Singularities in Respiratory Dynamics by Recurrence Quantification Analysis of Lung Sounds. *Chaos, Solitons and Fractals*,Vol. **21**, p.869–877.

Deep Breeze Ltd. (2008). *Deep Breeze - VRIxp*. [online]. [Accessed 12 May 2008]. Available form World Wide Web: <http://www.deepbreeze.com/deepbreeze/home/products/vrixp.aspx>

Earis, J. and Cheetham, B. (2000). Current Methods used for Computerized Respiratory Sound Analysis. *Eur. Resp. Rev.*,Vol. **10**(77), pp.586-590.

Earis, J. E. and Cheetham, B. M. (2000). Future Perspectives for Respiratory Sound Research. *Eur. Resp. Rev.*,Vol. **10**(77), p.641–646.

Enderle, J., Blanchard, S., and Bronzino, J. (2005). *Introduction Biomedical Engineering 2nd Edition*. London: Elsevier Academic Press.

Ethnomed.org. (2005-2007). *Treating Drug-Resistant Tuberculosis*. [online]. [Accessed 7 Aug 2007]. Available form World Wide Web: <http://ethnomed.org/ethnomed/clin_topics/tb/cdc_resistance.html>

Farabee, M. (2001). *The Respiratory System*. [online]. [Accessed Feb 2007]. Available form World Wide Web: <http://www.emc.maricopa.edu/faculty/farabee/BIOBK/BioBookRespsys.html>

Fauci, A. S. (2007). *World TB Day March 24,2007*. [online]. [Accessed May 2008]. Available form World Wide Web: <http://www3.niaid.nih.gov/about/directors/news/tb_07.htm>

Figola, R. and Beasley, D. (2000). *Theory and Design for Mechanical Measurements.* New Jersey: John Wiley & Sons, Inc.

Gnitecki, J. and Moussavi, Z. M. (2007). Respiratory Sound Analysis. *Medicine and Biology Magazine*, pp.20-29.

Gnitecki, J., Moussavi, Z., and Pasterkamp, H. (2003). Recursive Least Squares Adaptive Noise Cancellation Filtering for Heart Sound Reduction in Lung Sounds Recordings. *Proc. IEE. ENG. Med. Biol Soci*,Vol. , pp.2416-2419.

Grosset, J. (2003). Mycobacterium Tuberculosis in the Extracellular Compartment: An Underestimated Adversary. *Antimicrob. Agents. Chemother.*,Vol. **47**(3), pp.833-836.

Güler, I., Polat, H., and Ergün, U. (2005). Combining Neural Network and Genetic Algorithm for Prediction of Lung Sounds. *J. Med. Sys.*,Vol. **29**(3), pp.217-231.

Hadjileontiadis, L. (2003). Discrimination Analysis of Discontinuous Breath Sounds using Higher-Order Crossings. *Med. Bio. Eng. Comput*,Vol. **41**, pp.445-455.

Jain, A. and Vepa, J. (2008). Lung Sound Analysis for Wheeze Episode Detection. *In*: *30th Annual International IEEE EMBS Conference, 2008*. Vancouver, British Columbia: IEEE, pp.1582 - 2585.

Jin, F., Sattar, F., and Goh, D. (2008). Automoatic Wheeze Detection Using Histograms of Sample Entropy. *In*: *30th Annual International IEEE EMBS Conference, 2008*. Vancouver: IEEE, pp.1890 - 1893.

Kandaswamy, A., Kumar, C., Ramanathan, R. P., Jayaraman, S., and N. Malmurugan. (2004). Neural Classification of Lung Sounds using Wavelet Coefficients. *Comp. Biol. Med.*,Vol. **34**, p.523–537.

Kraman, S. S., Wodicka, G. R., Pressler, G. A., and Pasterkamp, H. (2006). Comparison of Lung Sound Transducers using a Bioacoustic Transducer. *J. App.Phys.*,Vol. **101**, pp.469-476.

Majumder, A. K. and Chowdhury, S. (1981). Recording and Preliminary Analysis of Respiratory Sounds from Tuberculosis Patients. *Med. & Biol. Eng. & Comput*,Vol. **19**, p.561 564.

Majumder, A. K. and Chowdhury, S. (1981). Recording and Preliminary Analysis of Respiratory Sounds from Tuberculosis Patients. *Med. & Biol. Eng. & Comput*,Vol. **19**, pp.561-564.

MAYO Clinic Staff. (2006). *Infectious Disease: Tuberculosis*. [online]. [Accessed 16 Mar 2007]. Available form World Wide Web: <http://www.mayoclinic.com/health/tuberculosis/DS00372>

Misiti, M., Misiti, Y., Oppenheim, G., and Poggi, J.-M. (2006). *Wavelet Toolbox For Use with Matlab*. Natick: The MathWorks Inc.

Moore, D., Evans, C., and Gilman, R. (2006). Microscopic-Observation Drug-Susceptibility Assay for the Diagnosis of TB. *N. Engl. J. Med.*,Vol. **355**(15), pp.1539-1550.

National Institute of Allergy and Infectious Deseases. (1996). *Tuberculosis*. [online]. [Accessed 17 July 2007]. Available form World Wide Web: <http://www3.niaid.nih.gov/news/newsreleases/1996/tbtip.htm>

nursebob.com. (2007). *Breath Sounds*. [online]. [Accessed 12 Feb 2007]. Available form World Wide Web: <http://rnbob.tripod.com/breath.htm>

Parish, T. and Stoker, N. (1999). Mycobacteria: Bugs and Bugbears (Two Steps Forward and One Step Back). *Mol. Biotechnol.*,Vol. **13**(3), pp.191-200.

Pasterkamp, H., Kraman, S., and Wodicka, G. (1997). Respiratory Sounds: Advances Beyond the Stethoscope. *Am. J. Respir. Crit. Care. Med.*,Vol. **156**, p.974–987.

Piirilä, P. and Sovijärvi, A. (1995). Crackles: Recording, Analysis and Clinical Significance. *Eu. Respir. J.*,Vol. **8**, pp.2139-2148.

PixSoft Inc. (2007). *The R.A.L.E Respiratory*. [online]. [Accessed 20 April 2007]. Available form World Wide Web: <http://www.rale.ca/Recordings.htm>

Reyes, B. A., Charleston-Villalobos, S., Gonzalez-Camarena, R., and Aljama-Corrales, T. (2008). Analysis of Discontinuous Adventitious Lung Sounds by Hilbert-Huang Spectrum. *In*: *30th Annual International IEEE EMBS Conference, 2008*. Vancouver: IEEE, pp.3620-3623.

Rossi, M., Sovijärvi, A., Piirilä, P., Vannuccini, L., Dalmasso, F., and Vanderschoot, J. (2000). Environmental and Subject Conditions and Breathing Manoeuvres for Respiratory Sound Recordings. *Eur. Respir. Rev.*,Vol. **10**(77), p. 611–615.

Sankur, B., Kahya, Y., Güler, E., and Engin, T. (1994). Comparason Of AR-Based Algorithims For Respiratory Sounds Classification. *Compw. Biol. Med.*,Vol. **24**(1), pp.67-76.

Sovijärvi, A., Malmberg, L., Charbonneau, G., Vanderschoot, J., Dalmasso, F., Sacco, C., Rossi, M., and Earis, J. (2000). Characteristics of Breath Sounds and Adventitious Respiratory Sounds. *Eur. Resp. Rev*,Vol. **10**(77), pp.591-596.

Sovijärvi, A., Vanderschoot, J., and Earis, J. (2000). Standardization of Computerized Respiratory Sound Analysis. *Eur. Respir. Rev.*,Vol. **10**(77), p.585.

Stethographics, Inc. (2007). *Multichannel STG™ System Overview*. [online]. [Accessed 19 June 2007]. Available form World Wide Web: <http://www.stethographics.com/main/products_multi_overview.html>

Taplidou, S. and Hadjileontiadis, L. (2007). Wheeze Detection Based on Time-Frequency Analysis of Breath Sounds. *Comput. Biol. Med.*,Vol. **37**, p.1073 – 1083.

The British Society for Antimicrobial Chemotherapy. (2008). *Multi-drug Resistant Tuberculosis*. [online]. [Accessed 5 Aug 2008].

The Institute of Fundamental Electronics. (2006). *Discontinuous Lung Sounds*. [online]. [Accessed 20 June 2007]. Available form World Wide Web: <http://www.ief.u-psud.fr/~gc/sounds.html>

Vannuccini, L., Earis, J., Helistö, P., Cheetham, B., Rossi, M., Sovijärvi, A., and Vanderschoot, J. (2000). Capturing and Preprocessing of Respiratory Sounds. *Eur. Respir. Rev.*,Vol. **10**(77), p.616–620.

World Health Oraganisation. (2006). *WHO Publications on Tuberculosis*. [online]. [Accessed Feb 2007]. Available form World Wide Web: <http://www.who.int/tb/publications/2006/tb_factsheet_2006_1_en.pdf>

World Health Organisation. (2006). *Global Tuberculosis Control: Surveillance, Planning, Financing*. Geneva.

World Medical Association General Assembly. (2004). *Declaration of Helsinki: Ethical Principles for Medical Research Involving Human Subjects*. Tokyo.

Yeginer, M. and Kahya, Y. (2007). Sensitivity of Pulmonary Crackle Parameters to Filter Cut-Off Frequency. *In*: *Proceedings of the 29th Annual International Conference of the IEEE EMBS, 2007*. Lyon, France:, pp.1062-1065.

Appendix A: ZonicBook Medallion Specifications

ZonicBook-Medallion Specifications

General Specifications

Environment

Operating: 0° to 50°C, 0° to 95% RH, non-condensing (ZonicBook only)

Storage: -20° to 70°C

Power Consumption: 8.5 watts max with +12 VDC power supply

Input Power Range: 9 to +15 VDC

Dimensions: 279 mm W x 216 mm D x 35 mm H (11" x 8.5" x 1.375")

Weight: 1.32 kg (2.9 lbs)

PC-Card (included): Requires one type III slot

PC-Card to ZonicBook Cable (included): 30 in.

Analog Inputs

Input Channels: 4, 8, or 16*

Input Connector: BNC

A/D: One 16-bit Sigma Delta converter per channel

Sampling: All input channels are sampled simultaneously, up to 51.2 kHz max per channel

Digital Decimation Filter: 92 dB stop-band attenuation

Dynamic Range: >80 dB typ

Amplitude Flatness: 1 dB typ

Bipolar Ranges: 25 mV to 25V full scale in 1.5 dB steps

Maximum Overvoltage: ±80 VDC

Input Bandwidth:
4- and 8-Channel ZonicBook: DC to 20 kHz
16-Channel ZonicBook: DC to 10 kHz

Input Coupling: AC, DC; switch selectable, per channel

AC Coupling: 1.6 Hz; -3 dB point

ICP Voltage (@ 4 mA): 24V ±.5V (no load), 20V bias max

Input Impedance

Single-Ended: 1M Ohm in parallel with 30 Pf

Differential: 2M Ohm in parallel with 30 Pf

Accuracy: 25 mV to 25V; ±2% (±0.2 dB)

Channel Match: +1 dB amplitude, +1° phase

Input Noise: ≤ ±3 LSB (RMS)

Total Harmonic Distortion: -62 dB typ

Signal to Noise and Distortion: -60 dB typ

Cross Talk: < 75 dB max; relative to full scale

Anti-Alias Filters: 80 dB alias rejection

Output Characteristics

Number of Channels: 1 BNC output per ZonicBook

Output Frequency Range: 2 kHz

Dynamic Range: 80 dB typ

Frequency Resolution: 0.001 Hz

Frequency Accuracy: 100 ppm

Amplitude Accuracy: 2.0% @ 1V; up to 1 kHz

Maximum Amplitude: 2.8V peak-peak

DAC Resolution: 16-bit Sigma Delta

Processing Characteristics

Analysis Frequency: 10 Hz to 20 kHz for 4- or 8-channel ZonicBooks; 10 Hz to 10 KHz for 16-channel ZonicBook; All input channels are sampled synchronous; Analysis Rate is set for all channels

Blocksize: 128 to 16,384 data samples per block of data (in powers of 2)

FFT Windows

Response Channels: None, Hanning, Flat Top, Exponential, 3 Term Blackman Harris

Force Channels: None, Rectangular, Cosine Taper

Integration/Differentiation (in frequency domain): Single and Double Differentiation; Single and Double Integration

Averaging: Linear, Exponential, Negative, Peak Hold, Time Synchronous

Acquisition Triggers: Free Run

User-Programmed Trigger: Level and Slope, Time and Date, Pre or Post data trigger delay

Octave Filter: A, B, and C Weighting

Display Types: Time, Trend, Auto Spectrum, Cross Spectrum, Spectrum, FRF, PSD, Transfer Function, 1/3 Octave, Full Octave, Coherence

Transfer Function Types: Inertance, Mobility, Compliance, Apparent Mass, Impedance, Dynamic Stiffness

Octave Types: 1/3, Full

Figure A- 1: ZonicBook Data Sheet

Appendix B: Microphone Housing Design

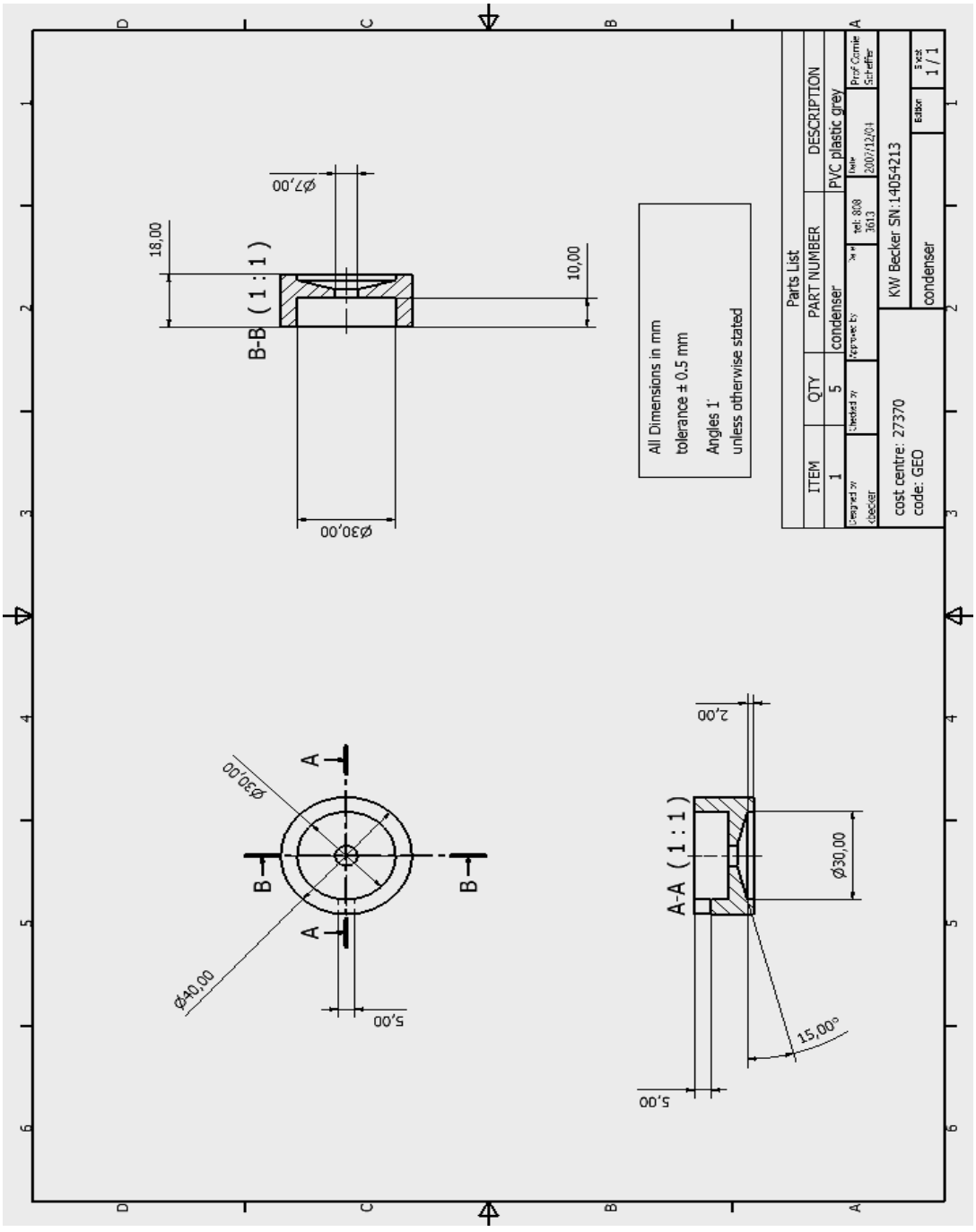

Figure B- 1: Housing Design

Appendix C: Schematic & Printed Circuit Board Designs

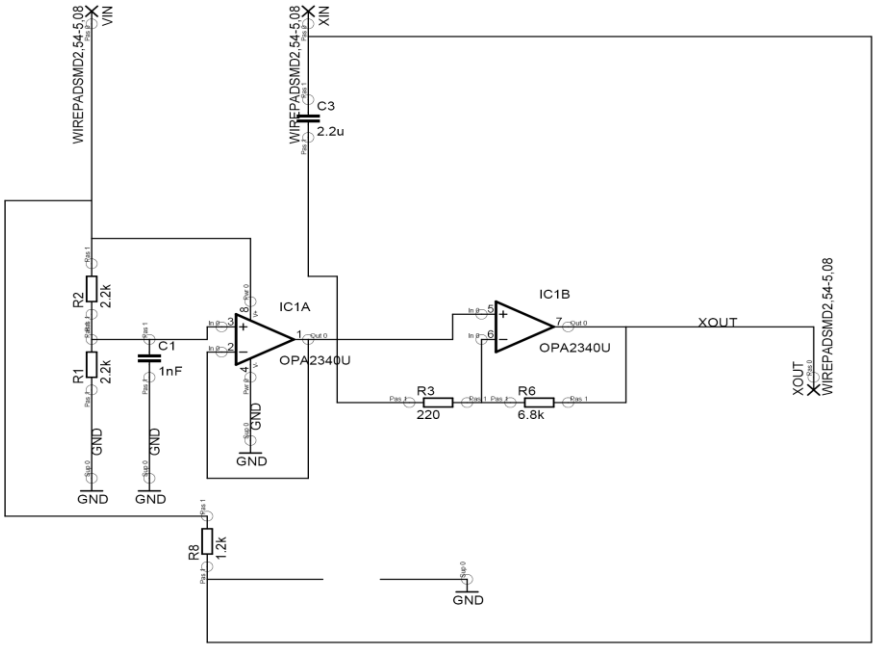

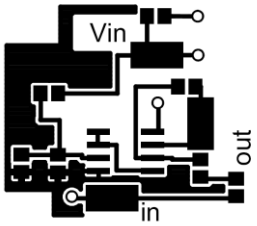

Not to scale

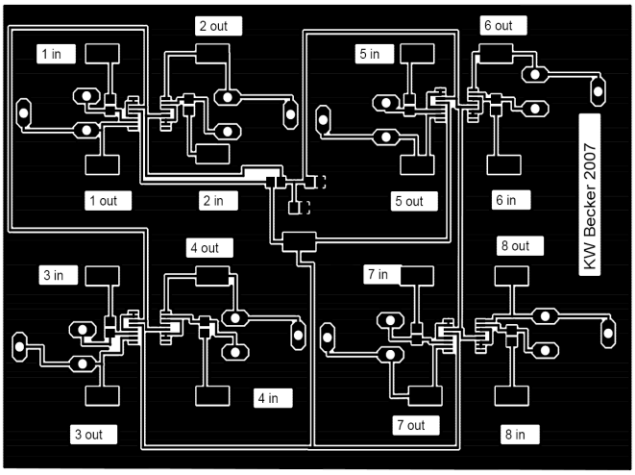

Not to scale

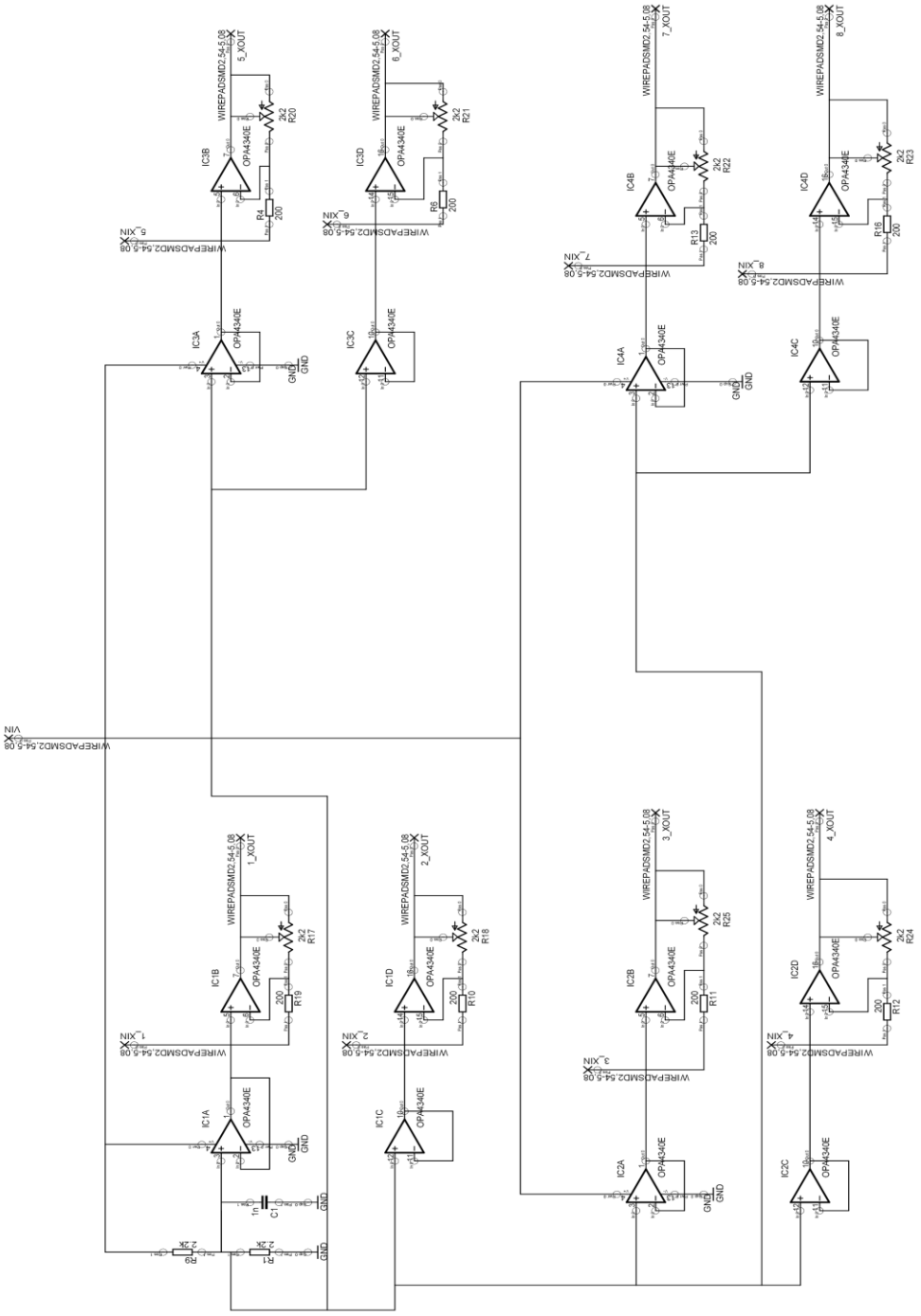

Appendix D: Effect of Aliasing Frequencies

When sampled an analogue signal is converted into a number at given time increments. These time increments are dependent on the sampling frequency which can play a significant role of reconstruction of the signal in digital form.

An example of this is where an analogue signals is sampled at a sampling frequency of <2 fm where fm is the maximum frequency (called the *nyquist* frequency). Because of the lower sampling frequency, a misinterpretation occurs in the result of an alias signal, as shown in Figure D- 1. (Figola and Beasley, 2000). When sampling an analogue signal to obtain it in digital form a phenomenon known as “aliasing” occurs. Aliasing is defined as a false frequency that can occur when a signal is sampled at a lower rate than at least double its highest frequency (Figola and Beasley, 2000). The nyquist frequency is defined as the minimum sampling frequency allowed when sampling the analogue domain to avoid aliasing and given by the formula:

$$f_s \geq 2f_m \tag{D1}$$

Where f_s is the sampling frequency.

Figure D- 1 illustrates a signal comprised of multiple frequencies ranging from 1550 Hz – 2150 Hz. The signal is sampled at 2000 Hz which is <2x maximum frequency. Therefore aliasing occurs which is seen in the reconstructed signal in the lower diagram of Figure D- 1.

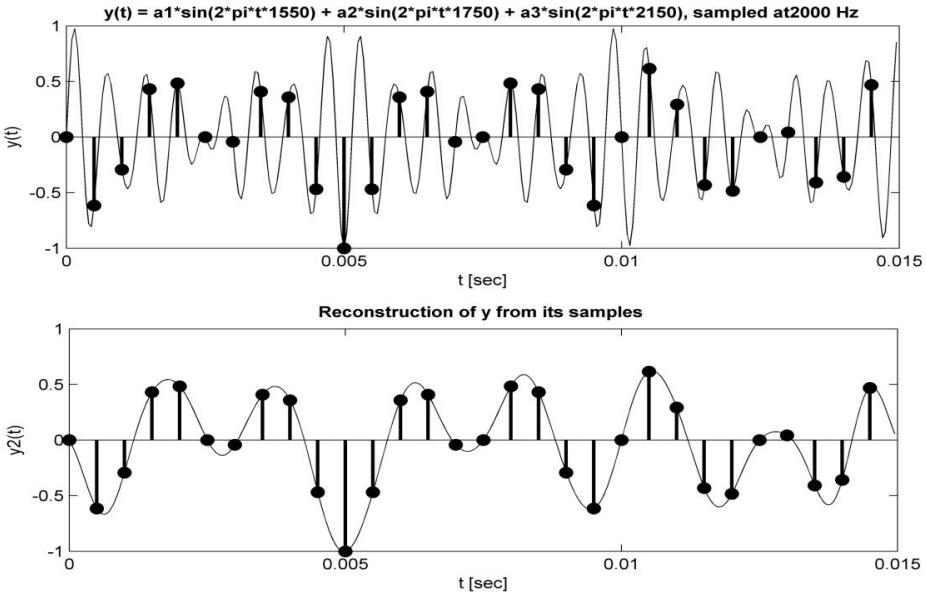

Figure D- 1: Aliasing Example

Appendix E: Illustrations of Graphical User Interfaces

The following illustrations show the three GUI's designed to successfully execute the necessary data preparation and signal analysis.

Figure E- 1 illustrates the "Open And View" GUI. Original recordings are loaded using the 'Load' button and plotted using the 'Run' button. Visual inspection of the first window would confirm correct breathing patterns and the further seven windows would allow for a decision of the quality of the recording. If satisfied the 'create and save' button would save the data in a matrix of eight columns (microphone 1 – 7 and respiratory strap in column 8). This matrix could be loaded into the Matlab ® workspace for further use.

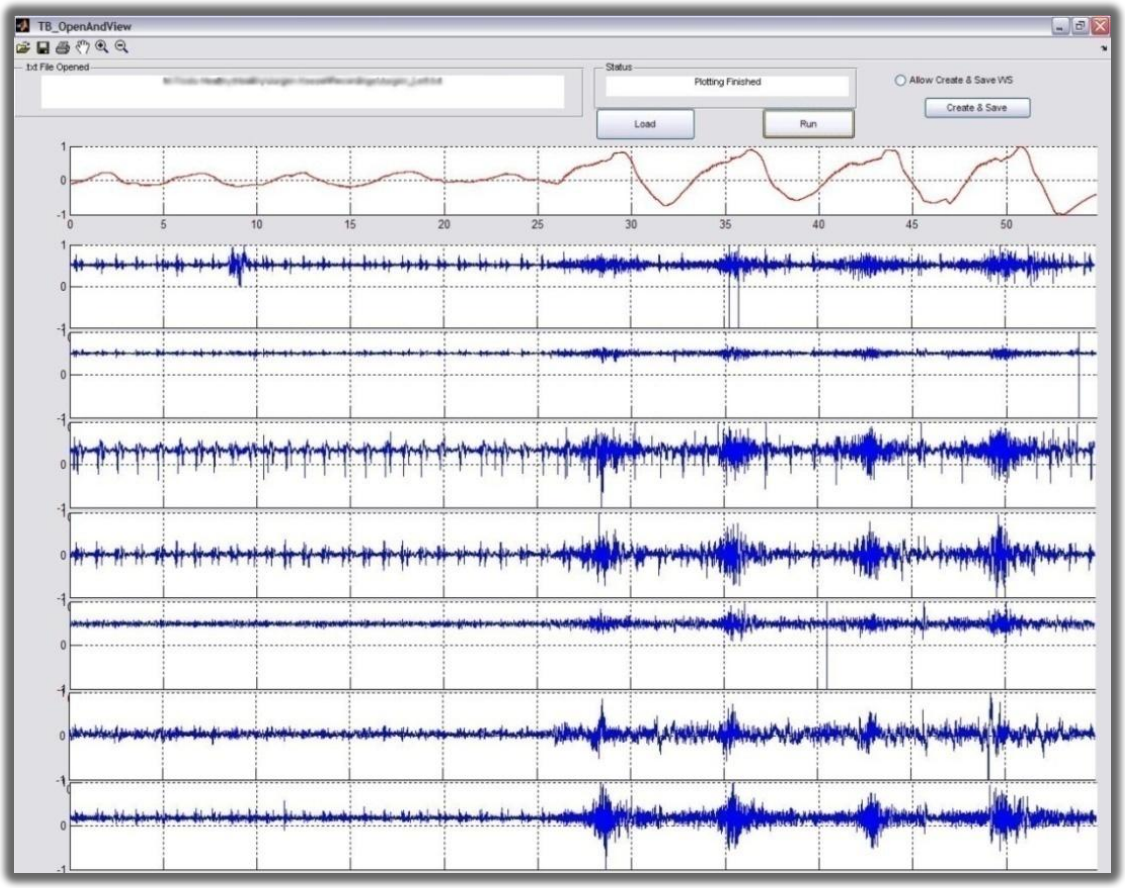

Figure E- 1: Open And View GUI

Figure E- 2 is an illustration of the following step to filter and split the respiratory recordings. Achievement of this was through the "Filter And Split GUI". The GUI

comprises of seven individual windows each with a separate 'Load' button to provide separate recordings from the same participant to be loaded individually. This insured that from a session of three recordings on the same chest, all the best quality breath cycles could be individually chosen and loaded.

Successive 'Filter' buttons carried out the task of opening simulink models to remove low frequency heart and muscle sounds as well as environmental noise. The output from the filters was 'Imported' back into the GUI and buttons on the far right executed the splitting of deep breaths into individual single breath data vectors.

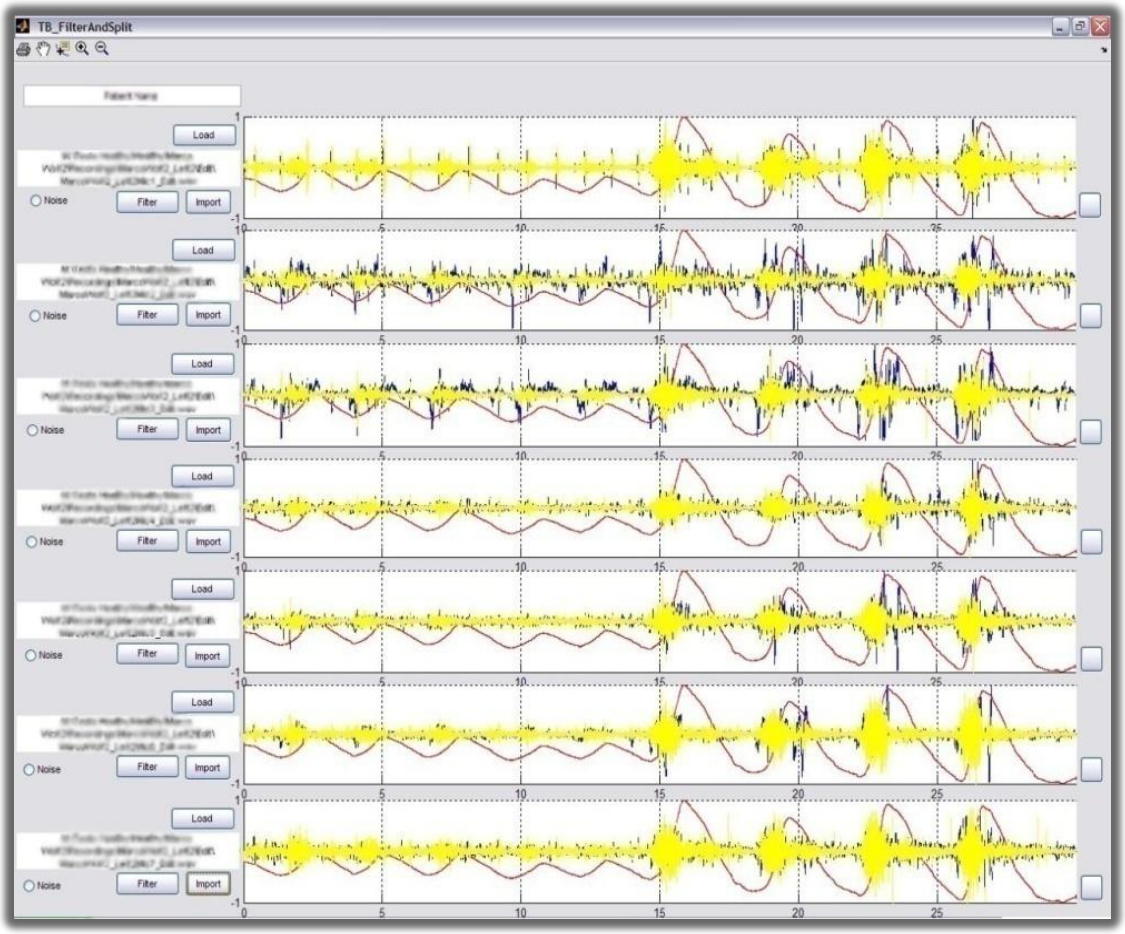

Figure E- 2: Filer And Split GUI

The third and final "TB Auscultation GUI" loaded the data from the previous GUI, illustrating them in separate windows (Figure E- 3). This can be seen in with the seven microphones placed in rows and three separate breath cycles in columns.

Loading of data was through the 'Load' button after which the 'Analyze' button performed all analysis techniques as described in Chapter 5.

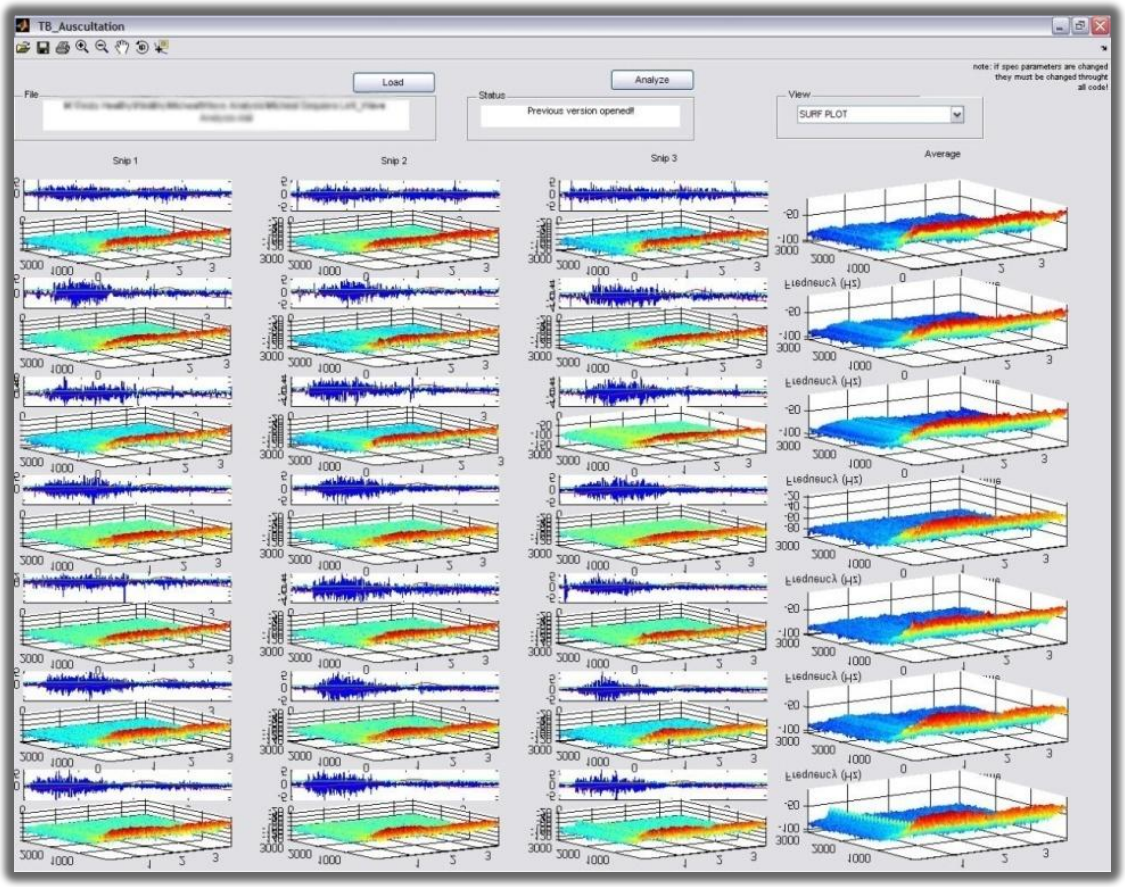

Figure E- 3: Auscultation GUI

Visualization on calculation of SOF factors for the data from the "TB_Aucultation" GUI was done separately using m.code files in Matlab and manual plotting of characteristics.

Appendix F: Organization of Data Measurements

Table F- 1 below provides an in-depth observation into the analysis and characteristic numbers allocated to signal analysis for the project. This includes the arrangement of data for the four time, frequency, wheeze and crackle analysis's done.

Table F- 1: Structure of Data Analysis

Signal Characteristic Name	Description	Characteristic Number
Timesig:		
Time	Data to plot the time signal	
rms	Root Mean Square of the entire breath signal.	1
Crstfac[1]:	Crest factor of the time signal.	2-13 [1]
Str8t (10x1)	Crest Factor of ten segments of signal.	2-11[1]
max	Maximum of those ten crest factors.	12 [1]
Avg	Average of all ten crest factors.	13 [1]
Segrms (10x1)	Root mean square of ten segments of signal.	14-23
segenergyV - totenergy (10x1)	Energy of each segment divided by energy of whole signal.	24-33
FFT:		
FreqMag	Vector of amplitudes at various frequencies.	
Maxampl – AND - pos	The position and value of the frequency with the highest amplitude.	34-35
Maxamp – V - totArea	Highest amplitude divided by the total area under the FFT plot.	36
Mean	The mean of the FFT.	37
Oct [4^2,8^3,16^4,32^5,64^6,128^7,256^8,512^9]:	Signal is broken into octave bands each 2^n wide where n is the position number.	38-45
octArea – V - totArea	Area of the octave segment divided by the total area of the FFT.	38^2,39^3,40^4,41^5, 42^6,43^7,44^8,45^9
WHEEZE:		
answer	Answer if wheeze signal characteristics are present in the signal or not.	46
CRACKLE:		

Wave Co-ef	Wavelet packet of the wavelet co-efficient.	
Cfs [33[10],34[11],37[12], 38[13]]:	The Crest Factor for wavelet packet chosen where those of node 33,34,37 and 38 of the wavelet tree.	47-85,86-124,125-163,167-202
Data	Data belonging to the chosen wavelet packets.	
Mode	The statistical mode of the wavelets.	47[10],86[11],125[12],164[13]
Mean	The statistical mean of the wavelets.	48[10],87[11],126[12], 165[13]
Median	The statistical median of the wavelets.	49[10],88[11],127[12], 166[13]
Max	The maximum value in the vector of wavelet co-efficient	50[10],89[11],128[12], 167[13]
Min	The minimum value in the vector of wavelet co-efficient	51[10],90[11],125[12], 168[13]
Deviation	The standard deviation of values in the vector of wavelet co-efficient.	52[10],91[11],130[12], 169[13]
Range	The difference between the maximum and minimum values.	53[10],92[11],131[12], 170[13]
Crstfac	Crest factor of the wavelet packet.	54-65[10],93-104[11],132-143[12],171-182[13]
Str8t (10x1)	Crest Factor of ten segments of the wavelet packet	54-63[10],93-102[11],132-141[12],171-180[13]
Max	Maximum of those ten crest factors	64[10],103[11], 142[12],181[13]
Avg	Average of those ten crest factors	65[10],104[11], 143[12],182[13]
Segrms	Root mean square of ten segments of signal	66-75[10],144-153[11],105-114[12],183-192[13]
Segenergy – V - totenergy	Area under each segment divided by area under vector of wavelet co-efficient.	76-85[10],115-124[11],154-163[12],193-202[13]

Figure F1 overleaf illustrates the high achy of measurements done on the respiratory signals.

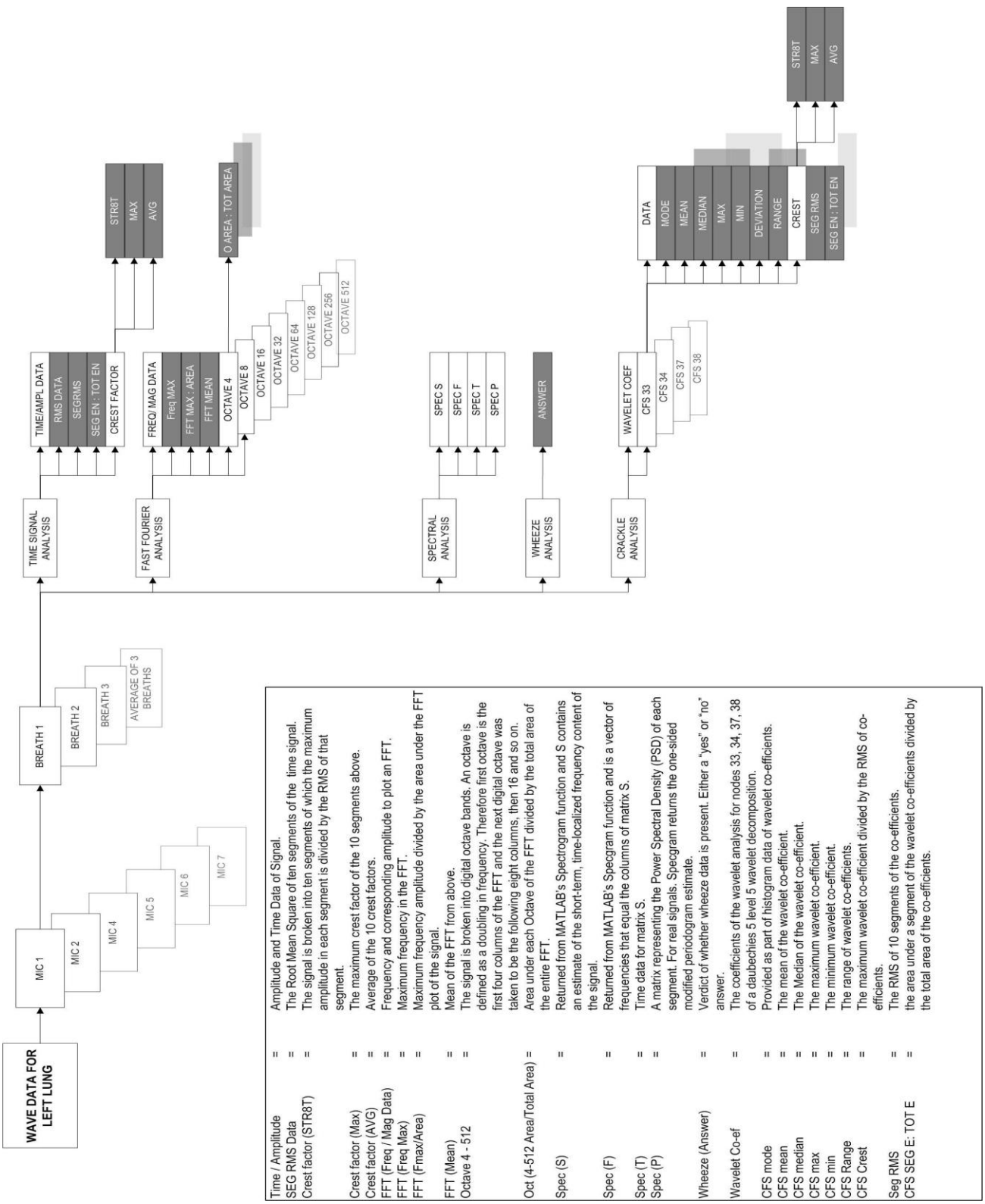

Appendix G: Explanation of Wavelet Analysis

In brief, wavelet analysis is similar to the Fourier transform analysis of a signal with a few variations over the FFT. Firstly the Fourier transform is the sum over all time of the signal $x(t)$ multiplied by a complex exponential where the exponential is a representation of real and imaginary sinusoidal components. This is accomplished using Equation H1 repeated below:

$$X(f) = \int_{-\infty}^{\infty} x(t)\, e^{-j2\pi ft} dt \qquad \text{(G1)}$$

The results of the transform are the Fourier coefficients $X(f)$, which when multiplied by a sinusoid of frequency f yield the sinusoidal components of the original signal.

Similarly, the definition of the continuous wavelet transform (CWT) is the sum over all time of the signal multiplied by scaled and shifted versions of a wavelet function Ψ. The results of the CWT are many wavelet coefficients C, which are a function of scale and position (Equation H2). (Misiti *et al.*, 2006)

$$C(scale, position) = \int_{-\infty}^{\infty} x(t)\Psi(scale, position, t)dt \qquad \text{(G2)}$$

Where $x(t)$ is the signal and Ψ a scaled and position of the so called *mother wavelet*. Thus, multiplying each coefficient by the appropriately scaled and shifted wavelet yields the constituent wavelets of the original signal. This has the advantage over the Fourier analysis in the sense that the sifted and scaled versions of the mother wavelet represent a windowing technique with variable-sized regions. Wavelet analysis allows the use of long time intervals more precise low-frequency information is required and shorter regions where high-frequency information is required.

Since wavelet analysis on every time and scale form would produce huge amounts of data, the analysis can be done on a discrete level using only scaled and shifted versions to powers of two. The result is a multiple level decomposition of arranged filters into which the signal goes in and the wavelet coefficients come out. This structure, as seen in Figure G- 1, illustrates that a signal S is filtered into its low frequency components (known as the *approximation (*A)) and its high frequency

components (known as *detail* (D)). The approximation is then down sampled by two and filtered at the next scaled and shifted version level.

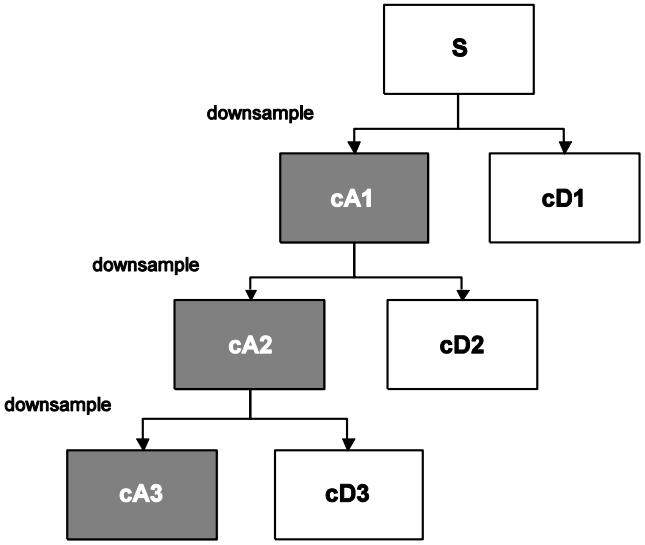

Figure G- 1: Wavelet Filtering and Down Sampling

Appendix H: Explanation of Neural Networks

A neural network can be modeled as an interconnected group of neurons that use a mathematical model for information processing. The system can be illustrated in Figure H- 1.

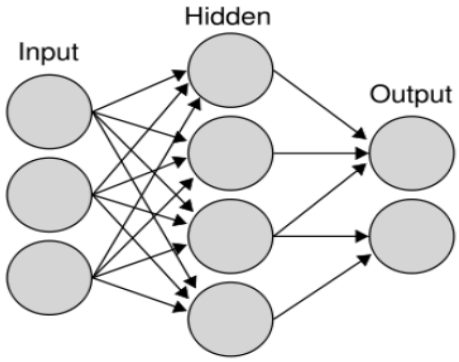

Figure H- 1: Neural Network Illustration

The figure shows that neurons are arranged as inputs, hidden neurons (can be in various layers), and outputs.

An artificial neural network (ANN) is a neural network defined by the function:

$$f : X \rightarrow Y \tag{H1}$$

This means the neural network uses a mathematical function to give a certain output Y from an input X. A widely used structure is the non-linear weighted sum of the function of the inner hidden neurons. Each hidden neuron represents a function $g(x)$ which carries a weight w. the function $f(x)$ is therefore given by:

$$f(x) = K\left(\sum_i w_i g_i(x)\right) \tag{H2}$$

were K is a predefined function such as a hyperbolic tangent.

The attractive ability of a neural network is its ability to learn. This essentially means that a neural network is given a set of inputs and its outputs are compared to what the correct answer should have been. This entails a cost function being drawn up for an optimal solution f^* where the cost C is minimized in order obtain an error as small as possible. This can be shown as:

$$C(f^*) \leq C(f) \tag{H3}$$

The neural network is trained to adjust the connection weights and biases in order to produce the desired output. At the training stage, the feature vectors are applied as input to the network and the network adjusts its variable parameters and the weights to understand the relationship between the inputs and outputs. The most frequently used training algorithm in classification problems is the back propagation (BP) algorithm along with a few modified BP algorithms. Adaptive learning rate BP, resilient BP, Levenberg–Marquardt, and scaled conjugate gradient BP algorithms were examined for training the ANN in this project.

Appendix I: Data Sheet for Electret Microphones

Panasonic Microphone Cartridges

Omnidirectional Back Electret Condenser Microphone Cartridge

Series: **WM-61A**
WM-61 B (pin type)

■ **Features**
- Small microphones for general use
- Back electret type designed for high resistance to vibrations, high signal-to-noise ratio
- High sensitivity type
- Microphone with pins for flexible PCB (WM-61B type)

■ **Sensitivity**

Vs = 2.0V RL = 2.2kΩ	–35 ± 4dB

■ **Specifications**

Sensitivity	–35±4dB (0db = 1V/pa, 1kHz)
Impedance	Less than 2.2 kΩ
Directivity	Omnidirectional
Frequency	20–20,000 Hz
Max. operation voltage	10V
Standard operation voltage	2V
Current consumption	Max. 0.5 mA
Sensitivity reduction	Within –3 dB at 1.5V
S/N ratio	More than 62 dB

■ **Typical Frequency Response Curve**

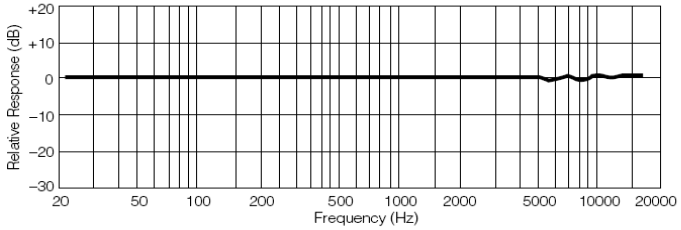

■ **Dimensions in mm** (not to scale)

WM-61A

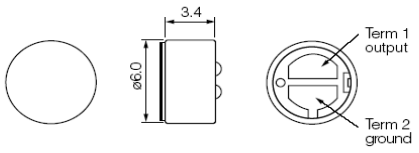

WM-61B

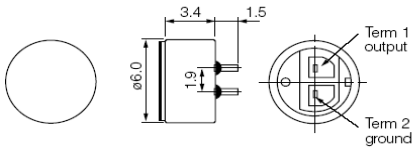

Figure I- 1: Electret Data Sheet

Appendix J: Evaluation Data for Neural Network Performance

Neural Network Parameter Varification: testing done on training data.

False Positives						
CV1	CV2	CV3	CV4	CV5	CV6	CV Average
2	3	4	5	4	1	3.17
3	4	2	5	4	3	3.50
3	3	1	5	3	5	3.33
3	2	3	4	3	0	2.50
3	3	3	5	3	3	3.33
2	6	3	3	1	4	3.17
4	2	4	2	3	4	3.17
3	4	2	3	2	3	2.83
2	4	4	2	3	3	3.00
4	3	4	4	3	4	3.67
				FP Average		3.17

False Negatives						
CV1	CV2	CV3	CV4	CV5	CV6	CV Average
4	4	5	5	3	7	4.67
5	5	4	6	6	6	5.33
5	5	5	3	5	3	4.33
5	6	5	4	5	6	5.17
4	5	5	5	4	5	4.67
7	4	4	5	5	4	4.83
5	5	5	5	5	6	5.17
4	6	5	4	5	4	4.67
4	5	5	5	4	5	4.67
7	4	4	5	4	5	4.83
				FN Average		4.83

True Positives						
CV1	CV2	CV3	CV4	CV5	CV6	CV Average
29	28	27	26	27	30	27.83
28	27	29	26	27	28	27.50
28	28	30	26	28	26	27.67
28	29	28	27	28	31	28.50
28	28	28	26	28	28	27.67
29	25	28	28	30	27	27.83
27	29	27	29	28	27	27.83
28	27	29	28	29	28	28.17
29	27	27	29	28	28	28.00
27	28	27	27	28	27	27.33
				TP Average		27.83

True Neagatives						
CV1	CV2	CV3	CV4	CV5	CV6	CV Average
22	22	21	21	23	19	21.33
21	21	22	20	20	20	20.67
21	21	21	23	21	23	21.67
21	20	21	22	21	20	20.83
22	21	21	21	22	21	21.33
19	22	22	21	21	22	21.17
21	21	21	21	21	20	20.83
22	20	21	22	21	22	21.33
22	21	21	21	22	21	21.33
19	22	22	21	22	21	21.17
				TN Average		21.17

Neural Network Reliability Test: testing done on foreign data.

False Positives						
CV1	CV2	CV3	CV4	CV5	CV6	CV Average
5	4	6	5	2	7	4.83
5	3	7	8	3	7	5.50
6	5	6	7	4	7	5.83
5	5	5	5	3	5	4.67
4	4	6	6	3	6	4.83
7	6	7	7	3	6	6.00
6	4	8	6	7	6	6.17
5	4	8	5	3	7	5.33
4	4	6	7	5	7	5.50
6	4	5	8	4	7	5.67
				FP Average		5.43

False Negatives						
CV1	CV2	CV3	CV4	CV5	CV6	CV Average
5	5	3	6	9	6	5.67
5	6	4	6	8	6	5.83
5	5	2	5	7	7	5.17
5	5	3	6	6	6	5.17
5	5	2	6	6	6	5.00
6	5	3	4	6	6	5.00
6	5	4	6	5	6	5.33
6	5	2	5	5	6	4.83
6	5	2	4	6	6	4.83
5	6	3	7	8	6	5.83
				FN Average		5.27

True Positives						
CV1	CV2	CV3	CV4	CV5	CV6	CV Average
26	27	25	26	29	24	26.17
26	28	24	23	28	24	25.50
25	26	25	24	27	24	25.17
26	26	26	26	28	26	26.33
27	27	25	25	28	25	26.17
24	25	24	24	28	25	25.00
25	27	23	25	24	25	24.83
26	27	23	26	28	24	25.67
27	27	25	24	26	24	25.50
25	27	26	23	27	24	25.33
				TP Average		25.57

True Neagatives						
CV1	CV2	CV3	CV4	CV5	CV6	CV Average
21	21	23	20	17	20	20.33
21	20	22	20	18	20	20.17
21	21	24	21	19	19	20.83
21	21	23	20	20	20	20.83
21	21	24	20	20	20	21.00
20	21	23	22	20	20	21.00
20	21	22	20	21	20	20.67
20	21	24	21	21	20	21.17
20	21	24	22	20	20	21.17
21	20	23	19	18	20	20.17
				TN Average		20.73